DESIGN STUDIES ON SOME NEW VARIANTS OF KLYSTRON AMPLIFIER

Ph. D. Thesis

DEEPENDER KANT

2013REC9569

DEPARTMENT OF ELECTRONICS AND COMMUNICATION ENGINEERING

MALAVIYA NATIONAL INSTITUTE OF TECHNOLOGY, JAIPUR

December, 2018

Design Studies on Some New Variants of Klystron Amplifier

Submitted in

fulfillment of the requirements for the degree of

Doctor of Philosophy

by

Deepender Kant

ID-2013REC9569

Under the Supervision of

Supervisor:
Dr. Vijay Janyani
Professor,
Department of ECE,
MNIT

Co-Supervisor:
Dr. L M Joshi
Ex- Chief Scientist,
CSIR-CEERI &
Professor, AcSIR

DEPARTMENT OF ELECTRONICS AND COMMUNICATION ENGINEERING

MALAVIYA NATIONAL INSTITUTE OF TECHNOLOGY, JAIPUR

December, 2018

Dedicated to my family

DECLARATION

I, Deepender Kant, declare that the thesis entitled, **"Design Studies on Some New Variants of Klystron Amplifier"** and the work presented in it are my own. I confirm that:

- This work was done wholly or mainly while in candidature for a research degree at this University.
- Where any part of this thesis has previously been submitted for a degree or any other qualification at this University or any other institution, this has been clearly stated.
- Where I have consulted the published work of others, this is always clearly attributed.
- Where I have quoted from the work of others, the source is always given. With the exception of such quotations, this thesis is entirely my own work.
- I have acknowledged all main sources of help.
- Where the thesis is based on work done by myself jointly with others, I have made clear exactly what was done by others and what I have contributed myself.

Date:

Deepender Kant
(2013REC9569)

CERTIFICATE

This is to certify that the thesis entitled "***Design Studies on Some New Variants of Klystron Amplifier***" being submitted by **Deepender Kant (2013REC9569)** is a bonafide research work carried out under our supervision and guidance in fulfillment of the requirement for the award of the degree of **Doctor of Philosophy** in the Department of Electronics & Communication Engineering, Malaviya National Institute of Technology Jaipur. The matter embodied in this thesis is original and has not been submitted to any other University or Institute for the award of any other degree.

Dr. Vijay Janyani
Professor,
Department of ECE,
MNIT

Dr. L M Joshi
Ex- Chief Scientist,
CSIR-CEERI &
Professor, AcSIR

ACKNOWLEDGEMENT

I wish to express my deep sense of gratitude to the special people who helped me by providing their assistance, suggestions and encouragement while doing my work presented in this thesis. I would like to acknowledge all of them for their support and help.

First of all, I am grateful to my Ph.D. supervisor Dr. Vijay Janyani for accepting me as his student and providing me a platform to conduct the research under his supervision. He always supported and allowed me to carry out the work without any boundaries. His enthusiasm, encouragement and faith in me have inspired me to do my work more passionately, without his continuous support this work would not have been possible. I wish to thank him for being available every time to overcome research and personal difficulties. I am highly indebted to him for giving me an opportunity to work under him and for his wholehearted support and suggestions. I feel myself lucky and honored to have a mentor like him.

I would like to thank Dr. L M Joshi, my co-supervisor at CSIR-CEERI, under whose able guidance, the project work has been carried out. He has been a constant source of inspiration and encouragement to me throughout the research work. His vast technical knowledge and insight in the field of microwave tubes have given me an excellent background in this field. I am grateful to him for guiding me throughout this journey by his important suggestions, support for fabrication work and valuable help at various stages of this work.

I would like to thank Prof. D. Boolchandani (HOD, ECE), Prof. K. K. Sharma (Ex-HOD), and Dr. Ghanshyam Singh Convener, DPGC for giving me time to time support and co-operation. I would also like to thank all other faculty members of Department of Electronics and Communication for many fruitful discussions and suggestions.

I wish to express my sincere thanks to Director, CSIR-CEERI for allowing me to do this research work and I am also grateful to Dr. Chandrashekhar, Ex-Director CSIR-CEERI for his encouragement and support.

I am also very thankful to my DREC committee members Dr. Ghanshyam Singh, Dr. Ritu Sharma and Dr. Ravi Kumar Maddila for their valuable suggestions and time to time support for making this thesis better. I firmly believe that their constructive

comments and timely feedbacks always give me a path to work upon for the better improvement. Thank you all for being in my research committee.

My deep sense of gratitude towards my colleagues at CSIR-CEERI Dr. A K Bandyopadhyay, Dr. Debasish Pal, Sh. Rakesh Meena, Sh. Bijendra Kumar, Sh. Vikram Singh and Sh. Nagaraju, for their continuous help and support while doing this work

I cannot forget my dear friends at MNIT Dr. Nikhil Deep Gupta, Dr. Amit Kumar, Sh. Bipin and Sh. Nitesh Kumar for helping me as much as they can. I really enjoyed their company in all ups and downs and learned many new things from them.

I would like to thank all my friends, family members and everybody else who helped me either directly or indirectly in completing this work. Last but not least, I thank almighty ***God*** for providing me strength and courage to complete the work.

(Deepender Kant)

ABSTRACT

Many of today's and future applications, such as communication, atmospheric sensing, military & high-energy physics applications require RF sources producing microwave power of several kilowatts to megawatt level. Klystron is one of the most popular devices used for such applications. It is essentially an amplifier which amplifies the microwaves in terms of gain and power. It is a velocity-modulated tube in which the velocity modulation process produces a density-modulated beam of electrons. The technology of conventional klystron has been quite matured and with increasing demand in terms of RF output power along with other performance parameters such as efficiency, gain etc., the new technologies like multi beam, sheet beam klystrons and extended interaction klystrons are becoming popular due to many advantages offered by them.

The aim of this dissertation work is to study some of the design aspects of above said devices including the design of a multi beam electron gun along with focusing structure, design development and characterization of multi beam and sheet beam klystron cavities and beam wave interaction study in multi beam klystrons. The study of multi beam klystron design has been done by considering the specification of a L/S band klystron, which has its applications in communication systems. The study has been done by converting some parameters of the existing single beam klystron into multi beam design parameters. A complete design of a conventional single beam klystron has been also covered in this work including thermal design aspects.

Contents

List of Figures:

List of Tables:

List of Abbreviations:

ECM:	Electronic Counter Measure
ECCM:	Electronic Counter Counter Measure
EW:	Electronic Warfare
IMPATT:	IMPact Avalanche ionization Transit Time
TRAPATT:	TRApped Plasma Avalanche Triggered Transit
MESFET:	MEtal Semiconductor Field Effect Transistor
BJT:	Bipolar Junction Transistor
PHEMT:	Pseudomorphic High Electron Mobility Transistor
FET:	Field Effect Transistor
GaAs:	Gallium Arsenide
GaN:	Gallium Nitride
AlGaN:	Aluminium Gallium Nitride
MW:	Mega Watt
GHz:	Giga Hertz
TWT:	Travelling Wave Tube
NEC:	Nippon Electronic Corporation
DNP:	Dynamic Nuclear Polarization
NMR:	Nuclear Magnetic Resonance
XDMR:	X-ray Detected Magnetic Resonance
ESR:	Electron Spin Resonance
CW:	Continuous Wave
SLAC:	Stanford Linear Accelerator Center
RF:	Radio Frequency
LHC:	Large Hadron Collider
LINAC:	Linear Accelerator
KAERI:	Korea Atomic Energy Research Institute
IPR:	Institute for Plasma Research
LHCD:	Lower Hybrid Current Drive
DSN:	Deep Space Network
BARC:	Bhabha Atomic Research Center
NLC:	Next Linear Collider
GeV:	Giga Electron Volt
HV:	High Voltage
MBK:	Multi Beam Klystron
SBK:	Sheet Beam Klystron
EIK:	Extended Interaction Klystron
ILC:	International Linear Collider
SMA:	Sub Miniature version A
VNA:	Vector Network Analyser
E-Cal:	Electronic Calibration
OFHC:	Oxygen Free High Conductivity

CHAPTER 1
INTRODUCTION

1.1 Microwaves – Applications and Sources

Microwaves are a form of electromagnetic radiation with wavelengths ranging from as long as one meter to as short as one millimeter, or equivalently, with frequencies between 300 MHz and 300 GHz. The word 'Microwaves' used in 1932 for the first time for wavelengths from 1mm to 1m, other terms proposed were 'Microrays' and 'Quasi-optical waves' but Microwaves accepted [1]. Microwaves play a vital role in many strategic and societal areas like radio astronomy, remote sensing, terrestrial and satellite communication, industrial heating, particle accelerators and military communications etc. Microwaves provide various advantages compared to low frequency regime such as reduction in antenna size, increased antenna directivity and less atmospheric absorption as microwaves are not much affected by snow, fog and cosmic or galactic noise as compared to optical and infrared waves. Microwaves ranging from S to Ku bands are commonly used for ground based communication. For space to space communication, millimeter waves are preferred to microwaves for compact antenna and waveguide systems. For very long distance communication, lower ranges of microwaves, in L and S bands, are preferred due to the availability of high power transmitters. Similarly in radar systems microwaves and millimeter waves are extensively used such as in airborne, marine and ground based radar, both for civil and military applications. Electronic Warfare systems, including Electronic Counter Measure (ECM) and Electronic Counter Counter Measure (ECCM), also use low and medium power microwave and millimeter waves. Considerable research and development efforts have also been directed towards the exploitation of high power microwaves (HPM) as weapons for the destruction of electronic equipment.

The design of a microwave circuit is not as easy as compared to the low frequency circuit design. Since the electron transit time is comparable with the time period of the wave, problems of lead inductance and inter electrode capacitance arise. Moreover at higher frequencies skin effect dominates and losses like radiation loss, dielectric loss etc. come into picture. Therefore low gain, high noise figure of devices and the most importantly, the inability to treat device's lumped parameters are the factors which become relevant at high frequencies which force circuit designer to adapt a more complex design philosophy for the generation and amplification of the microwaves. A variety of such microwave sources including many types of vacuum tubes as well as solid-state semiconductor devices have been invented over last six to seven decades [2-22]. Before the advent of solid-state devices such as Gunn, IMPATT,

TRAPATT diodes etc., vacuum tubes were the only available choice for use throughout the entire microwave range. In vacuum tubes, the electron beam moves in vacuum without any collision, therefore no heat loss due to their kinetic energy during electron current flow through the device. Ideally, the heat is produced only in the collector where electron beam is dumped after interaction whereas in solid state devices the electron current drifts through a solid surface of material resulting in the loss of kinetic energy of electrons while travelling between emitter and collector. Therefore electron mobility is very less in semiconductor materials than in vacuum, the device sizes are very small and the maximum power which can be generated or amplified by a solid-state device is very much less than vacuum devices popularly known as microwave tubes [2-4]. The solid state devices are used at low power range but there are numerous applications where medium to high power microwave is required and vacuum tubes can only meet such requirements. Solid state technology works at comparatively low power levels. The major advantages of this technology are low production cost, mass production and small size. Microwave tubes, on the other hand, have the advantages of high powers, high gains, wide bandwidths, high reliability, long life, etc.

Therefore vacuum technology and solid state technology are the two competing technologies for sources of microwaves and vacuum technology dominates when the requirement is very high average power and peak power as shown in Figure 1.1. The semiconductor devices like MEtal Semiconductor Field Effect Transistors (MESFET) are superior for higher frequency than Bipolar Junction Transistor (BJT) due to their higher transit frequency. Further by using GaAs rather than silicon in MESFET gives additional advantages due to higher electron mobility and facilitating for fabrication of GaAs substrate, thereby eliminating the microwave power absorption in substrate due to free carrier absorption. Pseudomorphic High Electron Mobility Transistor (PHEMT) is a useful device in the field of wireless communication and is a type of Field Effect Transistor (FET) where a heavily doped wide band gap layer is grown on the top of a thin un-doped GaAs layer and hence forming a quantum well which results a dramatic increase in the mobility of electrons. Impact Avalanche ionization Transit Time (Imp ATT) is basically a diode which takes advantage of avalanche breakdown combined with transit time of charge carriers so as to provide a negative resistance region and thereby acts as an oscillator. Apart from the semiconductor devices listed in the Figure 1.1 there is a newer microwave device i.e. GaN based transistors which has tremendous growth over last two decades since its invention in 1993 with poor initial performance [23]. They have been used worldwide as commercial power amplifiers in S and X bands [24] and by incorporating the new device structures their operational frequency has been reached into

millimeter and sub millimeter range [25-26]. The amplifiers based on AlGaN/GaN technology have been proven very promising devices with higher output power, larger bandwidth and increased efficiency [27-33].

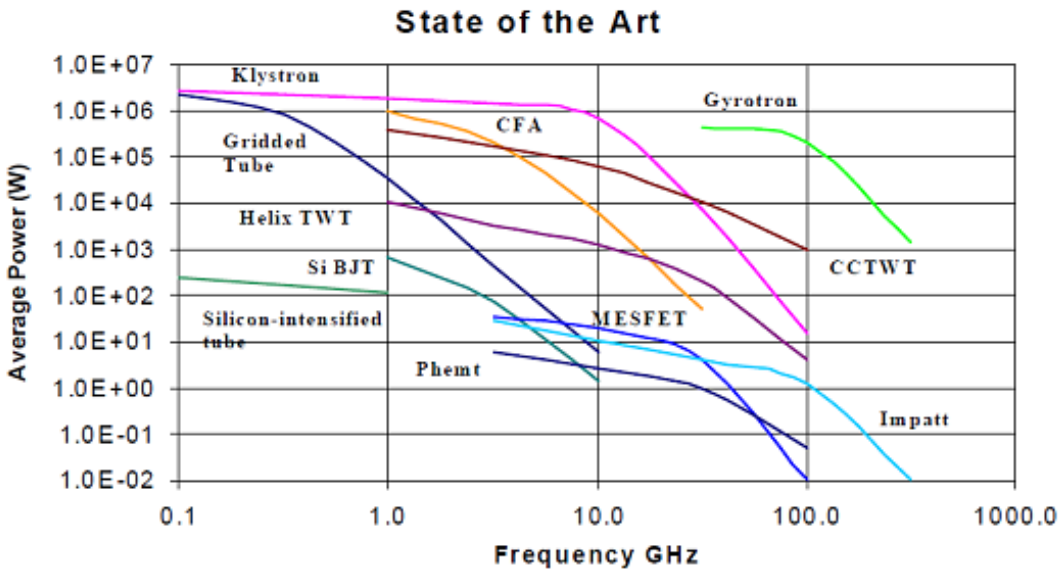

Fig. 1.1: Power levels and the frequency range for various microwave sources

(Source: Google images; after R. Parker, NRL)

The vacuum technology has been and will continue to be the enabling technology for entire classes of high-power, high frequency amplifiers for use in both military and commercial systems. In addition to this, high power microwave amplifiers and oscillators are being used in scientific research areas such as high energy particle accelerators and plasma heating for controlled thermonuclear fusion. Commercial satellites for communication systems and broadcasting, microwave ovens for industrial and domestic heating and many medical system such as hypothermia applicators are heavily dependent on vacuum electronic devices for their reliable performance at high power and high efficiency [34]. Figure 1.2 shows the range of power and frequency for these key applications [35]. The factor 'Pf^2' can be given as *figure of merit* for the ability of a vacuum device to generate RF power, where 'P' is the average power in Megawatts (MW) and 'f' is the operating frequency in GHz. The Figure 1.3 shows a doubling of the factor 'Pf^2' every two years for vacuum electronics devices over last several decades.

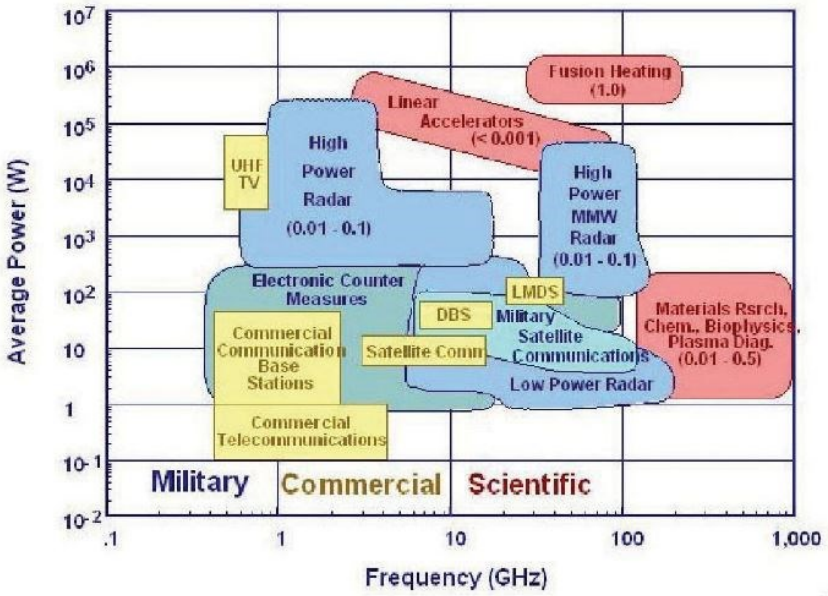

Fig. 1.2: Applications of high power microwave sources

(Source: Vacuum Electronics: Status and Trends, Baruch Levush etal.)

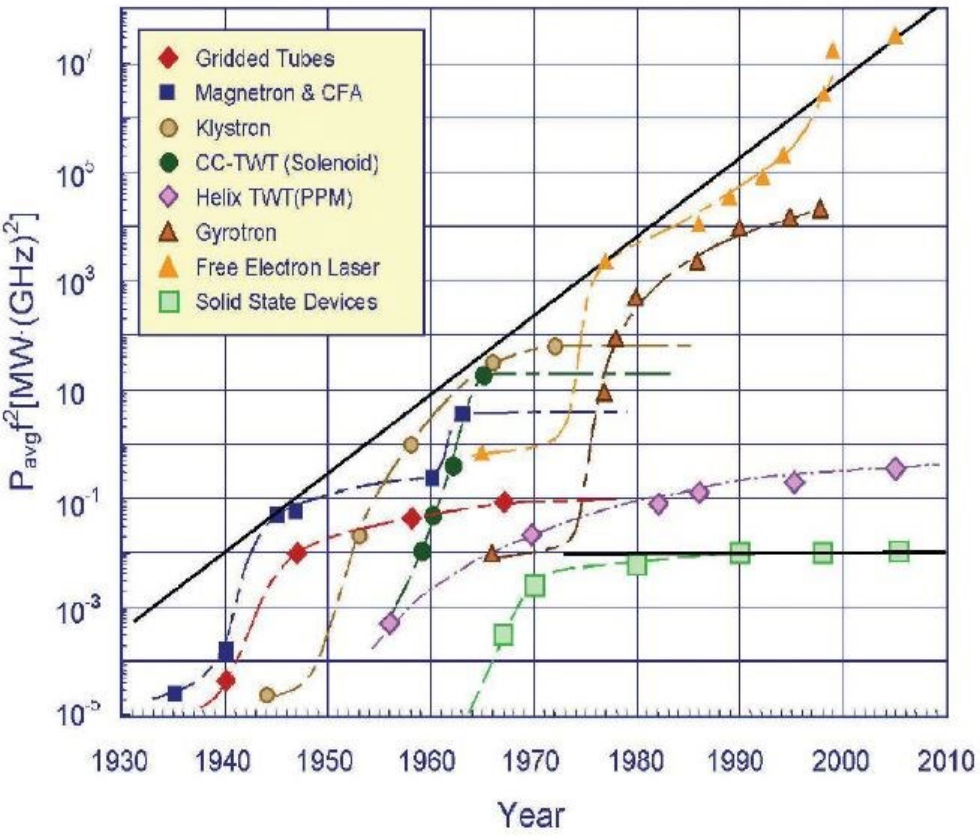

Fig. 1.3: Progress in factor 'Pf^2 for vacuum electronics over the years

(Source: Vacuum Electronics: Status and Trends, Baruch Levush etal.)

Chapter 1. *Introduction*

In a microwave tube, the interaction takes place between an electron beam and RF waves supported by an electromagnetic structure so as to convert the kinetic energy of electron beam into RF amplification. The most commonly used microwave tubes are:

1. Travelling Wave Tube (TWT)
2. Magnetron
3. Gyrotron
4. Klystron

The oscillators as well as the amplifiers can be made in microwave tubes. Magnetrons and Gyrotrons are the oscillators and TWTs, klystrons are the amplifiers [2-5], [10-14]. Although Gyrotron is much popular fast wave device, Gyro-TWT and Gyro-klystron are also under research under this category [36],[37].

The microwave tubes can be classified in various ways based on the mechanism of conversion of spontaneous radiation from individual electrons into coherent radiation by bunching the electrons in a proper phase with respect to RF wave by adjusting the beam, magnetic field and interaction structure parameters. Some of the classifications are as follows;

(i) **O-type/M-Type and Kinetic/Potential Energy conversion type devices:** In an O-type microwave tube, like TWT and klystron, which is also a kinetic energy conversion device, a DC axial magnetic field is used to constrain the electrons to move in the axial direction of the interaction structure. The magnetic field in such a device however does not take part in the interaction between the electron beam and RF waves. In an M-type tube, like magnetron and Crossed Field Amplifier (CFA), which is also a potential energy conversion device, a DC magnetic field is used along with a DC electric field at right angle to it, both in turn at right angle to the axial direction. The magnetic field takes a dominant role in the interaction process in an M-type tube.

(ii) **Fast wave and Slow Wave devices:** A Gyrotron may be considered as a fast-wave type, since in this type a fast waveguide mode i.e. with phase velocity greater than the speed of light, is destabilized, whereas TWT, klystron are called slow-wave type devices where a slow waveguide mode, with phase velocity less than the speed of light, is destabilized.

(iii) **Cerenkov, transition, and bremsstrahlung radiation types:** A microwave tube like TWT belong to the Cerenkov radiation type, in which electrons move in a medium with a speed greater than the phase velocity of electromagnetic waves in

the medium and the klystron belongs to the family of transition radiation type, the latter associated with electrons passing through the boundary between two media with different refractive indices or passing through perturbations in a medium such as conducting grids and a gap between conducting surfaces. Similarly, a Gyrotron may be categorized as a bremsstrahlung radiation type, in which radiation occurs when electrons bremsstrahlung, that is move with a varying velocity (that is, with an acceleration/ deceleration) in electric and/or magnetic fields and the electron beam is made periodic in its cyclotron motion The operation of the device is essentially based on cyclotron resonance maser (CRM) instability [38], [39].

The traveling wave tube (TWT) is the most popular microwave tube and has the largest market among all tubes. TWTs are used in most electronic warfare systems, satellites and radar systems particularly in phased array systems. Of particular note is the performance of the X-band TWT on the Voyager I satellite, which was in operation for 28 years in space [40]. They can be used as a driver in Microwave Power Modules (MPM) for electronic warfare and also as the final amplifiers in a large percentage of communications satellites and systems.
This is a linear-beam, O-type device and commonly used RF circuit in TWTs are

(i) Helix for broadband application (being a non-resonant structure) and
(ii) Coupled cavity for high power application.

Traveling wave tubes are used from frequencies below 1 GHz to over 100 GHz. Power generation capabilities range from watts to megawatts. For helix TWTs, bandwidths may be as high as 2 octaves or more. For coupled-cavity TWTs, bandwidths in the 10–20% range are common [40].

TWT was invented by Kompfner [41] in early 1943, since then the technology of TWT has been changed dramatically except its basic principle [42] resulting in an increase in the overall DC to RF conversion efficiency from about 1% (including solenoid power) to today's 73% with the future potential to approach 75% or even 80% for commercial satellite communication applications. The efficiency enhancement for TWTs from Thales Electron devices is shown in Fig. 1.4 but it is more or less same characteristics for other manufacturers also like Hughes Electron Dynamics, Nippon Electronic Corporation (NEC) etc. [43-52]. Efficiencies of 100 to 200 W Ku-band TWT´s around 70% have been reported by all these space TWT manufacturers at least with engineering models. The Fig. 1.5 shows a survey of various types of TWTs used for space applications.

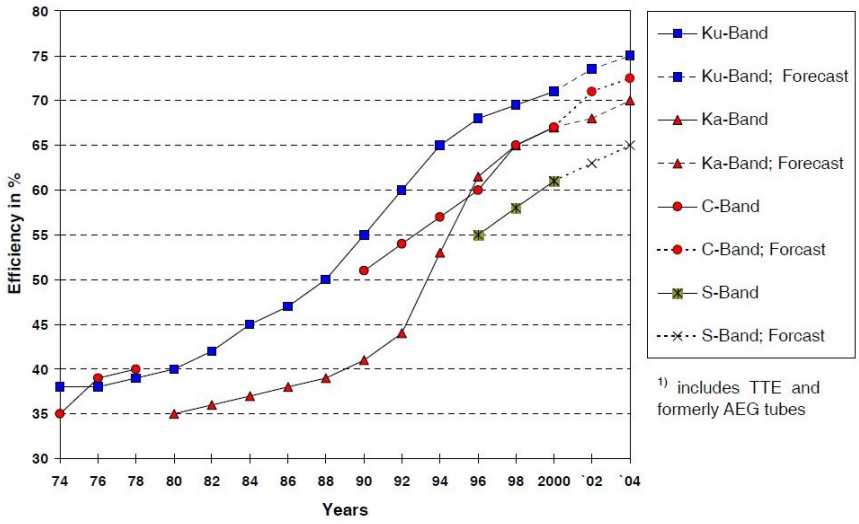

Fig. 1.4: Progress in efficiency for Thales satellite TWTs over the years

(Source: From History to Future of Satellite TWT Amplifiers" Dr. Günter Kornfeld ; Thales Electron Devices GmbH, Germany)

Band / Frequency /GHz	power / efficiency in production	Power / efficiency under development	Application
L-band / 1.5	130 – 160 W / 55 %	130 – 170 W / 59 % 50 – 90 W / 59 %	Direct Digital Radio (Africanstar) possible use for Navigation / Galileo
S-band / 2.3 – 2.6	70 – 90 W / 59 % 200 – 240 W / 58 %	70 – 130 W / 62 %	communication / TV-broadcast direct digital radio for automotive
C-band / 3.4 – 4.2	20 – 130 W/ 60 - 65 %	20 – 150 W / 64 - 70 %	telecommunication /broadcast.
C-band / 5 to 6	5 kW; pulsed TWT		SAR, for earth observation, Radar TWT
X-band / 7 - 8.5	25 / 120–170 W / 60 %	120 – 170 W / 69 %	scientific applications with deep space mission
X-band / 7 - 8	4 kW;pulsed TWT		Earth observation, radar TWT
Ku-band/10.7 – 12.75 Ku-band/10.7 – 12.75	25 – 200 W / 62 – 66 %	25 – 200 W / 65 – 73 % 300 W / 68 %	Telecommunication and Broadcasting Internet Multimedia-Services (fixed and mobile)
Ku-band / 13 – 15 or 12-18	100 W; pulsed TWT		Altimeter; Radar application
Ka-band / 17 – 22 and 23	15 –140 W / 55 – 66 %	15–150 W / 58 – 68 % 200 W / 65 %	Telecommunication and Multimedia Services
Ka-band / 27 – 32	20 – 30 / 54 %	20 – 40 W / 50 %	Deep Space Mission, Scientific
Q-band / 40 – 45	40 – 250 W / 25 – 35 %	40 – 100 W / > 45 %	Multimedia Services for low Orbit Satellites or Stratosphere Balloons
V-band / 58 – 64	20 W / 35 %	20 – 35 W / 45 %	Inter Satellite Links for Multimedia Services

Fig. 1.5: Survey of Space TWT Applications

(Source: From History to Future of Satellite TWT Amplifiers" Dr. Günter Kornfeld ; Thales Electron Devices GmbH, Germany)

The magnetron since its invention in 1941 by Randaal and Boot has been the most extensively used sources in radar transmitters as well as in heating applications. The magnetron generally has coaxial structure with a cylindrical cathode at the center and an outer electrons rotates azimuthally in the coaxial space between an inner cathode and an outer anode block containing coupled resonant cavities arranged periodically around the azimuth. The electrons rotate in the inter electrode space under the combined effect of a radial electrostatic field and an axial magneto static field. The interaction between an azimuthally traveling wave associated with the coupled cavities and the synchronously rotating electron layer produces a radial electron drift toward the anode coupled with electron velocity modulation. This action produces electron bunching in space and subsequent generation of coherent microwave power. Magnetron oscillation builds up from random noise at frequencies determined by the resonant anode structure. Magnetrons are especially useful as pulsed oscillators in simple light weight systems and in airborne radar systems. Besides the usual cavity-slot configuration, magnetrons have also been developed in other configurations, namely, the coaxial, inverted and rising configurations [53-57]. Rising sun magnetrons are capable of generating high powers at mm wavelengths.

Gyro-devices have been implemented in oscillator and amplifier configurations. Gyrotron can generate unprecedented average and peak power levels at millimeter wavelengths with high efficiency. Gyrotron belongs to the cyclotron mode interaction, fast-wave, kinetic energy conversion and bremsstrahlung radiation type device where cyclotron resonance interaction takes place between gyrating electrons and a fast waveguide mode in an open-ended resonator. Unlike in conventional microwave tubes, transverse rather than axial kinetic energy is converted into RF energy. The bunching, which is essentially azimuthal, is based on the relativistic dependence of gyrating electrons and hence that of their cyclotron frequency. In such tubes larger interaction structure dimensions can be taken than in conventional slow-wave microwave tubes. This reduces losses in the wall of the structures. The operating frequency is controlled by the electron cyclotron frequency and hence by the background magnetic field used in the device. In order to reduce the required magnetic field, a higher beam harmonic operation is called for [36-40]. Gyro-amplifiers have been also developed using klystron and TWT like interaction circuits. The primary applications for Gyrotrons are the cyclotron resonance heating of fusion plasmas, ceramic sintering, and metal joining. The invention of Gyrotron has opened up a new research field in high power Tera hertz science and technology where these devices are used as powerful

and frequency tunable source of coherent radiation [58-69] including the high-precision spectroscopic techniques (DNP-NMR, ESR and XDMR etc.), new medical technologies and treatment and characterization of advanced materials [68].

Klystrons are high gain but narrowband amplifiers that find wide use in various communication and radar systems, material processing and particle accelerators for medical, industrial and scientific applications including nuclear waste transmutation and energy production by sub-critical reactors. Klystron tube is basically an amplifier device, which amplifies the microwaves in terms of gain and power output. It is a velocity-modulated tube in which the velocity modulation process produces a density-modulated beam of electrons. Here the interaction between electron beam and RF fields takes place at discrete locations i.e. resonator cavities placed along the beam path and the RF signal is carried from cavity to cavity by the electron beam. Klystrons have been built at frequencies from 0.5 to 35 GHz, delivering CW power over 1 MW and pulsed power over 100 MW. The gain of a typical klystron ranges from 10 dB to 70 dB [70–71] and the power output is over 1 MW for CW and may be more than 150 MW for pulsed operation. Some developments include a tunable long pulse (10 sec) klystron with an output power of 1MW in the frequency range 1.7-2.3 GHz [72], multi-megawatt multi-beam multi-cavity klystron for high energy physics, especially for electron synchrotron or storage rings for 300-600 MHz frequency range [73], high power (63 MW) stable klystron for Stanford linear accelerator center (SLAC) and 60 kW, 800 MHz klystron with overall efficiency of 71% using a multistage depressed collector [74].

1.2 Klystron Amplifier and Its Applications Areas

A schematic diagram of a multi cavity klystron tube is shown in Fig. 1.6. It consists of the following major components:

(i) Electron gun.
(ii) Focusing system
(iii) RF interaction structure.
(iv) Collector
(v) Output RF window

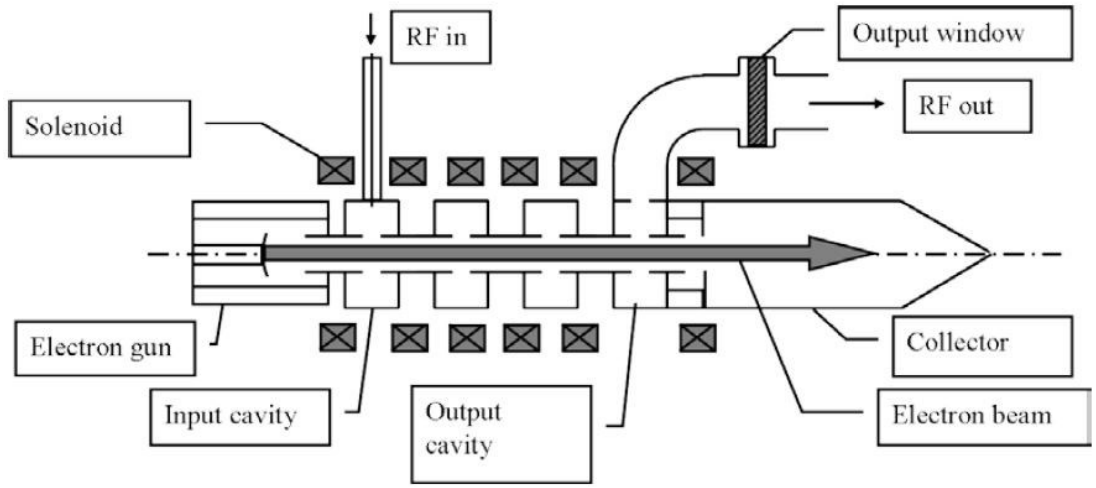

Fig. 1.6: Schematic Diagram of Single Beam Multi cavity Klystron

(Source: Google images; Radio Frequency Power Generation, R. G. Carter)

Electron Gun**:** It consists of a heater, cathode, grid, beam focusing electrode (BFE) and anode. Electrons are emitted by the cathode and are drawn toward the anode, which is operated at a positive potential with respect to the cathode. The electrons are formed into a narrow beam by either electrostatic or magnetic focusing techniques; this ensures that the electron beam does not spread out. The control grid is used to govern the number of electrons that reach the anode region. It may also be used to turn the tube completely on or off in certain pulsed amplifier applications.

Focusing system**:** An axial magnetic field is used to keep the beam abstain from spreading as it traverses the tube, which is usually through an electromagnet.

RF Interaction Structure**:** In this region, the interaction between the electron beam from electron gun and modulating signal coming from input cavity of the tube takes place. This region has two main components--:

(a) Resonant Cavities:

The RF resonant cavity is an important part of klystron and plays a vital role in the RF performance of the tube like its gain, bandwidth, efficiency, etc. that depends upon the proper choice of cavity parameters. The exchange of energy between accelerated electron beam and RF signal takes place at the gap of cavity.

(b) Drift tube:

Drift tube is the space between two successive cavities. The drift tubes are designed to be non-propagating at the frequency of operation. In the drift length the electrons group into bunches after undergoing a change in velocity while passing through the cavity gap. The choice of proper drift length is aimed for maximum bunching effect, which depends on plasma frequency and velocity of electrons.

Collector**:** Collector is the portion of Klystron where electrons are collected. When the electrons enter the collector, magnetic field ceases to act on the beam and beam spreads due to space charge forces. Slow electrons, which are normally major portion of beam, make steep angles with axis. The striking electrons produce heat on collector surface which is removed by proper cooling arrangement. The collector is designed to dissipate heat without any structural damage by increasing its surface area.

Output RF Window**:** Microwave window is a passive component of microwave tube through which the output RF power is coupled out with minimum loss with ultra-high vacuum and normal atmospheric pressure on either side of it.

Operating principle [1]: In the Klystron, the dc electron beam is accelerated to a high velocity before it is passed through the modulating electric field of the input cavity.

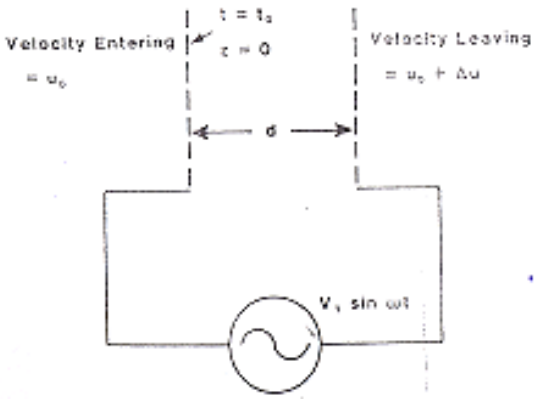

Fig. 1.7: Velocity Modulation of Electron Beam

In Fig 1.7, the input cavity is represented by a pair of grids spaced by distance ‘d’. A sinusoidal voltage is applied to the grids. When the high-velocity electron beam is passed through the modulating field, some electrons have their velocities increased (when the right-hand grid of

Fig.1.8 is positive with respect to the left-hand grid), some electrons have their velocities decreased when the voltage is reversed, and a few have their velocities unchanged. As a result, the electrons are said to be velocity modulated. Because the velocity change of the electrons is generally small, the electrons remain very close to their dc beam positions, and so essentially no density modulation occurs within the modulating gap.

After the beam leaves the modulating gap, those electrons that had have their velocity increased gradually overtake the slower electrons. This process is illustrated in Fig. 1.4, which is known as an Applegate diagram. Axial electron positions are plotted as a function of time so that the slopes of the various lines represent electron velocities.

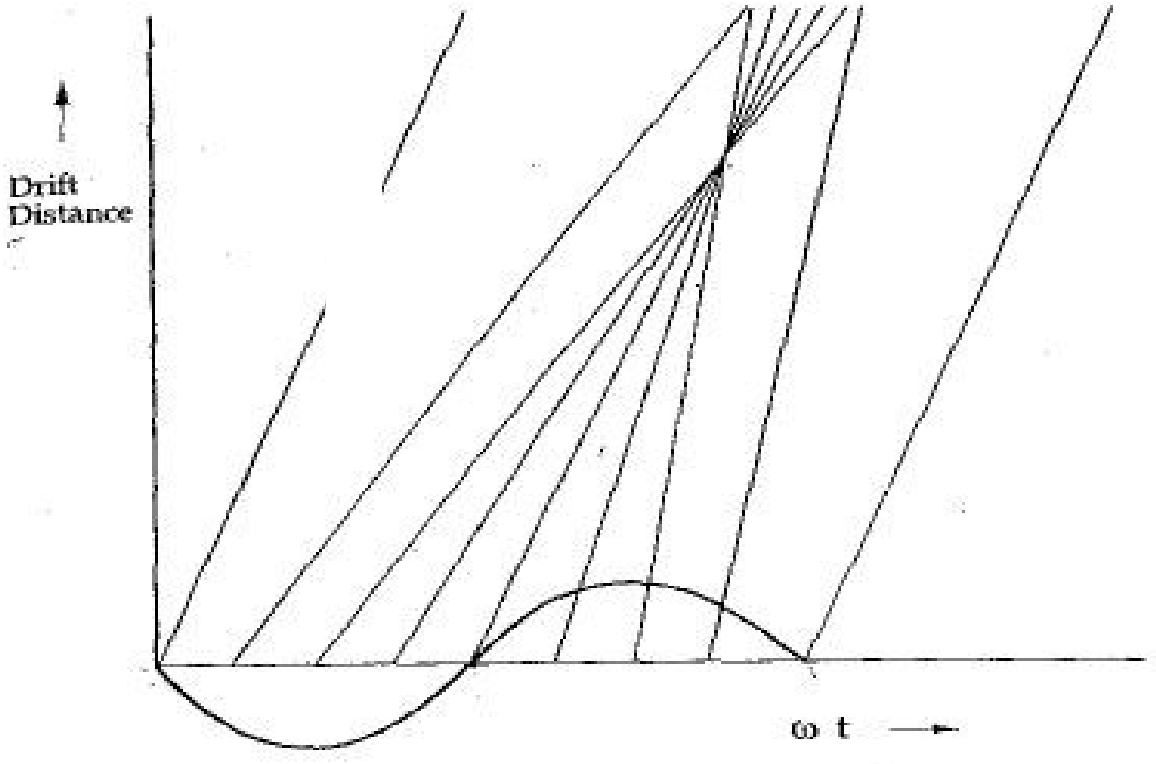

Fig. 1.8: Applegate diagram for electrons in a field free drift region

(Source: Power Klystron Today, Smith, Phillips)

In Fig.1.8, space charge forces between electrons are ignored, so the electron trajectories are shown to cross. In practice, at small and medium drive signal levels, space-charge forces prevent electron trajectories from crossing. Modified Applegate diagram considering the effect of space charge is shown in Fig. 1.9.

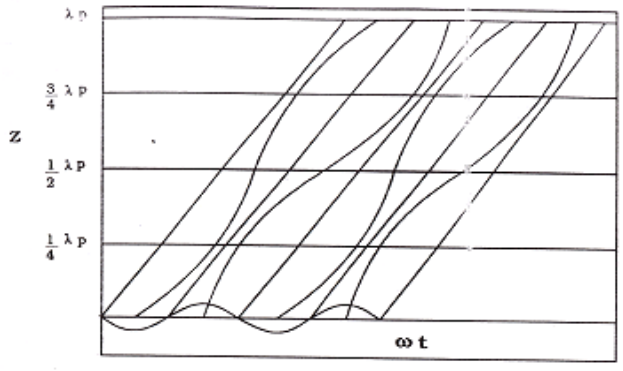

Fig. 1.9: Modified Applegate diagram showing the effect of space charge

(Source: Power Klystron Today, Smith, Phillips)

Here in the figure λ_p is the wavelength corresponding to plasma frequency, the frequency at which electron oscillates in-between the bunches.

The function of the intermediate cavities [40], [75] is to increase the gain, and usually the bandwidth of the amplifier. The location of the first intermediate cavity is one quarter of the plasma wavelength from the input cavity. RF current is induced in the intermediate cavities. This current and the impedance of the cavity produce a voltage across the gap that enhances the modulation of the beam to produce further current growth.

The location of the third cavity is shown to be less than $\lambda_p/4$ from the second cavity. The reason is, due to the result of the nonlinear beam behavior. The velocities of the electrons are so high that space-charge forces have little effect during the bunching process. As a result, that optimum bunch (containing maximum fundamental current) occurs before the beam has drifted a quarter of the plasma wavelength. In Klystrons, the next-to-final cavity is called the penultimate cavity. The distance between the penultimate cavity and the final cavity is less than quarter of plasma wavelength for the same reason as above. In principle, the gain of the klystron amplifier can be increased indefinitely by adding additional cavities along the beam.

The possibility of increasing the bandwidth by adding idler cavities was postulated in the 1940s. However, increasing the bandwidth in this way is not as easy as it first appears to be because the cavities of a klystron are all coupled to the same electron beam and so their tuning characteristics are not independent. If not tuned properly, some of the idler cavities will demodulate the beam and produce holes (regions of reduced gain) in the frequency response, hence stagger tuning is needed. In addition it is necessary to have an output structure that can cover the required bandwidth. The common approach for design is to find out the bandwidth

which can reasonably be expected of the output stage and then to design RF drive section having sufficient bandwidth with the required device gain. Normally, the gain is limited to 50 to 60 dB. at higher levels, the shot noise of the beam is increasingly amplified, and the signal-to-noise ratio of the output is reduced. In addition, to obtain stability, there must be no feedback from output to input, either because of leakage of transmission line connections, RF modulation of collector leads, and feedback to the electron gun, or reflected electrons within the beam.

Features of klystron amplifier: High-power Klystron features include:

1. High efficiency and high gain
2. High power performance but narrow bandwidth
3. High reliability and longer life

Applications of klystron amplifiers: Klystrons are widely used for following applications

1. Communication
2. High-energy accelerators
3. Thermonuclear fusion
4. Surveillance radars.
5. Industrial microwave heating etc.

All particle accelerators require high-power radio-frequency sources which should be amplifiers to achieve sufficient frequency and phase stability. The range of frequencies employed is from about 50 MHz to 30 GHz or higher with power range from 10 kW to 2 MW or more for continuous power and up to 150 MW for pulsed power. CERN is using 400 MHz, 300 kW CW power klystrons as RF source in its LHC accelerator and Fig.1.10 shows various klystrons used for different pulsed accelerators [76-77].

L*ab*	**Accelerator Name**	**Type**	**Frequency (MHz)**	**Power (MW pk)**	**Duty**
GSI	FAIR Linac	Linac	325	2.5	0.08 %
ESS	ESS DTL	Linac	352.2	1.3 and 2.5	5 %
ORNL	SNS RFQ & DTL	Linac	402.5	2.5	8 %
ESS	ESS Elliptical	Linac	704.4	2	4 %
ORNL	SNS CCL	Linac	805	5	9 %

Fig. 1.10: RF power amplifiers for pulsed accelerators

(*Source: Radio frequency power generation; R G Carter*)

Thales Electron Devices, France has produced TH2161's family of CW klystrons for synchrotron and storage rings which are capable to deliver 180,250 and 300 kW CW power levels at 500 MHz [78]. SLAC and CPI has jointly done Cooperative Research and Development Agreement (CRADA) for development of UHF super power klystrons as a 476 MHz RF source for use in storage rings at SLAC [79]. Korea Atomic energy Research Institute (KAERI) has used 350 MHz, 1 MW klystron for its Korea Multipurpose Accelerator Complex (KOMAC) project to accelerate a 20mA proton beam from 50keV to 3MeV[80]. Similarly 700 MHz klystrons were used high power proton Linacs at Los Alamos [81]. Litton has used L-5822-90 S-band klystron at 2856 MHz for its high energy medical linear accelerator system [82]. S-band klystron with 150 MW pulsed power with 3μS pulse at 60 Hz have been used at Linear collider test facility at DESY [83]. The high power pulsed klystrons have been manufactured at higher frequencies also such as 11.4 GHz/75 MW (E3761) and 5.7 GHz/50 MW (E3758) by Toshiba Electron Tubes and Devices, Japan [84].

High CW power klystron are also used globally for fusion experiments. The lower hybrid heating system of TORE SUPRA (CEA facility at Cadarache, France) includes 16 TH2103 klystrons delivering 500 kW each at 3.7 GHz . These klystrons operating in long pulses (up to 210s) have contributed to the achievement of a record energy in excess of 1 Gigajoule deposited in a plasma during a single shot [85]. Institute for Plasma Research (IPR), Gandhinagar, Gujarat uses 3.7 GHz, 500 kW power klystrons (same as above) for Lower Hybrid Current Drive (LHCD) system in the Indian Tokamak.

For the exploration of the solar system and the universe, NASA has established Deep Space Network (DSN) which is an international network of antennas that supports interplanetary spacecraft missions, Earth-orbiting missions and radio and radar astronomy observations. It consists of three deep-space communications facilities which are placed at about 120 degrees apart around the globe. At each facility, 220-ft antennas are powered by a 500-kW, CW S-band klystron and two 150-kW, X-band klystrons being operated in parallel. There is also another 25-kW X-band klystron. S-band is used for communications with orbiting spacecraft and the high-power X-band tubes are used in a radar mode [86]. Baron Gen3 Radar being used for superior weather detection in every meteorological environment from convective and tropical to arctic environment, uses 1 MW S-band klystron system [87]. Although magnetrons and TWTs are also used in weather radars [88] but klystron has a longer life time and is a better choice for high peak and average power. For industrial heating systems, NEC has developed several high-efficiency klystrons with power level 15 kW to 100 kW and 75% efficiency by

adopting second harmonic bunching and selecting low beam perveance [89]. These klystrons are expected to be applied to scientific and medical applications as well as to new industrial applications.

Applications of klystron for various national requirements (in Indian context) :
Several systems based on the klystron as a microwave power source are being developed in the country by various agencies for many societal as well as advanced scientific applications. Some of the examples are given as follows.

The following systems are being developed by various Department of Atomic Energy (DAE) units like **BARC, Mumbai and RRCAT, Indore** based on k*lystron* as its RF power source;

(i) ***X Rays Radiography for Cargo Inspection & Security Systems:***

This utility has immense potential in the industry and can play a vital role in strengthening the security of a nation, too. Many countries are now employing the X rays cargo scanning systems for checking the inflow of illegal arms, drugs, narcotics, ammunitions, explosives etc. By installing these devices flow of such goods can be detected. BARC in collaboration with Electronics Corporation of India Limited (ECIL) has initiated a project to develop a prototype cargo scanning system [90]. Such a system has following three major components:

(a) Electron accelerator for generating the X-rays,
(b) Radiographic and imaging techniques for constructing and viewing the images and
(c) Container handling system inclusive of overall electromechanical controls.

The role of klystron lies as RF source in the electron accelerator which will have a beam energy of about 10 MeV with an average beam current of 0.2 mA. The S-band Klystrons (at 2856 MHz) with a peak power of 6 MW and average power of 24 kW will be required, which are being developed at CSIR-CEERI as discussed later in Chapter 2.

(ii) ***Industrial Linear Accelerator for Food Processing:***

Electrons have mass and an electric charge and therefore, are absorbed fairly quickly as they penetrate dense materials. For food products with densities similar to water (1 g/cm^3), two-sided treatment with electron beam will penetrate through approximately 3.5 inches. However, in reality, packages with depths much greater than 3.5 inches can be decontaminated or disinfested with e-beam because most commercially packaged foods have a lower overall density than water. A 5-10 MeV Electron Accelerator based irradiation facility for food and agriculture products has been installed at one vegetable market in Indore by RRCAT [91]. The

klystron specifications for this accelerator are almost same as stated above for BARC system except a slight increase in its average power (25 kW).

(iii) Accelerator Driven Sub-critical System:

Accelerator Driven Subcritical Systems (ADSS) are being conceived as possible solutions to the problem of shortage of fissile material in the country and stockpiling of long lived nuclear wastes. In this case, proton/deuteron beams having energy in the range of 1-2 GeV & power of a few tens of a MW, are allowed to strike the Pb or Bi target, externally. The intense flux of neutrons thus produced through spallation mechanism can be used either for fission of the fissile material for producing power, or converting the fertile material into a fissile one and for transmutation of the long lived nuclear wastes into short lived one. One such type of proton accelerator with 1 GeV beam energy and beam current more than 10 mA is under development at BARC [92] which will require 352.2 MHz klystrons with power level in the range of 1 MW CW, as RF source for the particle acceleration.

(iv) Treatment of pathogenic germs:

Food and agricultural products are treated with ionizing radiation to accomplish different objectives like reduction of pathogenic bacteria and parasites that cause food borne diseases; or lengthening the shelf-life of fresh fruits, vegetables by decreasing the normal biological changes associated with growth and maturation processes, such as ripening or sprouting. Radiation processing of food has become important due to mounting concern over food born diseases, and growing international trade in food products that must meet stiff import standards of quality and quarantine. A 10 MeV, 10 kW Linear accelerator based electron beam radiation processing facility for agriculture use [91], [93] is being set up at RRCAT, Indore with S-band klystron as power source.

In the field of medical science for cancer treatment medical linac machines are being used which replace cobalt-60 machines used earlier but now phased out in many countries and the klystron is being used as power source in these machines. SAMEER, Mumbai is developing such medical LINAC's using klystron and magnetron as RF source [94]. The magnetrons are being used in the existing 4-6 MeV LINAC's whereas klystrons will be used in the upcoming 15 MeV or higher energy level machines, the operating frequency of RF sources in these medical linear accelerators is 2998 MHz.

1.3 **Klystron History and New Trends in Technology:**

Considering all above national needs, there is huge requirement of various types of klystron with increased power level along with improved performance features such as efficiency, gain and its compactness etc. Although many of these requirements are fulfilled by import but considering the strategic importance of these devices and for some customized applications, a dedicated research for indigenous developments in this area is being pursued at few laboratories in India. CSIR-CEERI, Pilani is one of the leading institutes among them.

Historical Timeline of Klystron: The invention of the klystron was the result of work done by many people [85], the very first of them was D.A.Rozhansky, a Professor of Physics at the Leningrad Polytechnic Institute, Russia who gave an idea for producing electron beams of varying density in 1932 but did not publish. Later in 1934, the first paper [95] on velocity modulation and electron bunching was published in a Springer Journal by Heil and Arsenjeva. However the research done by them was not converted into a physical device.

The invention of klystron had not been possible without invention of a microwave resonator for which the credit goes to W. W. Hansen, an Associate Professor of Physics at Stanford University, who published a paper in the Journal of Applied Physics with the title "A Type of Electrical Resonator" in 1937 [96].

In the same year Varian Brothers invented first 'two cavity klystron' using the Hansen cavity along with their own concept of velocity modulation. The device was named "klystron" by the Stanford Classics Department, after the old Greek verb (κλύζω) which means 'waves washing on the seashore' [97].

The research and development of most of the microwave tubes including klystron was very intense during World War II period due to their extreme importance in Radars and many other high power microwave applications in military. But the 'Power Klystrons' were not available during WWII due to lack of adequate beam optics. Later with improvements in electron beam optics after the work done by J. R. Pierce at Bell Labs [98] and many other critical components designed for the first time like high-voltage modulators and insulators, in 1948, the Stanford klystron having three cavities and wound-on electromagnet for beam-focusing eventually reached a power output of 30 MW with 1-microsecond pulses. It was the first microwave source with multi megawatt power and was used for the S-Band Mark III electron accelerator. The following Fig. 1.11 shows the growth of klystron [86] device over the years. Today, scientific high-energy particle accelerators are setting the pace in the development of very high-power klystrons. The "Next Linear Collider" (NLC) is designed, initially, as a 500-GeV collider (of

30 km. length and requiring 4000 klystrons of 75 MW peak power) and ultimately a 1-TeV e^+e^- machine. In parallel to increasing power and frequency, the research on EIK, multi beam and sheet beam versions of klystron is also ongoing.

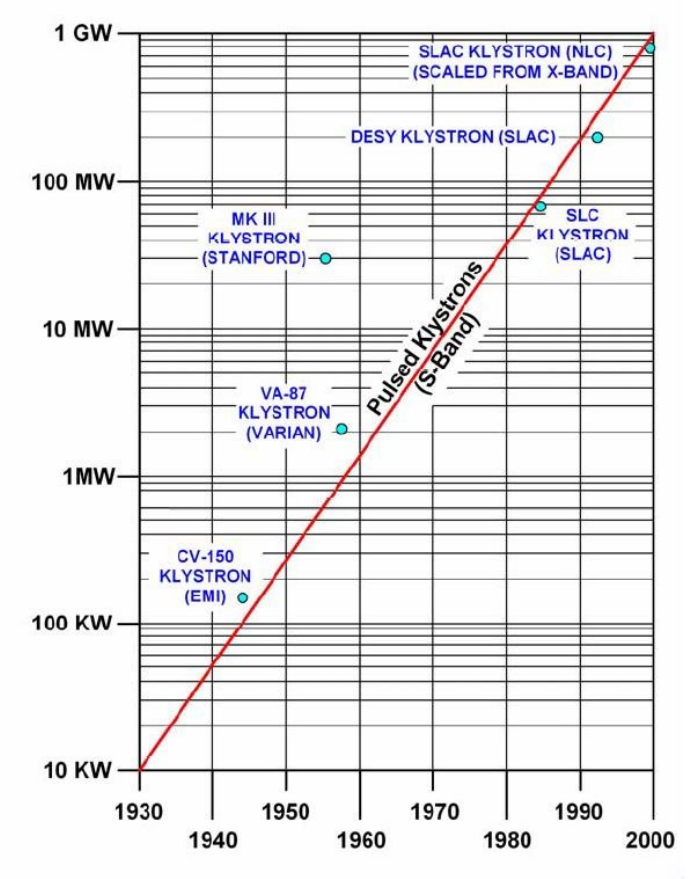

Fig. 1.11: Klystron power growth over the years since its invention (*Source: High Power Klystrons: Theory and Practice at the Stanford Linear Accelerator Center, G Caryotakis)*

Limitations of single beam klystron:

In a single beam klystron, a low perveance (ratio of beam current to 3/2 power of beam voltage), high voltage beam must be used to get high power with good efficiency and that is likely to lead to reduce reliability because of voltage breakdown. For obtaining high power, if we take the low voltage to avoid the voltage breakdown, we have to use the high perveance. Because of high perveance of the beam, the space charge repulsion will be higher so as to affect the bunching of electrons resulting in poor amplification of RF and loss in efficiency. The solution of the problem may be to use multiple low perveance electron beams in a single interaction structure i.e. multiple beam electron gun followed by multi-beam cavity. A cut section of these type of computer simulated electron beam structures is shown in the Figure 1.12 and corresponding cavity is shown in Figure 1.13.

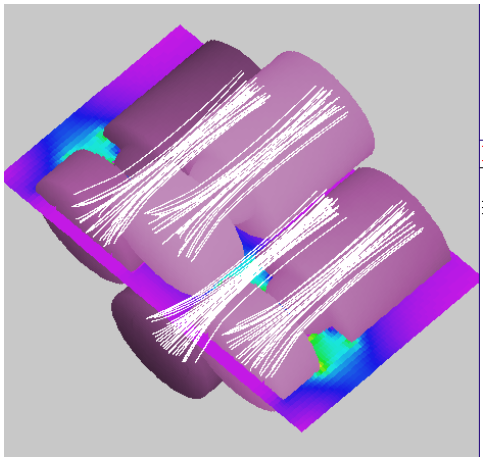

Fig. 1.12: A multi beam electron gun

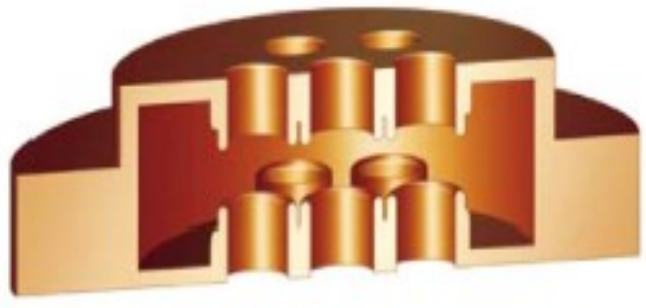

Fig. 1.13: A multi beam klystron cavity

Multi Beam Klystron:

In multi-beam Klystron (MBK), several electron beams are used to interact with the RF signal in a single interaction structure. MBK provides a number of advantages over single beam klystron.

- The operating voltage is reduced significantly (2 to 10 times) with a consequent reduction in the dimensions and weight of the devices and their power supplies.
- The current and perveance of the individual beam are not high but the total current and perveance of the entire multi-beam stream can be high. The lower perveance of individual beams results in higher efficiency.
- The individual low perveance beams are better focused and bunched and give up their energies to the field of the resonator in an efficient manner resulting in an excellent performance
- The increased reliability of the HV power supply and smaller size at a given power level with fewer risks of gun arcing and also possible increase in pulse length.

The key challenges for the multiple-beam approach are the issues of beam generation and transport therefore design of multi-beam electron gun is a critical task in MBK, due to focusing required for multiple beams in a single interaction structure.

The disadvantage of MBK is that it requires separate drift tube for each beamlet which makes the fabrication difficult for large number of beamlets and at higher frequencies where the device size is smaller. This leads to the development of Sheet Beam Klystron (SBK). SBK is nothing but MBK with the beamlets arranged linearly to form a sheet. Thus it comprises all the advantages of MBK except a change in its geometry from cylindrical to planar geometry.

Sheet Beam Klystron:

SBK is expected to give better performance in both high and low frequency regimes. The working of sheet beam klystron is similar to that of conventional two cavity klystron but the only difference is that here rectangular beam is used instead of cylindrical beam. As a result, both the surface area and the cross sectional area are increased. For example, 11.4 GHz and 100 MW peak power klystron designed with sheet and cylindrical beam has the following parameters shown in Figure 1.14. The sheet beam shown here is not an exactly unrolled geometrical version of the cylindrical beam but it only indicates that how beam cross section can be increased while converting a cylindrical beam into a sheet beam. The beam area given here is taken from the referred paper for comparing the cylindrical and sheet beam klystron having same output power and frequency.

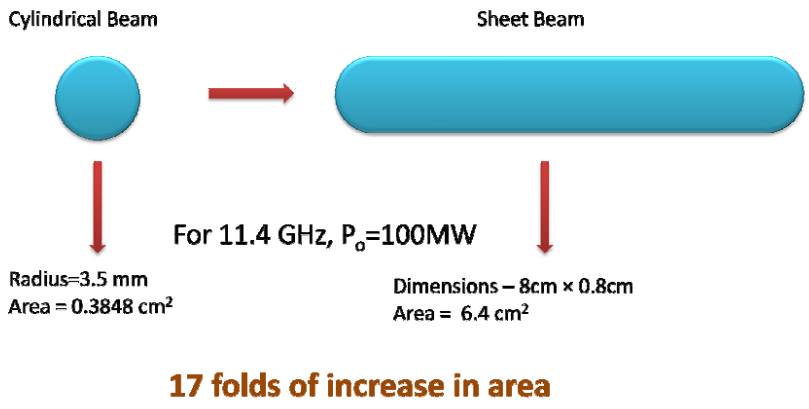

Fig. 1.14: Sheet beam Vs cylindrical beam

(Ref: A sheet beam klystron paper design, G Caryotakis)

The advantages of using the sheet beam are:

1. Increased beam surface area: The number of electrons exposed to the field is increased and hence the beam wave interaction is more efficient

2. Increased beam cross sectional area, therefore:

- reduced current density
- increased current for the same voltage
- reduction in the necessary Brillouin field

3. Power scales down in cylindrical beam klystron as $1/f^2$ but in sheet beam klystron the power scales down as 1/f where f is operating frequency.

Thus SBK is a promising device in the high frequency regime for certain applications where the huge Gyrotrons cannot be installed but there are certain issues in the development of sheet beam klystron as described below:

1. Need to generate high aspect ratio sheet beam: The high aspect ratio sheet beam as the name suggests needs non uniform electron optics for the formation of such a beam.

2. Ideal focusing structure for the sheet beam: The off axis beam i.e. beam offset from the central axis will always face difficulty in focusing due to the axis symmetric field provided.

3. The issue of 'diocotron instability' is another major challenge in propagation of a sheet beam. Space charge forces at the beam edge and axial magnetic field give rise to (E x B) drift, the drift has opposite direction on either ends of the beam width. This shear stress induces 'diocotron instability' which tries to break the beam. Finally with time a rectangular beam is transformed into an elliptical beam and then circular in the worst case.

4. Designing an efficient RF interaction structure: The RF structure should provide uniform field to the overall cross section of the beam. Developing such a cavity becomes a critical task, such cavities are also over-moded which makes the design further critical.

5. Requirement of extremely precise fabrication: Dimensional tolerances are generally of the order of 10^{-3} λ which at millimeter wavelength requires micrometer tolerances. This needs high precision machining techniques and good fabrication skills.

Extended Interaction Klystron (EIK):

A problem common among many of the approaches providing high RF power, is the extremely high RF gradient in the output circuit, which presents an obstacle to long-pulse operation. RF breakdown is a function of frequency and pulse duration. The presence of a high-density electron beam traveling through the interaction gaps of the output structure in these devices adds to the severity of the problem. The problem gets more difficult when the pulse width is increased. Attempts to solve this high-peak-power, repetitive, long-pulse problem involved some sort of extended interaction mechanism, in which extraction of RF power at output cavity is split over multiple gaps. The multi-gap RF circuit has a simple, rugged geometry and is characterized by its high impedance [99]. This supports efficient modulation and energy exchange between the RF field and the electron beam over a broad instantaneous bandwidth. While comparing an extended interaction cavity with a single gap output cavity, of course, the bandwidth is increased but more important is the fact that the power-handling capability is increased because the total output voltage, which would be applied across a single gap in a conventional klystron, is divided among the multiple gaps in the extended interaction structure [40]. Fig. 1.15 shows a five gap interaction structure in comparison with a single gap klystron cavity.

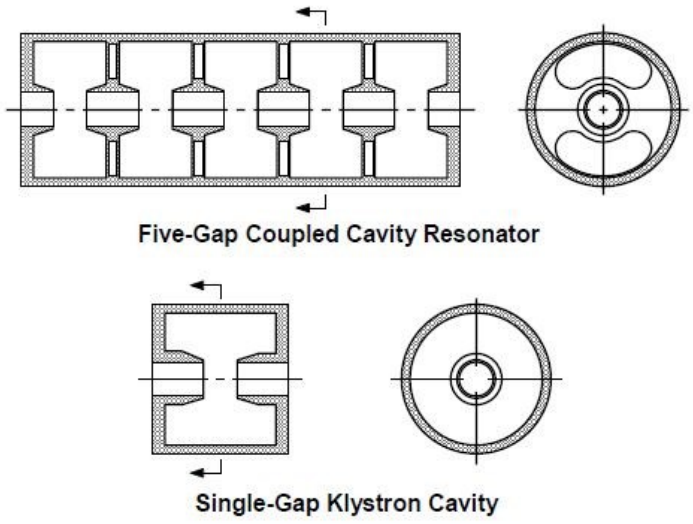

Fig. 1.15: Five-gap Vs Single-gap Klystron Cavity

(Source: A.S Gilmour, Klystons, TWTs, Crossed-Field Amplifier and Gyrotrons)

The EIK is an optimum blend between the klystron and coupled-cavity TWT technologies achieving high peak power, efficiency, bandwidth and reliability at millimeter and sub-millimeter frequencies. However now a days most of the research work for EIK is being carried out in sheet beam klystron technology.

In summary, the following figure 1.16 summarizes the different phases of trends in klystron technologies.

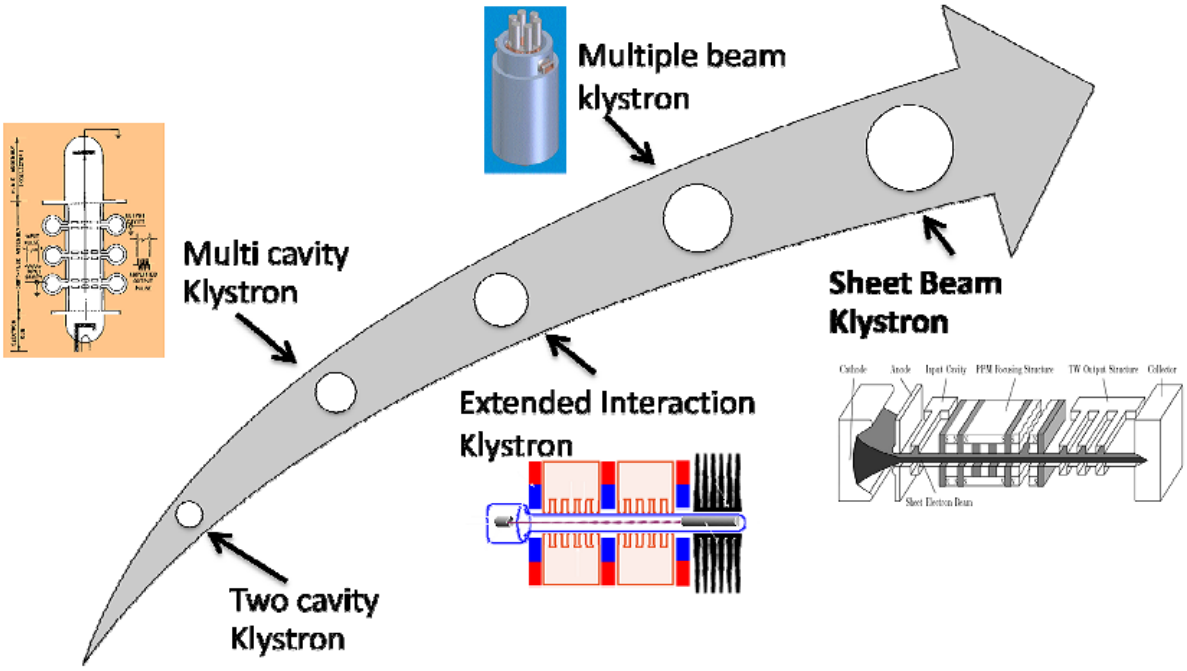

Fig. 1.16: Various phases in the Klystron technology

Current status of MBK development:

A wide variety of medium to high power multi-beam klystrons have been developed in Russia in various frequency ranges (ranging from L to Ku band). The U.S., France and Japan have industrial programs to develop high power multiple beam klystrons for accelerator and X-ray Free Electron Laser (FEL) applications.

Fig. 1.17 shows TESLA Linear Collider multiple-beam klystron (MBK), TH1801, made by Thales Electron Devices, France. It uses seven beams having each beam micropervance equal to 0.5, propagating into separate drift tubes but with common RF cavities. A common collector is used to collect the beam after extracting their energy at the output cavity gap. The operating frequency of the device is 1300 MHz and the power output is 10 MW (peak), 150 kW (average) with the maximum pulse duration of 1.5 milliseconds [86].

Fig. 1.17: The Thales MBK **Fig. 1.18: The CPI MBK**

(*Source: High Power Klystrons: Theory and Practice at the Stanford Linear Accelerator Center, G Caryotakis)*

Fig. 1.18 shows CPI VKL-8301, which was built for TESLA to the same specification. It is also a multi beam klystron, but its design is fundamentally different. This device employs six beams, on a larger "bolt circle" and without a centre beam. In comparison to the Thales MBK, this arrangement employs individual intermediate cavities and hence facilitating the use of larger cathodes and lower cathode current densities. This has resulted in a longer life of the VKL-8301 than the TH1801 [86].

Toshiba, Japan has supplied E-3736 multi beam klystrons at 1.3 GHz, 10 MW/150kW for Tesla Technology Collaboration, DESY, Germany and for European X-FEL project [100-101].

Recently Chinese have reported the design of a 40 beam C-band klystron at 5.71 GHz delivering 4 MW peak power with 80% efficiency [102]. Earlier Institute of Electronics, Chinese Academy of Sciences (IECAS), China has developed many types of multi beam klystrons for frequency range L to Ku band with different power level [103-104] i.e. KS4116A S-band MBK, KC4079L C-band MBK, KX4127 X-band MBK etc.

In Indian context Research and development program on multi beam klystrons has been recently started. CSIR-CEERI and DRDO-MTRDC are mainly working in this field.

Current status of SBK development:

Though the concept of SBK was first proposed by Kovalenko in 1937, till now the commercial availability of such tubes is not reported although some research institutions have developed and tested few lab prototypes of sheet beam klystrons. The continuing research in this area is quite promising and gives consistent encouragement towards the successful development of this device. Round the globe intense research is being carried out for SBK at all frequency as depicted in Figure 1.19.

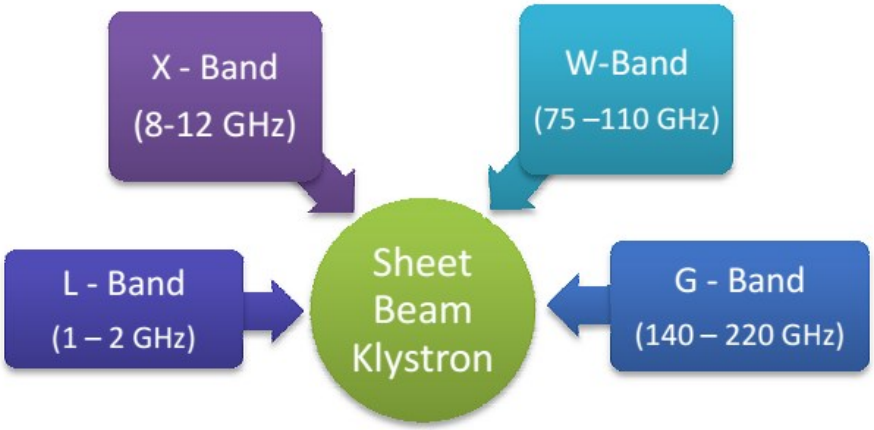

Fig. 1.19: Frequency bands over which the SBK research is being carried out

Sheet beam klystron is a promising device for the future need of higher power at higher frequency and many organizations like Stanford Linear Accelerator Center (SLAC), Calabazas Creek Research (CCR), US Naval Research Laboratory (NRL), Institute of Electronics Chinese Academy of Science (IECAS) etc. are working in this research area and a number of research papers from these institutes are available after their findings.

At SLAC, the logistics of the Next Linear Collider (NLC) initially required several thousand 75-MW X-band klystrons for the 500 GeV versions of the machine. The baseline NLC klystron has a pulse length of approximately 3 microseconds and the number of PPM-focused klystrons is approximately 1600, which is a large number of fairly complicated tubes. A klystron with twice the output would be very desirable, especially if a 1-TeV NLC were to be considered but 150 MW peak and a 50 kW average power at 11.4 GHz is uncomfortably high with a single beam therefore SLAC had invested a lot of research into the design and development of a sheet beam klystron (SBK) at 11.4 GHz/ 150 MW and developed it successfully [105-106].

As said above that 'The Institute of Electronics, Chinese Academy of Sciences' has also worked for the above specified klystron with same power level and frequency [107-108] and they are also working for W-band klystron with power level of 30 kW. It has been reported

recently [109] that their X band SBK was tested at CPI in 2009 and W-band SBK has been tested in NRL in 2013.

Apart from this SLAC has developed and tested 10 MW, 1.3 GHz SBK [110] for International Linear Collider (ILC), W- band SBK having 100 kW peak power with 2% duty [111-112] and is currently continuing research for a S-band SBK at 2.1 GHz for U.S. Navy's FEL source [113-114].

1.4 Objectives and Goals to be Achieved

The objective of the proposed research work is to investigate the different design aspects of the above said klystron technologies. This study will be carried out through following steps:

(i) Analytical design through available literature
(ii) Simulation through software tools
(iii) Design optimization for the given specification
(iv) Development of few structures
(v) Characterization of the developed structure

The goals for the proposed research work have been set as follows:

(i) Design of a multi beam electron gun
(ii) Design of focusing structure for the multi beam transportation
(iii) Beam wave interaction simulation in multi beam interaction structure
(iv) Design and development of multi beam RF cavity and its characterization
(v) Design and development of a sheet beam cavity and its characterization

An overview of the work: The specifications for the target multi beam klystron has been chosen around one L/S band klystron with projected applications in the field of communication systems for defense forces. The motivation behind the present research work is to design an improved version of an existing 1 kW CW power L/S band klystron already developed at CSIR-CEERI [115]. The new version requires 2 kW CW power with increased bandwidth and efficiency. The conventional design with single beam approach has not been able to meet the improved performance features therefore a multi beam design approach has been adopted. A five beam electron gun has been designed and simulated using some commercial software tools such as CST Studio Suite, Opera and Trak etc. The initial design parameters are derived with some analytical formulas available through literature and optimization of parameters is carried

out through computer codes. The design of a compatible five beam RF cavity also has been carried, the cavity has been fabricated and characterized for its resonant frequency. Further the beam wave interaction study for this klystron has been carried out. A sheet beam klystron cavity also has been designed and fabricated, the resonant frequency for sheet beam cavity has been measured.

In addition, a complete design of a low frequency high CW power klystron (single beam) has been also completed as a part of another ongoing development activity of a 352.2 MHz 100 kW CW power Klystron at CSIR-CEERI. The experimentally measured results of electron gun for this klystron are presented. Later a multi beam version of this experimentally validated electron gun is also designed and cross-validated through different codes. The publications brought out during the course of this research are listed in Annexure I.

The specifications for the proposed L/S band Klystron are as given in Table 1.1.

Table 1.1: L/S band Klystron Specifications

Quantity	Value
Operating Frequency (Tunable)	1800-2200 MHz
Output Power	2 kW CW
Efficiency (proposed)	40% (min.)
Bandwidth	>15 MHz
Number of Beams	5

As reported in previous section that the main challenges for the multiple-beam approach are the generation and transportation of multiple electron beams therefore the design of electron gun is the most difficult task in the design of a multi beam klystron, due to focusing required for the off-axis multiple electron beams in a single interaction structure.

Several approaches have been used for focusing in MBK;

The article [116] of A.V.Malykhin, P.V.Nevsky, V.I.Pasmannik, E.P.Yakushkin, "High-power multi-beam klystron with reverse magnetic focusing system" suggests usage of higher order modes in the RF cavities allowing larger space for the multiple (18) cathode emitters which in turn allows lower cathode loading. They also use some sort of reverse magnetic field to ensure magnetic focusing. They also use a screen to magnetically isolate the cathode. The

main drawback in their design is the positioning of the screen is very critical for proper beam transport. Moreover, due to the presence of the neighboring modes the available bandwidth of the device may be compromised.

The article [117] of Bernard Vancil, Robert Mueller, Kenneth W. Hawken, Edwin G. Wintucky and Carol L. Kory, "A Medium Power Electrostatically Focused Multiple-Beam Klystron" suggests to focus the electron beam electrostatically thereby eliminating the complete magnetic focusing system. The drawback in this concept is multiple power supplies are to be used for realizing of these device and suitable electrical isolation should be provided between different sections of the device. Thermal management and ruggedness of this type of device is another serious limitation of this concept.

Reference may be taken from the article [118] of Ashok Nehra, L.M. Joshi, S. Kaushik and R.K. Gupta, "Effect of Aperture in a Pole Piece for Focusing of Multi Beam Electron Gun" which suggests the use of square aperture of the pole-pieces for interception less beam transport. In this approach also the position of the pole-piece becomes a critical issues for proper beam transport. From the fabrication point of view, cutting exactly square pole-pieces and alignment of the same may become a bottleneck especially when the number of beams are high.

The reference [119] of the US patent US 6768265 B1 suggests the electron beam formation from cathodes which have their own electrostatic (Beam Focusing Electrode (BFE) as well as magnetic focusing structure via pole piece shaping and confined flow. In this case also the positioning of the pole-piece in front of the cathode as well as shaping of the pole-pieces are critical.

Reference [120] can be made to the US patent no US 7005789 B2 which suggests the usage of confined flow in the case of multiple beam klystrons via usage of a flux equalizer, which essentially equalizes the magnetic flux of the off axis electron beams. This approach allows one to use confined focusing of the electron beam but add to the complexity of the design and shaping of the pole-pieces, i.e. the flux equalizer.

Pub. No.: US 2013/0229109 A1 suggests the usage of cathode emitters [121] placed along a particular PCD in a Multibeam electron gun. However here also the pole-piece is placed after the cathode and have the similar criticality of placing the pole-piece at a particular location.

The Approach and Methodology:

The main objective of the present work is to suggest a technique for focusing of electron beams in a multi beam klystron provided that the emission surfaces are planar. Conventionally spherical cathodes are used in most of the microwave tubes to get the increased electron emission density and the electromagnet along with pole pieces at both ends with fixed locations, is used to achieve the required magnetic field along the beam axis. Normally the electron gun side pole piece is located between the cathode and anode to shape the magnetic field lines. However we have presented a five beam electron gun design compatible to a L-band klystron with an output power of 2 kW. The electron gun uses five planar emission surfaces along with a BFE cup surrounding the emission region for shaping of the electron trajectories. A metallic cylinder with five drift tunnels cut through it, is defined as an 'anode cum drift region' to observe the beam propagation and the electromagnet is placed surrounding the structure.

The soft iron pole pieces, to limit the magnetic field lines are put at both ends the of electromagnet. However the electron gun side pole piece has been put behind the cathode instead in front of the cathode location (as is conventional practice) on the beam axis. Also the pole piece has five apertures cut through it with same diameter as the drift tunnels to match the latter. The 3D simulation of this five beam electron gun has been done and optimization has been carried out to achieve the desired beam current without any interception along any of the drift tunnels.

A major advantage of the approach used is that the pole piece location behind the cathode is not much sensitive while the pole piece location between cathode and anode is very much sensitive and it must be placed at an accurate plane there.

For carrying out the design study as per the defined objectives, several simulations have been performed after some analytical estimation. There are several commercial codes available at CSIR-CEERI which have been utilized for optimization of our designed structures i.e.

- CST Studio Suite
- AJDISK
- MAGIC
- ANSYS
- OPERA

A brief introduction of these codes have been listed in Appendix 3.

1.5 Organization of the Thesis

The thesis is organized as follows; Chapter 1 starts with an overview of Microwaves and its applications. Various types of sources for generation and amplification of microwaves with different types of applications have been covered then specifically a klystron amplifier has been discussed in detail. The current and future trends in klystron technology have been discussed. Chapter 1 concludes by defining the objective and goals for the research work reported in the thesis. Chapter 2 presents initially the conventional approach while designing a single beam klystron including analytical formulas from literature followed by design approach of multi beam klystrons. The conversion of existing single beam klystron parameters into a multi beam klystron with similar performance parameters have been presented. The simulation results of few multi beam RF cavity structures are presented. Chapter 3 starts with the design of an electron gun for the proposed L/S band multi beam klystron and its optimization. Initially the design of gun has been carried out by applying an analytic magnetic field, there after an electromagnet has been designed. The design of electron gun along with electromagnet has been presented followed by the sensitivity analysis of magnetic field.

Chapter 4 presents the design and simulation for a compatible multi beam RF cavity for the above said electron gun followed by its development and characterization results. Chapter 5 starts with modelling of RF interaction structure after finalizing the design of RF cavity, the RF interaction structure has been optimized with CST code so as to give the desired output power and hence concluding design study of the multi beam approach.

Chapter 6 gives an introduction about the sheet beam klystron technology and its main challenges, a sheet beam klystron cavity has been simulated and optimized. The results of cavity frequency measured on its cold test model are also presented.

In the last, chapter 7 gives some insight into the complete design of a conventional single beam klystron of 100 kW output power at 352.2 MHz which is an ongoing development activity at CSIR-CEERI. Some of the experimental results under this activity are also presented.

Finally the thesis has been concluded along with a note on future work which may be carried out further after the presented work.

CHAPTER 2
STUDY OF DESIGN PARAMETERS FOR A MULTI BEAM KLYSTRON

A microwave tube is mainly specified by its operating frequency, output power, gain, bandwidth and efficiency. Generally in all microwave tubes DC voltage is used for accelerating electron beam and kinetic energy/potential energy of the beam is used for microwave generation or amplification depending upon the nature of interaction in the device. The efficiency signifies the 'figure of merit' for this interaction and if input RF power is given to the device (in case of an amplifier) then another parameter 'gain' comes into picture as a ratio of output and input RF power. The term 'bandwidth' tells about the frequency band over which the device is capable to provide output power within specified level. Therefore efficiency, gain and bandwidth are the performance parameters of the device and their optimization may be required as per user's demand along with target output power at the desired frequency. The design of any microwave tube mainly involves following steps:

(i) The generation and transportation of the electron beam i.e. the design of electron gun along with focusing mechanism

(ii) The interaction of the electron beam with RF field i.e. optimization of beam wave interaction process

(iii) The design of input and output RF couplers

(iv) Collection of the spent beam i.e. Structural and thermal design of collector

2.1 Design Parameters of a Single Beam Klystron:

The design of a conventional klystron includes the design of electron gun, design of RF cavity (re-entrant type) followed by beam-wave interaction simulation and thermal design of collector as mentioned earlier. Later in Chapter 7, a complete design study for a single beam 352.2 MHz, 100 kW power klystron is presented.

Design of Electron Gun parameters: The parameters involved with electron gun design are beam voltage, beam current and beam radius. The required output power along with target efficiency will give the DC input power of the device; then an appropriate combination of beam voltage and beam current is chosen as per the chosen perveance of electron gun and power supply parameters. Once the beam voltage is fixed then depending upon the frequency of operation of the device, the drift tube (beam tunnel) radius can be calculated as shown in the

design of RF cavity section. The beam radius can be computed thereafter based upon the fill factor of the tube.

Design of RF cavity and interaction structure: The parameters required for initial design of a re-entrant cavity are drift tube radius, gap length, cavity height and cavity diameter. There are conflicting conditions in deciding the 'gap diameter' and 'gap spacing' , while for good interaction both the parameters should be small compared with the transit time of electron through gap, a too small gap diameter imposes severe complication due to higher beam interception. There is possibility of RF voltage breakdown in case of a narrow gap. Therefore both the parameters are to be decided keeping the set specifications in mind. Once the gap and drift tube dimensions are fixed, other dimensions of the cavity such as diameter and height are decided to get desired resonant frequency. Small gap reentrant type resonator oscillates when its height is somewhat less than $\lambda/4$. The height of cavity is chosen such that it is less than $\lambda/4$ over the whole frequency range of operation [3].

The gap spacing is given by the relation $\beta_e d = 0.9$ where β_e is the electron wave number [2], [3]. The drift tube radius can be taken [122] as $1/\gamma$ as a first approximation (γ= wave propagation constant), later it can be optimized with software.

Computation of Parameters for RF Section:

- **Size of the cavity:** For cylindrical cavity, the relation between the resonant frequency of TM_{nml} mode and radius is given by [12] :

$$f_r = \frac{1}{2\pi\sqrt{\mu\varepsilon}}\sqrt{\left(\frac{X_{nm}}{a}\right)^2 + \left(\frac{l\pi}{d}\right)^2} \qquad \text{(Eq. 2.1)}$$

  where, μ is the dielectric permeability of medium and ε is the dielectric permittivity of medium

  X_{nm}= m^{th} root of Bessel function $J_n(x)=0$, such that $J_n(X_{nm})=0$

  a= radius of cavity; l= length of cavity; d= diameter of cavity

  For rectangular cavity, the equation is:

$$f_r = \frac{1}{2\pi\sqrt{\mu\varepsilon}}\sqrt{\left(\frac{n}{a}\right)^2 + \left(\frac{m}{b}\right)^2 + \left(\frac{l}{c}\right)^2} \qquad \text{(Eq. 2.2)}$$

  Where a, b, c are the dimensions of the cavity along x, y and z directions respectively

- **DC Electron Velocity (u_0):** This is the velocity with which the electron beams are accelerated from the cathode to the interaction structure. The velocity is given by

$$u_0 = \sqrt{2\,\frac{e}{m}\,V} \qquad \text{(Eq. 2.3)}$$

Putting e= 1.6x10^{-19} C and m=9.1x10^{-31} kg, we get $u_0 = 0.593 \times 10^6 \sqrt{V_0}$ m/sec.

- **Electron wave number (β_e):** It is the ratio of the angular frequency and dc velocity of the electrons.

$$\beta_e = \frac{\omega}{u_0} \qquad \text{(Eq. 2.4)}$$

- **Wave Propagation Constant** $\gamma = \sqrt{(\beta_e^2 - k^2)}$ (Eq. 2.5)

  where k= free space wave number = $2\pi f/c$ (Eq. 2.6)

- **Drift tube radius (a):** It is taken as the inverse of the electron wave number. It is given by

$$a = 1/\gamma \qquad \text{(Eq. 2.7)}$$

- **Beam radius (b):** For proper beam transport, the beam fill factor (i.e. ratio of beam radius to drift tunnel radius) of 60-70% is considered.

$$b = 0.7 \times a \text{ (for 70\% filling)} \qquad \text{(Eq. 2.8)}$$

- **Charge density (ρ):** The charge density in the electron beam is expressed as

$$\rho = \frac{I}{\pi b^2 u_0} \qquad \text{(Eq. 2.9)}$$

where, I = beam current

- **Plasma frequency (ω_p):** Due to space charge effects, the electrons oscillate between the bunches. The frequency with which they oscillate is known as electron plasma frequency. The expression for plasma frequency is only applicable to a beam of infinite diameter. It is given by

$$\omega_p = \sqrt{\frac{e\rho}{m\varepsilon_0}} \qquad \text{(Eq. 2.10)}$$

where, ε_0 is the permittivity of free space. Its value is 8.854x10^{11} farad/m

- **Reduced plasma frequency (ω_q):** Due to boundary imposed on the electron beam by the drift tube walls in the longitudinal direction, the natural plasma frequency is disturbed and we obtain the reduced plasma frequency expressed as

$$\omega_q = \text{Plasma reduction factor} \times \omega_p \quad \text{(Eq. 2.11)}$$

where plasma reduction factor may be taken from empirical curves [3], [75]

Additionally, we define the reduced plasma wavelength (λ_q) as

$$\lambda_q = \frac{2\pi u_0}{\omega_q} \quad \text{(Eq. 2.12)}$$

- **Length of drift tube (L):** The cavities are placed at those locations along the drift tube, where the electron bunches are most intense. The length of the drift tubes between the cavities is given by

$$L = \frac{\lambda_q}{4} \quad \text{(Eq. 2.13)}$$

Once the parameters of a klystron RF cavity are computed then by iterative simulation process all parameters are optimized to get the desired performance parameters of RF cavity like its frequency, 'Q' and shunt impedance. The input and output cavities are separately designed and simulated along with RF coupling mechanism. Later on the complete RF interaction structure is simulated to optimize the beam wave interaction process through iterative simulation so as to achieve the desired performance parameters of the device like its gain and efficiency etc. by varying the different cavity parameters and their mutual spacing.

Thermal design of collector: The main function of collector is to collect the spent beam. The electron beam that acquires kinetic energy through the acceleration in the gun, delivers part of its energy to RF field in the process of interaction in the RF section. The final energy exchange takes place in the output cavity. The collector is placed next to output cavity. The energy still left in the beam, which depends on the efficiency of RF interaction, is allowed to be dissipated on the collector resulting in heating of latter. The collector is designed to remove the heat efficiently thus produced [123]. Also electrons impinging the collector surface may produce secondary electrons, which under favorable conditions, may travel towards RF interaction region resulting in instabilities and other undesirable effects. It is therefore necessary to design the collector so as to trap the secondary electrons in the collector itself. Thermal design of collector is done through computational code like ANSYS under varying flow conditions of the cooling liquid so as to limit the collector surface temperature in safe zone.

2.2 Derivation and Selection of Multi Beam Design Parameters:

In Multi-beam Klystron (MBK), several electron beams are used to propagate and interact with the RF signal in a single interaction structure. As it uses many lower perveance beams, while overall perveance is same as of the single beam device, the beam voltage is significantly lower (for same DC input power) than single beam klystron. This results in an increased reliability of the HV power supply and smaller size at a given power level with fewer risks of gun arcing and possible increase in pulse length. The device efficiency also will be higher with lower perveance of individual beams. Design of multi-beam electron gun is the most difficult task in the MBK design process due to the focusing required for the off-axis multiple beams in a single interaction structure.

Some initial work at CSIR-CEERI, towards multi beam klystron was based on the approach by using multiple single beam gun structures configured in a periodic circular manner and propagating these beams through a multi beam cavity. However it has been found that to fabricate multiple electron guns in a single envelope but without changing the electrical parameters of design, will make no sensible advantage of the multi beam approach. The beam voltage per beam-let in the multi beam structure should be reduced according to the number of beams taken so as to take advantage of lower operating beam voltage. Considering this we have computed the design parameters of a multi beam klystron by deriving them from their single beam counterpart by following some scaling laws, reported in a published paper [124]. These laws relate the electron beam parameters such as beam voltage, beam current etc. of the single beam device and its equivalent multi-beam device respectively, depending upon the number of beams chosen for the multi-beam design. The beam voltage and beam current parameters for the desired N-beam klystron i.e. V_{MBK} and $(I_b)_{MBK}$ will be given by the following conversion formulas where N is the number of beams and 'J' represents the beam current density. Similarly V_{SBK} and $(I_b)_{SBK}$ are the beam voltage and current in the single beam design. The suffix '1' in Equation (2.16) denotes the *beam current density per beamlet* of MBK.

$$V_{MBK} = \frac{V_{SBK}}{N^{\frac{2}{5}}} \qquad \text{(Eq. 2.14)}$$

$$(I_b)_{MBK} = (I_b)_{SBK}\, N^{\frac{2}{5}} \qquad \text{(Eq. 2.15)}$$

$$(J_1)_{MBK} = (J)_{SBK}\, N^{\frac{2}{5}} \qquad \text{(Eq. 2.16)}$$

After converting the beam parameters for the both klystron specifications the RF cavity parameters can be derived by the same procedure as stated above but now there will be N drift tubes with N gaps in a single cylindrical cavity. Accordingly the converted parameters are used for simulation of the multi beam cavity and optimized through iterative simulation process. The scaling laws use following assumptions [124];

(i) The perveance of a single beamlet in the multiple-beam klystron is the same as the perveance of the entire beam in the single-beam klystron;
(ii) The power and efficiency of the multiple-beam and single-beam klystrons are identical;
(iii) The electron current density in both cases is limited by space charge effects.

Once the beam parameters are found using scaling laws with a chosen value of N (number of beams in the multi beam design), the placement of drift tubes in the cavity is another point of consideration.

Depending on the geometry of the resonators, the MBKs fall into two groups [40]:

i. Fundamental mode MBK (FM MBK) (Figure 2.1)
ii. Higher order mode MBK (HM MBK) (Figure 2.2)

Advantages of FM MBK:

a. Large instantaneous bandwidth can be obtained.
b. A large number of beams can be used, so operating voltage can be kept low.
c. Beam focussing is easier.

Disadvantages of FM MBK:

a. Cathode loading is high because beams are close together.
b. Limited life of cathode for high loading.
c. Limited peak power at shorter wavelengths (3 to 4 cm).

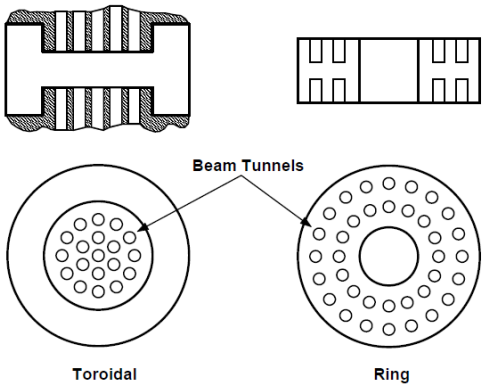

Fig.2.1: Cross section of FM MBK *(Source: A.S Gilmour, Klystons, TWTs, Crossed-Field Amplifier and Gyrotrons)*

The ring type FM MBK cavity is a modification to the toroidal cavity for obtaining increased pulse power. The main advantage is that a large number of cathodes can be placed at concentric rows at large diameters. We have used this configuration.

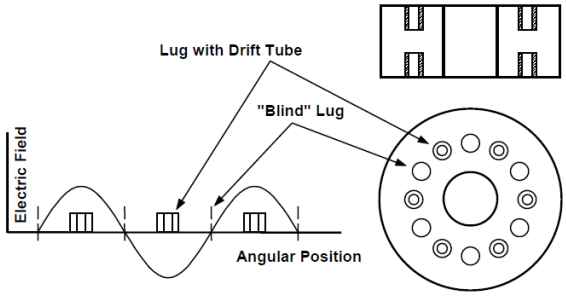

Fig. 2.2: Cross section of HM MBK *(Source: A.S Gilmour, Klystons, TWTs, Crossed-Field Amplifier and Gyrotrons)*

Advantages of HM MBK:

a. Low loading effect on the cathode.
b. Devices can be operated at higher power levels because of large separation between beams.

Disadvantages of HM MBK:

a. Bandwidth is very narrow.
b. Difficult beam focusing as the distance of the beams from the center increases.
c. Mode separation between higher order operating mode and neighboring mode is small, which interfere with the state of the operating mode.

Therefore after choosing an appropriate topology of drift tunnels, the simulation of RF cavity is carried out in a suitable 3-D computer code to find out the desired cavity parameters by variation in cavity radius and multiple gaps. Similarly the multi beam electron gun is separately simulated and optimized for the performance parameters of the desired characteristics of the electron beams. Design of a multi beam electron gun followed by a compatible multi beam klystron cavity has been done in the following chapters.

2.3 Simulation for Some Multi Beam Cavities of Existing Klystrons:

Different types of single beam klystrons are under design and development stages at CSIR-CEERI, Pilani. A study has been carried out to convert the design parameters of RF cavity for a single beam design into its equivalent multi beam design by following the laws of scaling. The main specifications of the two klystrons which are under development at CSIR-CEERI for different applications are listed in the following Tables.

Table 2.1: C Band Klystron Specifications

Parameters	Specifications
Frequency (MHz)	5000
Output power	250 kW CW
Gain (dB)	45
Efficiency (%)	50
Beam voltage (kV)	50
Beam current (A)	10

Table 2.2: S Band Klystron Specifications

Parameters	Specifications
Frequency (MHz)	2856.0
Output power	6.0 MW peak 24 kW average
Gain (dB)	45
Efficiency (%)	45
Beam voltage (kV)	130
Beam current (A)	100

Analytical estimation of cavity parameters for single beam design:

From the theory stated earlier we can get the initial dimensions of a cavity as a starting input for the software as shown below for the C-band klystron.

1. D.C. velocity of electron (u_0) = $0.593 \times 10^6 \sqrt{(V_o)}$ m/s

   here V_o is the beam voltage, here it is taken 50,000 volts

   = $0.593 \times 10^6 \sqrt{50000} = 132.6 \times 10^6$ m/s

2. Angular frequency (ω) = $2.\pi.f$ = 31.416 E 9 rad. for f = 5000 MHz

3. Electron wave number (β_e) = ω/u_o = 236.92

4. Wave Propagation Constant $\gamma_e = \sqrt{(\beta_e^2 - k^2)}$ = 212.52

   where k= free space wave number = $2\pi f/c$ = 104.72

5. Drift tube radius (a): The drift tube radius 'a' is given as $a = 1/\gamma_e$. = .00470 m; its wall thickness is initially taken 2.0 mm (if needed it can be optimized through software)

6. Cavity gap (d):

   Taking $\beta_e d = 0.9$ with β_e = 236.92 ;

   d = .00379 m; let us start with d = .003 m.

7. Cavity height 'h' = $\lambda/4$ = ¼ $(3 \times 10^8/5 \times 10^9)$

   = .015 m;

8. Cavity radius 'r' = $(3 \times 10^8 \times 2.405) / 2 \times \pi \times 5 \times 10^9$

   = .0229 m. for cylindrical pillbox design; let us start with the value r = .02

Similar calculations can be shown for the design of S-band klystron cavity as follows.

1. D.C. velocity of electron (u_0) = $0.593 \times 10^6 \sqrt{(V_o)}$ m/s

   here V_o is the beam voltage, here it is taken 130,000 volts

   = $0.593 \times 10^6 \sqrt{130000} = 213.81 \times 10^6$ m/s

2. Angular frequency (ω) = $2.\pi.f$ = 17.94 E 9 rad. for f = 2856 MHz

3. Electron wave number (β_e) = ω/u_o = 83.93

4. Wave Propagation Constant $\gamma_e = \sqrt{(\beta_e^2 - k^2)}$ = 58.87

   where k= free space wave number = $2\pi f/c$ = 59.82

5. Drift tube radius (a): The drift tube radius 'a' is given as $a = 1/\gamma_e$. = .0169 m; its wall thickness is initially taken 2.0 mm (if needed it can be optimized through software)

6. Cavity gap (d):

   Taking $\beta_e d = 0.9$ with β_e = 83.93 ;

   d = .01072 m; let us start with d = .0107 m.

7. Cavity height 'h' = $\lambda/4$ = ¼ ($3x10^8/2856x10^6$)

= .02626 m; let us start with h = 0.0255 m.

8. Cavity radius 'r' = $(3x10^8 \times 2.405) / 2 \times \pi \times 2856 \times 10^6$

= .0402 m. for cylindrical pillbox design; let us start with the value r = .04

Simulation of single beam cavity structures in CST Microwave Studio:

The C-band cavity with the above dimensions is simulated in CST Microwave Studio, the result of simulation is shown in Fig. 2.3 where the electric field lines at the cavity gap are shown and eigen mode frequency is found to be 4.265 GHz. The result is as per expectations, the radius should be decreased further to get the desired frequency of 5.0 GHz, due to re-entrant design.

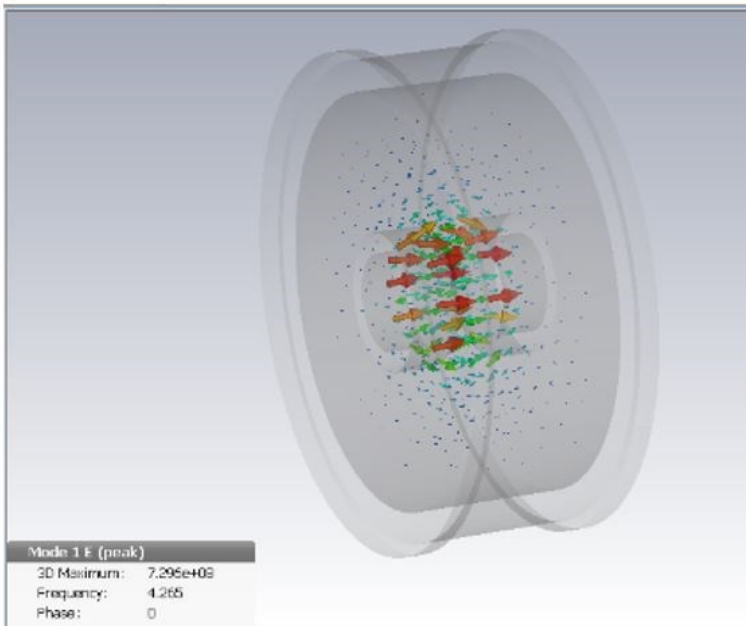

Fig. 2.3: Simulation result of cavity in CST Microwave Studio

The cavity dimensions are optimized by iterative simulation process and the output result for the desired frequency is shown in Fig. 2.4 below, where the eigen mode frequency is found as 5.0 GHz.

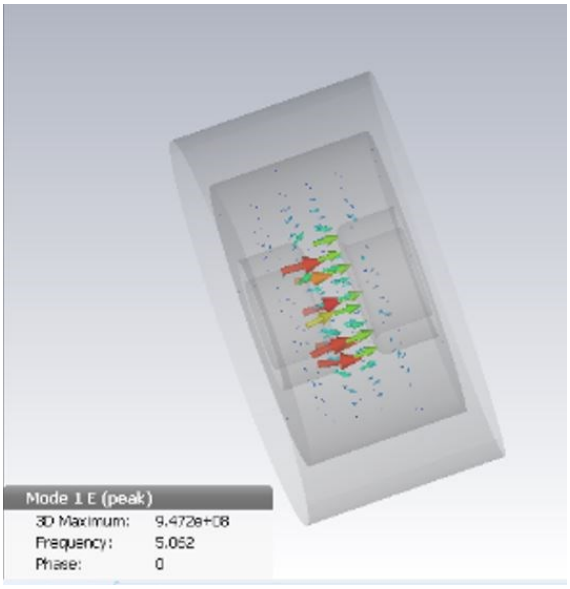

Fig. 2.4: Eigen mode simulation result for C-band cavity

Similarly the optimized simulation result for a S-band single beam cavity structure is shown in Fig. 2.5 where the a frequency of 2857 MHz is displayed as output result after running the eigen mode solver.

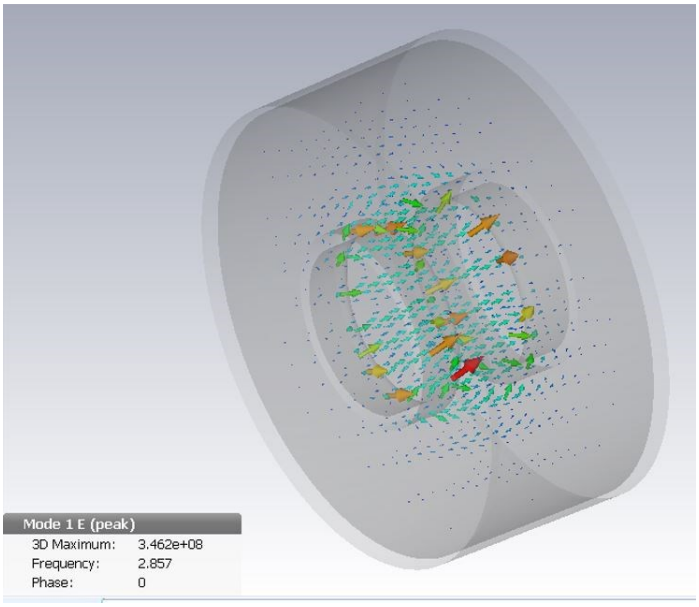

Fig. 2.5: Simulation of frequency for the S-Band Klystron

The optimized dimensions through simulations for both the single beam cavity structures are listed in Table 2.3. These cavities have been fabricated with these dimensions and also have been successfully tested for their designed frequencies.

Table 2.3: Design Parameters of Single beam Cavities

Parameter (in mm)	C-Band Cavity	S-Band Cavity
Drift tube radius	4.25	12.0
Beam radius *	3.0	8.0
Cavity gap	3.5	10.0
Cavity height	15.0	25.5
Cavity radius	13.5	31.0
Drift tube wall thickness	2.0	2.0

*Although the beam radius r_b is not a cavity related parameter but it is mentioned here due to its relevance while converting this design into an equivalent multi beam design and this is taken approximately 70% of drift tube radius considering 'beam fill factor' as 0.7)

Converting to the eight beam RF cavity design:

The design parameters for an equivalent multi beam cavity can be derived through some computations by following the scaling laws. We have considered eight beam cavity designs for both the above structures (N=8).

Calculations For C-band klystron cavity;

Perveance for single beam design is = $10 / (500000)^{3/2}$ = .894 μP

and by Eq. 2.14 $V_{MBK} = 50000/ (8)^{2/5} = 21.764$ kV

Considering the same perveance in each beam-let, the current per beam will be

$I_1 = .894 \times 10^{-6} \times (21764)^{3/2} = 2.87$ A

Total power with eight beams at 50% efficiency will be

$P_{MBK} = 8 \times (0.5) \times (2.87) \times (21764)$

$= 250$ kW

So we have chosen about 21.8 kV and 2.9 A as beam voltage and current per beam-let respectively, for an equivalent eight beam design. Now to find the drift tube radius in the multi beam structure we may first calculate S_1 which is beam cross section area for each beam-let in the MBK design by the following equation.

$(I_b)_{MBK} = 2.9 \times 8 = 23.2$ A $= N *(J_1)_{MBK} * S_1$ (Eq. 2.17)

where the current density per beam-let $(J_1)_{MBK}$ can be computed by Eq. 2.16 by putting the value $J_{SBK} = I_{SBK}/ \pi * (r_b)^2 = 10/ \pi (.003)^2 = 353677.65$ A/m^2

$(J_1)_{MBK} = 352677.65 *(8)^{2/5} = 812537.8725$; by putting this value in Eq. 2.17 we get

$S_1 = 3.57 \times 10^{-6}$ m^2

Therefore beam radius per beam-let in MBK will be $(r_1)_{MBK}$ = 1.066 mm
Considering a beam fill factor of 70 % we will get the drift tube diameter as about 3.05 mm;

With all of the above computed parameters, the desired eight beam cavity has been simulated in CST Microwave Studio. A multiple beam cavity can be simulated by three dimensional codes only because of its asymmetric cavity structure. The simulation of the eight beam RF cavity for C-Band klystron has been done by placement of the eight drift tubes as shown in the Fig. 2.6 and the simulated eigen mode frequency is found 5.016 GHz as displayed in Fig. 2.7 and it is indicated by the electric field lines shown across all drift gaps that E-field is concentrated between the multiple gaps which is the necessary condition for a good interaction between the RF field and electron beam propagating through the RF interaction structure.

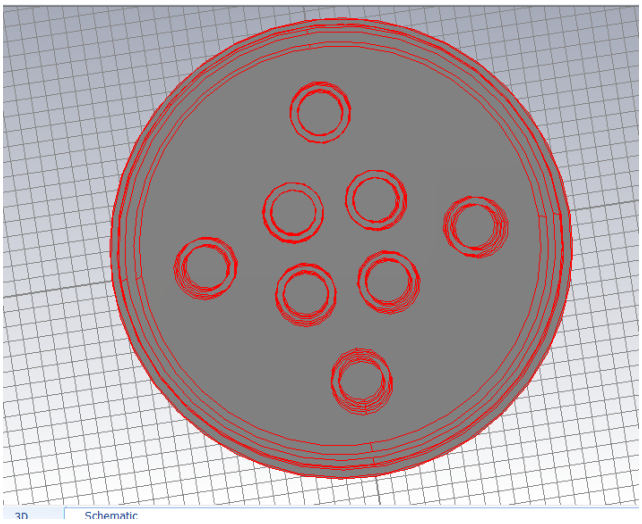

Fig. 2.6: Placement of the drift tubes

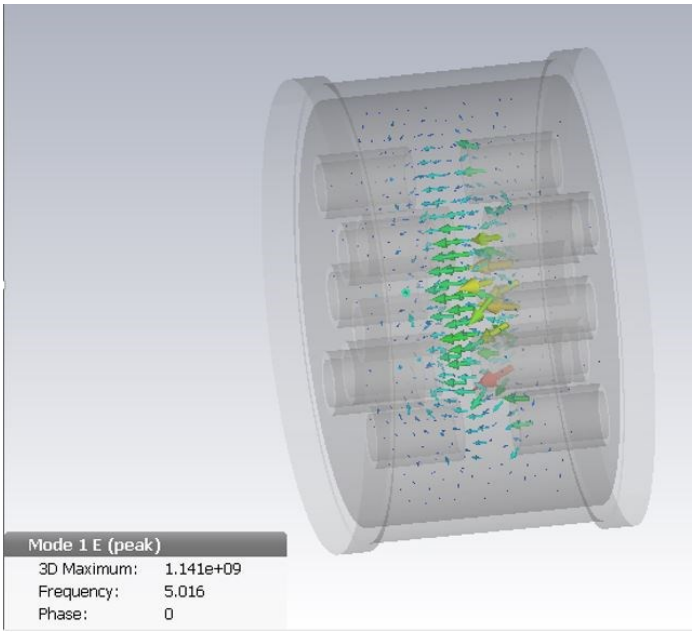

Fig. 2.7: The Eigen Mode frequency 5 GHz found in CST

Similar computations have been done for getting the design parameters for the S-band eight beam cavity and the computed parameters are listed in the Table 2.4 along with C-band eight beam cavity parameters as obtained above. The simulation result for S-band multi beam cavity is shown in Fig. 2.8 with the desired frequency of 2856 MHz.

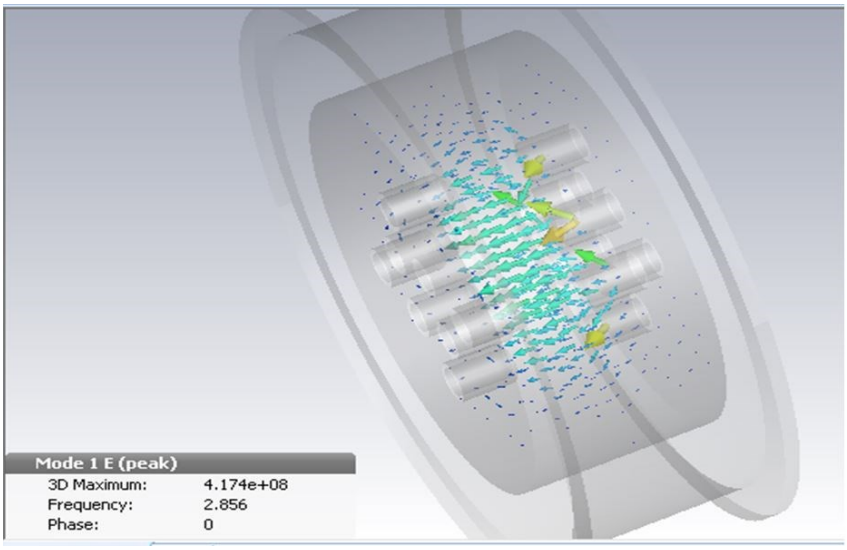

Fig. 2.8: The Eigen Mode frequency 2.856 GHz found in CST

Table 2.4: Design Parameters of the Multi-beam Cavities

Parameter (in mm)	C-Band Eight Beam Cavity	S-Band Eight Beam Cavity
Each Drift tube radius	1.5	2.15
Cavity gaps	3.6	8.5
Cavity height	15.0	25.5
Cavity radius	13.5	30.0
Drift tube wall thickness	0.5	0.85

Thus by applying the scaling laws, the design of two types of multi beam cavity structures have been simulated i.e. one at 5 GHz frequency, another at 2856 MHz frequency. After setting a design approach for the multi beam cavities, following chapter presents the design for a multi beam electron gun for a L/S band klystron and subsequent chapters will present RF interaction study in multi beam klystron.

Publication Outcome (1)

Deepender Kant, LM Joshi, Vijay Janyani, "Design of a Multi Beam Klystron Cavity from Its Single Beam Parameters", 2nd International Conference on Communication Systems (ICCS-2015) at BKBIET Pilani, October 18-20, 2015.

(Peer reviewed international conference with publication in the 'Journal of American Institute of Physics')

AIP Conf. Proc. 1715, 020049 (2016) doi: 10.1063/1.4942731

CHAPTER 3
DESIGN STUDIES FOR A MULTI BEAM ELECTRON GUN

The target specifications of a multiple beam electron gun for a klystron are fixed by considering the design parameters of a "One kw (CW) power tunable D/E band Klystron" developed earlier [115] at CSIR-CEERI, Pilani and used for tropo-scatter communication applications. The electron gun parameters for this device are listed in Table 3.1 and one actual photograph of the device is shown in Fig 3.1. Although the achieved efficiency of this klystron was low at about 30.3% but the device had a tunable range of frequencies from 1.7 GHz to 2.4 GHz, as required for its intended applications.

Fig. 3.1: One kW (CW) power klystron

Table 3.1: Specifications of 1 kW klystron

Parameter	Value
Beam Current	550 mA
Beam Voltage	6 kV
Beam Radius	2.2 mm
Beam-to-tunnel fill factor	0.6

The new requirement is of a klystron for operation at 1.8 GHz -2 GHz but with 2 kW CW output power with higher efficiency and wider instantaneous bandwidth. Development of a multi beam klystron is being proposed to meet the desired specifications. For ease of fabrication and handling, it is planned to design a five beam device. The idea is to work out each design parameter for the five beam device by conversion of the design parameters taken from its single

beam counterpart using the scaling laws. The target specifications for the proposed device are as given in Table 3.2.

Table 3.2: Specifications of 2 kW power klystron

Quantity	Value
Operating Frequency (Tunable)	1800-2000 MHz
Output Power	2 kW CW
Efficiency (proposed)	40% (min.)
Bandwidth	>15 MHz
Number of Beams	5

The MBK output power is given by following equation [124]:

$$\mathbf{P_{mbk} = N\ \eta\ I_1\ V_{mbk}}\ ;$$

where η is the efficiency of power extraction from each beamlet, N is the number of beams, and I_1 is the beam current per beamlet and V_{mbk} is beam voltage. For a five beam MBK with 250 mA current per beam and a beam voltage of 4 kV, the calculated output power is 2 kW.

3.1 Design and Simulation Approach for a Multi Beam Electron Gun

The desired electron gun has been simulated in two steps, first the single beam gun is designed using Trak code to find the optimum electrode shapes to achieve the required value of current. Here we have chosen a planar cathode and the confined flow focusing [3], [125] is used for magnetic field. The simulation of a single beam electron gun along with focusing field is shown in Fig. 3.2. The computed beam current is 256 mA at a beam voltage of 4 kV. Other Electron-gun design parameters are as listed in Table 3.3.

Table 3.3: Electron-gun Design Parameters

Parameter	Value
Anode cathode distance	5 mm
BFE angle with respect to beam axis	67.5^0
Drift tube radius	3.3 mm
Beam radius	2.2 mm
Cathode diameter	4.4 mm

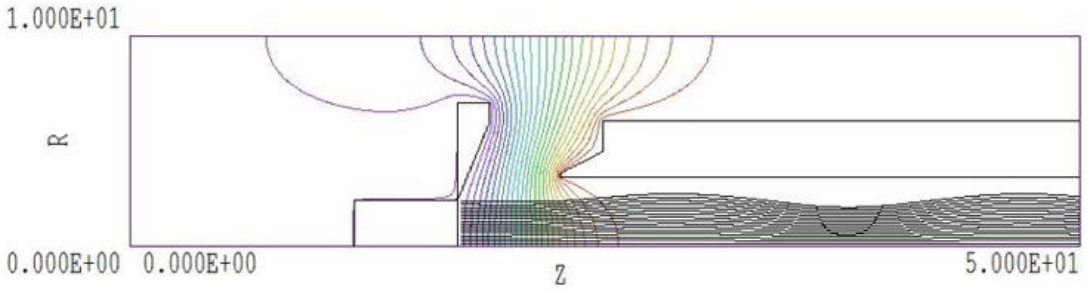

Fig. 3.2: The simulated electron gun in Trak

The value of the magnetic field for focusing of electron beam with above mentioned parameters is found using following well known relation [40] :

$$(B_b)^2 = 69\ I_b / (V_b)^{0.5} (R_b)^2$$

where B_b is the Brilliouin field value in gauss, V_b is the beam voltage and R_b is the beam radius. Thus the calculated value of B_b is 237 gauss and for confined flow focusing the value of the required magnetic field is taken 2-3 times [40] of Brilliouin field value so the chosen value for the focusing magnetic field in the present case is taken about 800 gauss. It is noted that the electron beam is laminar with no interception but with minor scalloping. The corresponding axial magnetic field is shown in the Fig. 3.3.

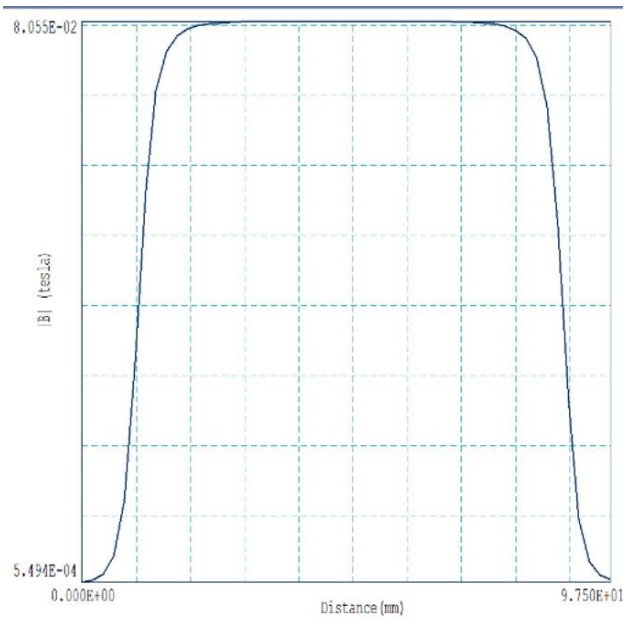

Fig. 3.3: The simulated magnetic field in Trak

Once the single beam gun design is optimized in Trak then the same structure has been simulated in CST Particle Studio as shown in Fig. 3.4 where particle trajectories under applied magnetic field are displayed and the value of beam current is found as 253.9 mA as shown in Fig. 3.5.

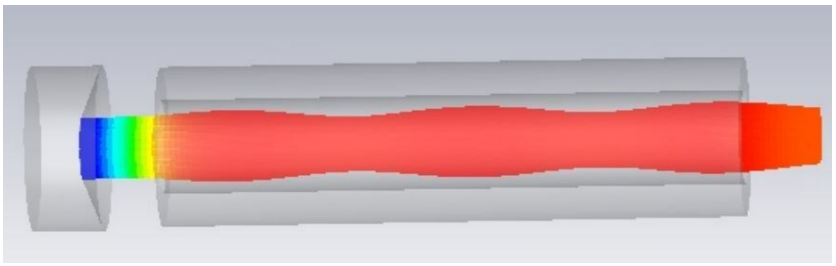

Fig. 3.4: The simulated electron trajectories in CST

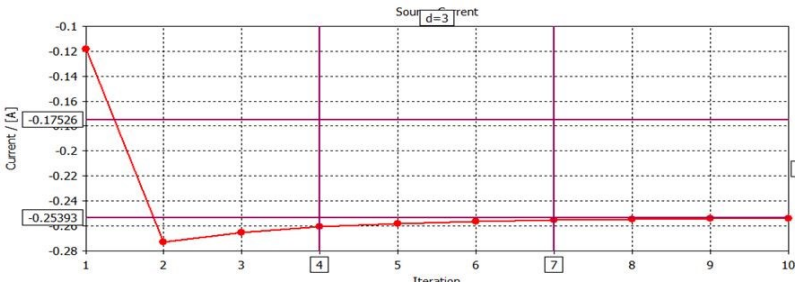

Fig. 3.5: The simulated beam current in CST

Now a five-beam structure has been modeled in CST as shown in the Fig. 3.6, with similar structural parameters of the above single beam gun. The five planar cathodes along with five beam forming electrodes (BFE) are considered on a single surface and the anode cylinder with five drift tunnels is placed at the simulated distance optimized earlier.

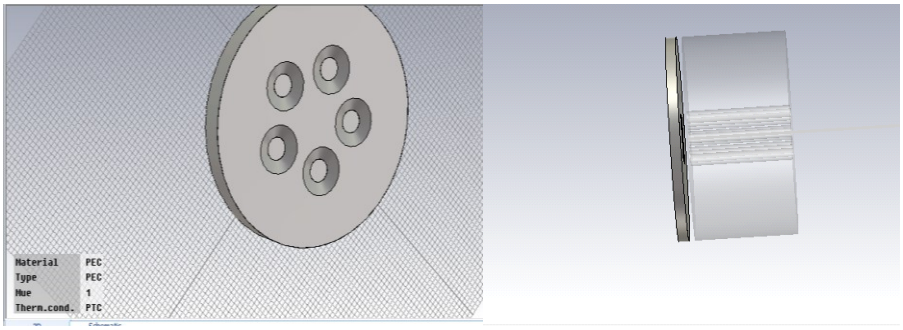

Fig. 3.6: Geometry of the five beam electron gun

The electron gun along with the required magnetic field, is simulated in CST particle studio and the simulation results for the beam trajectories at 4 kV are shown in Fig. 3.7. It may be observed that the beam trajectories are well focused along the simulated drift section.

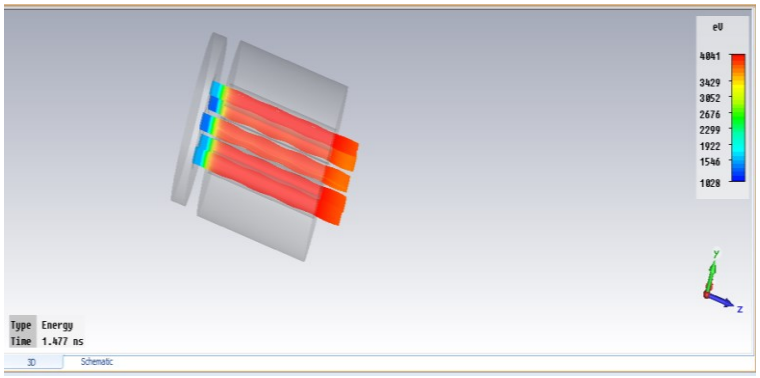

Fig. 3.7: Beam Trajectories with focusing magnetic field

The obtained value of total beam current is about 1250 mA as shown in the Fig. 3.8 and it is clear that the total beam current of five beam structure is almost five time of single beam current value as obtained through Trak and CST codes.

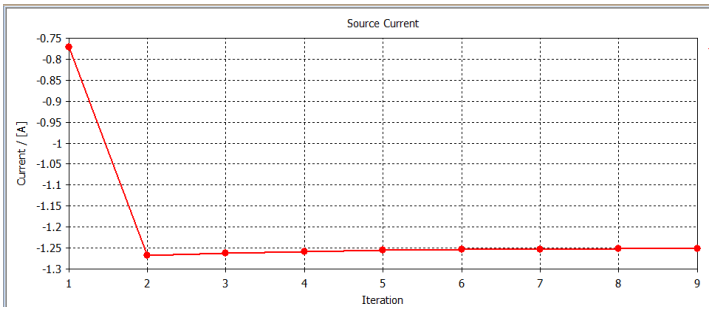

Fig. 3.8: Simulated value of the beam current

The above design of a five beam electron gun for a L-band klystron is based on applying analytical magnetic field values through software. Practically electromagnet is mostly used in klystron for getting the desired magnetic field at the axis of the device. The design of electromagnet for a particular klystron is done by considering the pole piece aperture and its location at both ends of the RF interaction structure, the number of coil turns, coil current in the electromagnet etc. This requires simulation of the electromagnet along with electron beam propagation. The five beam electron gun has been simulated along with electromagnet to achieve the desired beam transmission characteristics.

3.2 Design of Magnetic Focusing System

The electron gun simulation without any applied magnetic field is shown in Fig.3.9 where electron trajectories are mostly intercepted by the anode structure, as given by the collision information. The design of electromagnet has been carried out by iterative simulations in CST EM Studio.

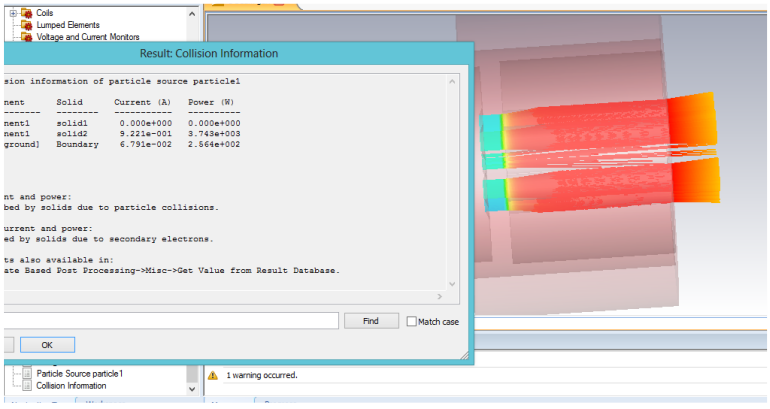

Fig. 3.9: Electron gun Simulation without Magnetic Field

The electromagnet is to be designed so as to provide this value of the magnetic field along each drift tunnel. The Figure 3.10 shows the modeling of the electromagnet in CST EM studio where a coil is defined along with pole piece structures on its both ends. A metallic cylinder with five drift tunnels is defined and the electromagnet is placed around the cylinder. The magnetic field can be measured after simulation, along the line defined at the axis of drift tunnel.

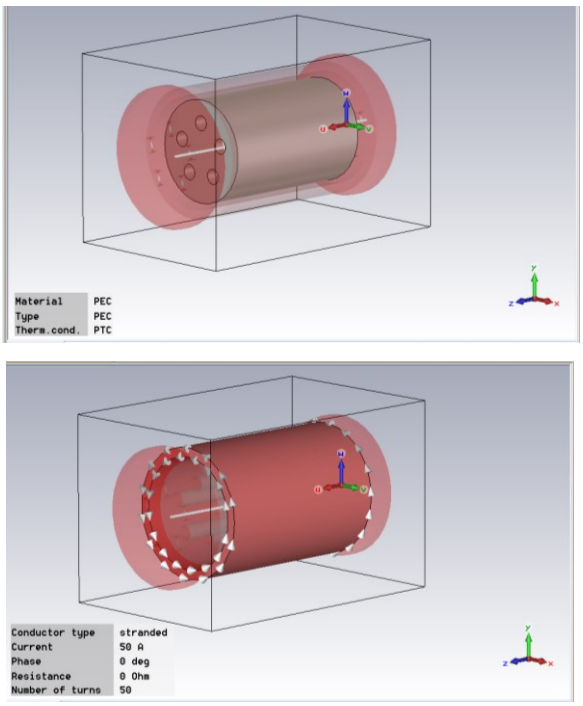

Fig. 3.10: Modeling of Electromagnet

The simulation of electromagnet has been carried out along with five beam electron gun structure so as to get the desired value of magnetic field at the drift tunnel axis. The Fig. 3.11 shows the electron gun surrounded by the electromagnet where one pole piece is placed behind the cathode and another at the end of the drift tunnel. The pole piece aperture can be varied for optimization of the magnetic field at the drift tunnel axis, also the product NI is varied for the electromagnet to get the desired value of magnetic field.

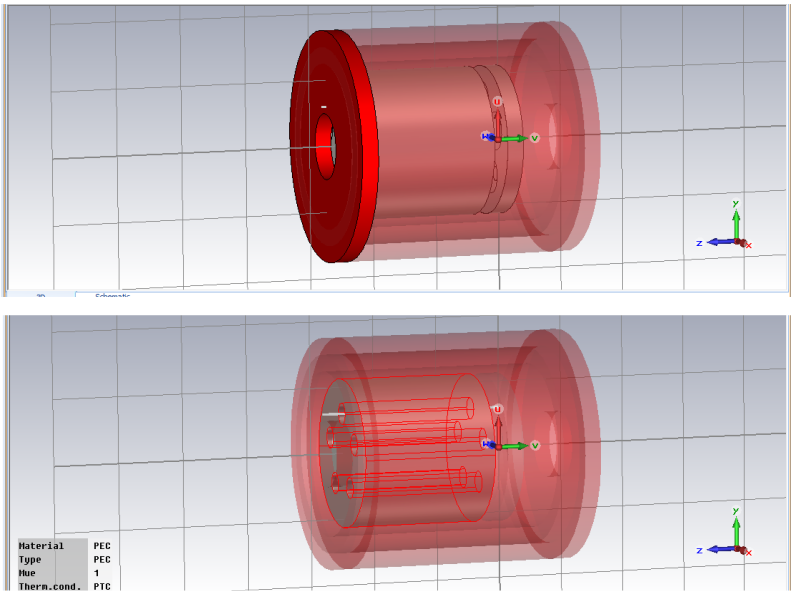

Fig. 3.11: Electron gun modelled with electromagnet

After iterative simulation process the desired value of magnetic field, measured along the line defined at drift tunnel axis, is shown in Fig. 3.12. The electron trajectories in presence of this magnetic field are also shown in Fig.3.13. The final value of NI is 5000 with 50A and 100 turns in the coil.

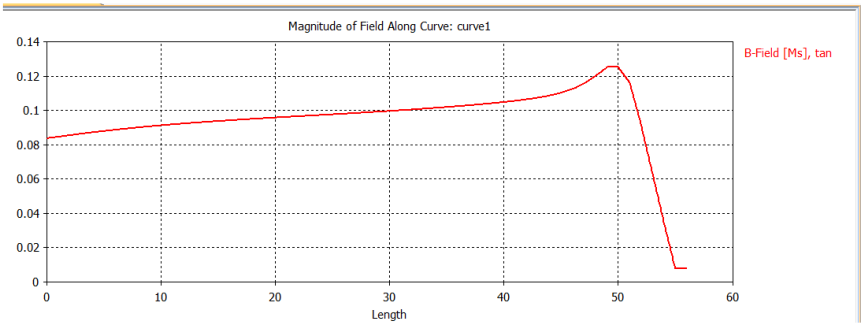

Fig. 3.12: The simulated magnetic field vale at drift tunnel axis

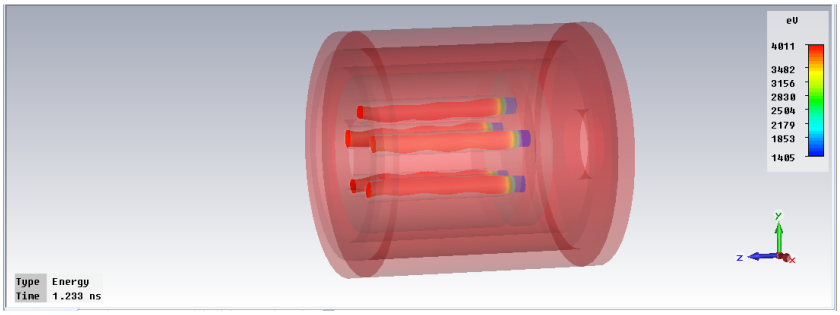

Fig. 3.13: The electron trajectories with magnetic field

The collision information in Fig. 3.14 shows that there is no beam interception at any of the drift axis and the dissipation is only at the termination. The beam current value is also found in Fig. 3.15, approx. 1250 mA as desired.

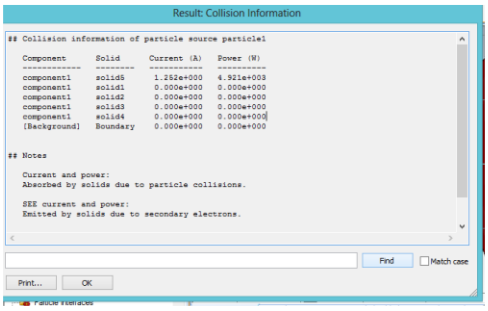

Fig. 3.14: The collision information

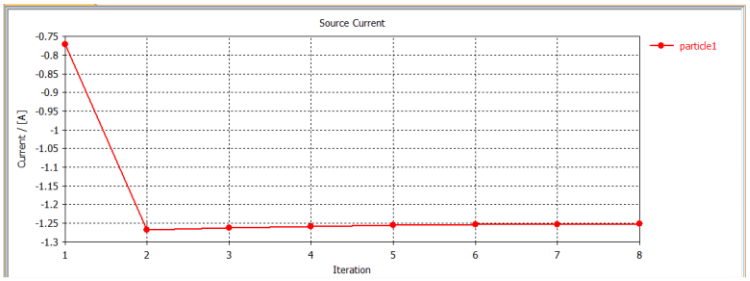

Fig. 3.15: The simulated current

3.3 Sensitivity Study of Focusing System

The simulations assume that electromagnet axis is perfectly aligned with principal axis of the electron gun however there may be the case that there is some angular misalignment between the two axes; then the focusing of electron beam will be disturbed and resulting the beam interception in beam tunnels. A sensitivity study has been carried out by varying the tilt angle between the two axes and it has been concluded that even $\pm 1^0$ tilt angle can produce interception current of 4-5 mA and further tilting enhances interception current greatly. It has been tried to study that whether increasing the NI value for electromagnet can reduce the interception current due to tilting or not. It has been concluded that at the most $\pm 1^0$ tilt can be corrected (with interception current less than 1 mA) with increased magnetic field to get the desired beam transmission. A tilt angle more than this will result in a much higher beam interception which cannot be corrected even by applying a higher magnetic field. Table 3.4 gives a summary of the results after iterative simulations with changing the different parameters of the focusing structure.

Table 3.4: Sensitivity of focusing system towards axis misalignment

Tilt angle (between the two axes) (deg.)	Interception current/total current (mA)	Magnetic field on drift axis with NI 3500 A T (gauss)	Correction applied/new magnetic field	Interception current after correction (mA)
0	0.0/1250	880	------	
+1	3.82/1255	865-870	4000 AT/ 980-990 G	.5
-1	4.45/1255	860-870	4000 AT/990 G 4400AT/1090 G	.9 .6
+2	173/1225	860-865	4000AT/ 980-990 G 4400AT/ 1080-1090 G	135 162
+3	390/1260	860-865		

3.4 Electromagnet with Multi Aperture Pole Piece:

All the simulations carried out till now are using the single pole piece aperture, as used conventionally however a study can be carried out by simulation with multi aperture pole piece as per the design of RF interaction structure. The pole piece has been modified with five apertures cut through it with same diameter as the drift tunnels to match the latter, to improve the focusing efficiency along individual drift tunnels. The 3D simulation of the electron gun has been done and optimization has been carried out to achieve the desired beam current without any interception along any of the drift tunnels.

The multi aperture pole piece design has resulted in reduced NI value for the required focusing. Fig. 3.16 shows the simulation for a single aperture (of 20mm diameter) pole piece where NI value is taken about 5000 (50 A, 100 turns) to get the required focusing so as no interception occurs in the drift tunnels.

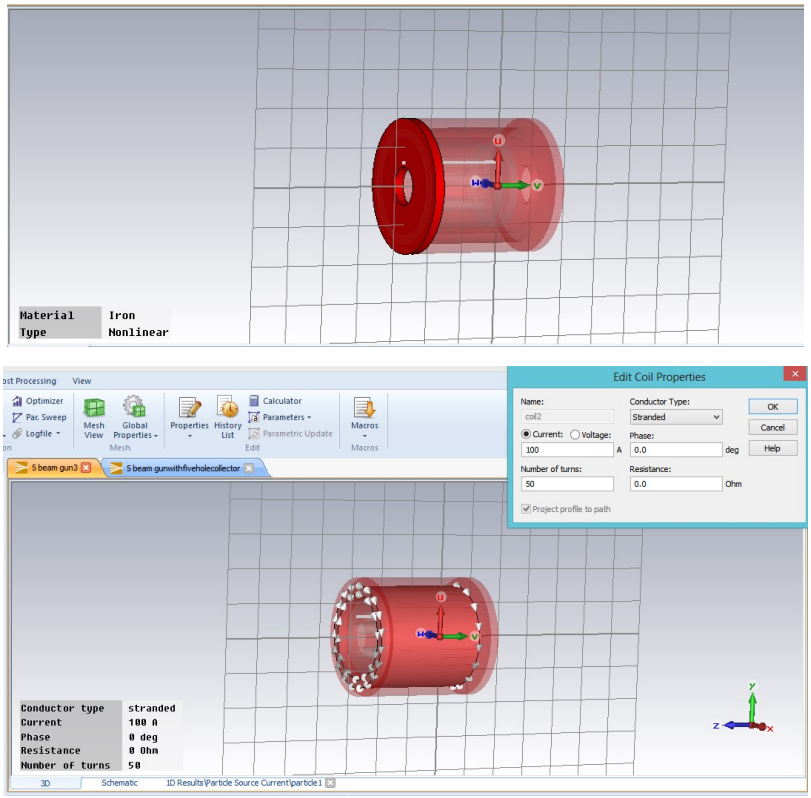

Fig. 3.16: Simulation with single aperture pole pieces

As reported earlier that there is no beam interception in the drift tunnels. However following Fig. 3.17 shows the simulation results with five aperture pole piece and also the required NI value i.e. 2400 (60 A, 40 turns) is very less as compared to single aperture case.

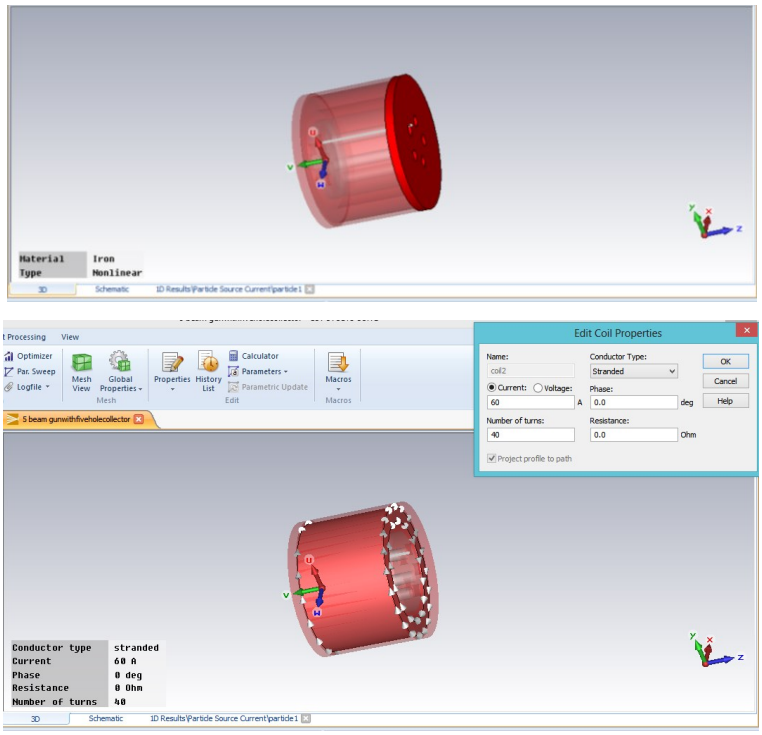

Fig. 3.17: Simulation with five aperture pole pieces

It is important to note that using with a NI of 2400 Amp.-turns, there is no beam interception with five hole pole pieces as shown in Fig. 3.18 where electron trajectories under applied magnetic field are shown along with collision information, also it was noted when NI= 2400 put in the previous simulation of single aperture case an interception current of about 160 mA appeared.

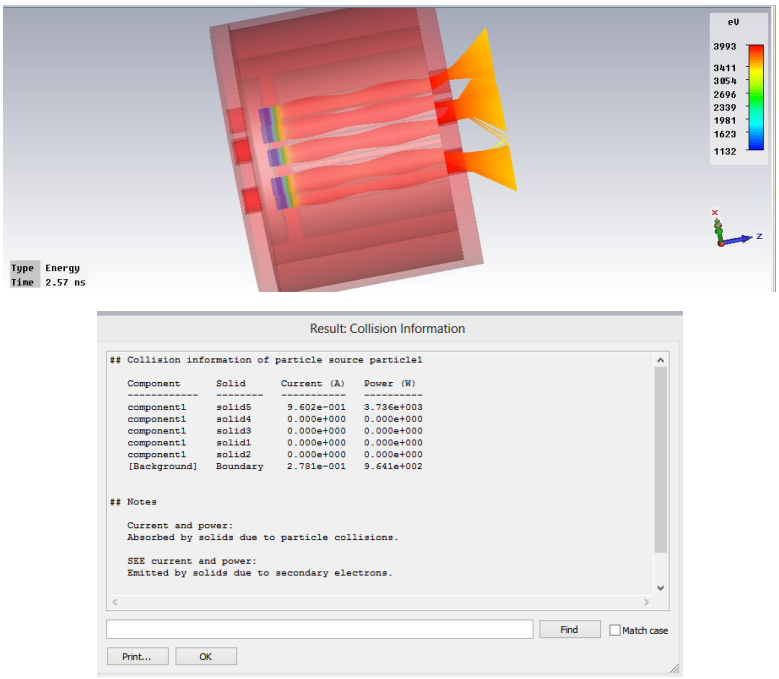

Fig. 3.18: Electron trajectories and collision information after simulation

3.5 Design of an Electron Gun for 325 MHz, 400 kW Eight Beam Klystron

Another klystron to be designed and developed at CSIR-CEERI is for 325 MHz, 400 kW power which is desirable for accelerator application [92] and considering the multi beam gun design approach as discussed in previous sections another electron gun with eight beams has been designed with following specifications of the intended klystron.

Table 3.5: Specifications of 325 MHz klystron

S. No.	Parameter	Value
1.	Frequency	325 MHz
2.	Output Power	400 kW
3.	Efficiency	45-50 %
4.	Gain	45 dB nominal

Considering 68 kV beam voltage and 12 A beam current for a single beam device capable to provide the 400 kW output power with the listed parameters, we can have electron gun design parameters for a multi beam (say 8 beams) klystron with scaling laws;

This gives;

V_{mbk} = 29.59 kV, $(I_1)_{mbk}$ = 1.5 A

Total I_{mbk} = 12 A

After converting the beam parameters, the RF cavity parameters can be derived having eight drift tubes with drift gaps in a single cylindrical cavity. Accordingly the multi beam parameters are used for simulation of the eight beam cavity in CST Microwave Studio and optimized through iterative simulation process. The eight drift tubes are located in the cylindrical cavity as shown in the Figure 3.19 and the results for Eigen mode frequency after simulation of both cavities are shown in Figures 3.20 and 3.21. It is also clear that the maximum E-field lines appear across all drift tube gaps as required for an efficient beam wave interaction process.

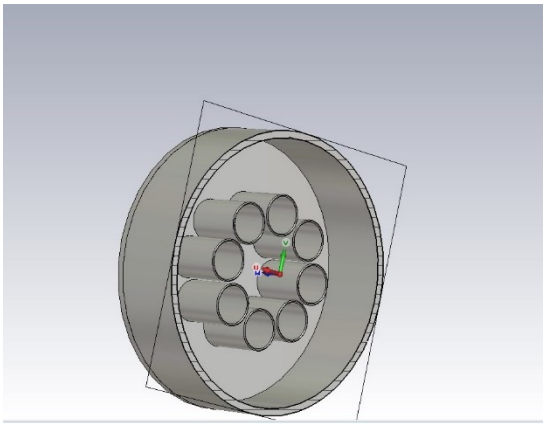

Fig. 3.19: Orientation of the drift tubes

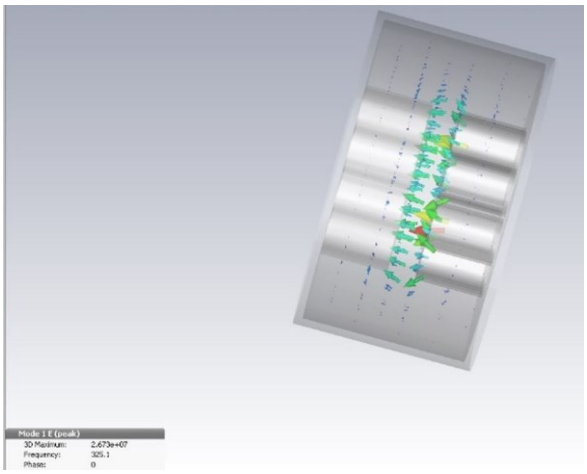

Fig 3.20: The Eigen Mode frequency 325 MHz found in CST

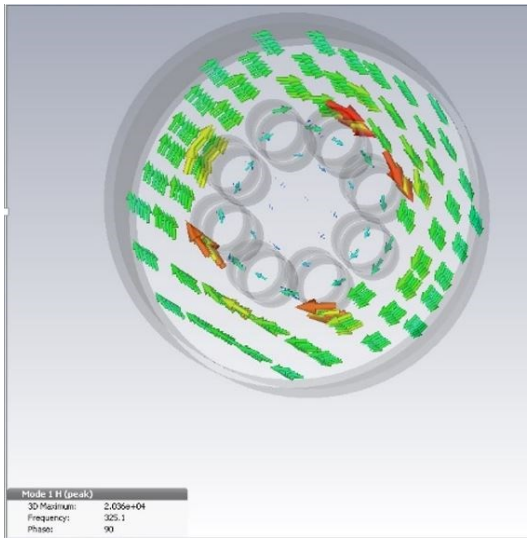

Fig 3.21: The Magnetic Field lines after eigen mode simulation

After simulation of the RF cavity with eight drift tubes and achieving the desired frequency, the electron gun design has been simulated and optimized through CST particle studio. The Fig. 3.22 shows modelling of electron gun showing cathode, anode and the emission area.

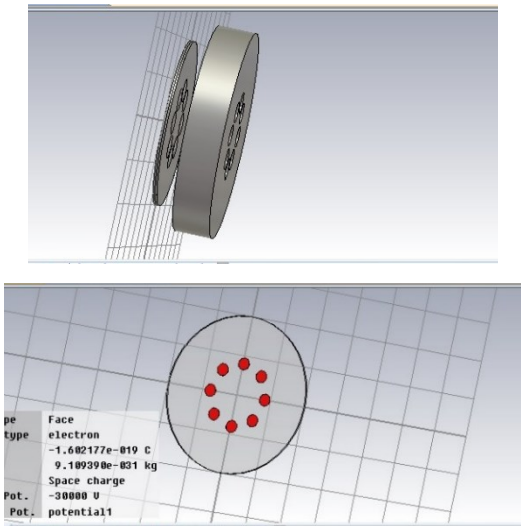

Fig. 3.22: Simulation of eight beam Electron gun

The magnetic field used for focusing of the electron beam has been applied through analytic mode, however in practical it will be electromagnet. The desired value of beam current has been achieved and the beam trajectories are shown in Fig.3.23 and it is shown by the collision information that there is no beam interception.

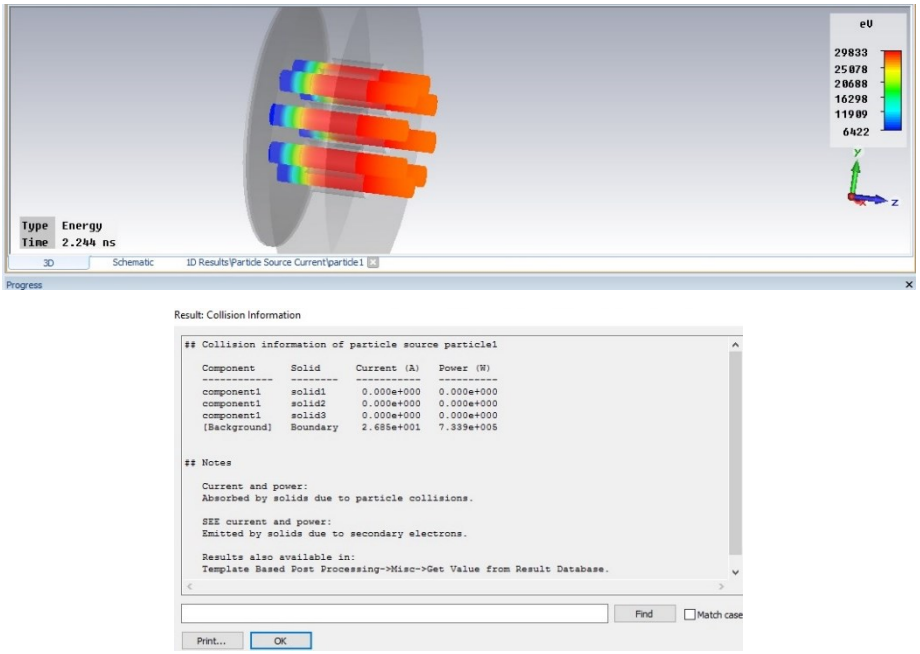

Fig. 3.23: Electron beam trajectories after simulation

In summary, for the design of a focusing field in a multi beam electron gun in our case, we have proposed two conditions;

(i) Electron gun side pole piece is put behind the cathode, instead of between cathode and anode

(ii) the both pole pieces have similar holes matched with the drift section for a better coupling of the magnetic field inside the drift tunnels.

Novelty in design:

The present work comprises of a methodology for focusing of the electron beams in a L- band multi beam klystron, operating in the frequency range of 1800-2000 MHz, with an output power of 2 kW (CW) and for its intended use in communication. The five beam electron gun compatible for the desired klystron has been designed and simulated through CST microwave studio. The desired beam current without any beam interception, has been achieved through simulation by using the proposed methodology. The novelty of the scheme, brought about by placing the pole piece behind the cathode and with similar pattern of holes through it for shaping of the magnetic field lines along each beam axis. The approach used is equally applicable for all electron guns having planar emission surfaces with any number of electron beams. *(An Indian Patent has been applied for this work as mentioned in Appendix 1)*

The following chapter will present the design of a compatible RF cavity for this design of electron gun for L/S band klystron.

CHAPTER 4
DEVELOPMENT AND CHARACTERIZATION OF MULTI BEAM RF CAVITY

After completing the design study of multi beam electron gun for the proposed klystron, the design of a compatible five beam RF cavity has been carried and simulated in CST Microwave Studio as well as in MAGIC. The RF cavity has been fabricated and characterized for its resonant frequency. While designing the cavity a 'beam fill factor' of 0.65 and beam coupling coefficient of 0.85 is considered.

4.1 Design and Simulation of L-band Multi Beam Cavity

The cavity radius for a simple cylindrical cavity operating in TM_{010} mode can be given as

$$R = \mathbf{c} * X_{np} / \omega_c \quad \text{(Eq 4.1)}$$

Here R = cavity radius, X_{np} = A Bessel function value = 2.405 for TM_{010} mode
ω_c = angular frequency = $2\pi f$ and c is velocity of light = $3x10^8$ m/sec;

Although the radius for a reentrant cavity will be lesser than this, it can be taken as an initial value to start the simulation. The design of reentrant type RF cavity with five drift tunnels has been optimized through iterative simulation process. Considering the beam radius of 2.2 mm from electron gun design and fill factor of 0.65, the drift tunnel radius will be 3.3 mm. The reentrant cavity's radius has been found to be 40 mm by simulation in CST and the five drift tunnels are placed azimuthally with the centers of the drift tunnels lying on a circle of 12 mm radius. Fig. 4.1 shows a model of the five beam cavity in CST Microwave Studio. The simulated value of resonant frequency of the cavity is 1.834 GHz as shown by the eigen mode simulation result in Fig. 4.2 and the vector plot for the electric field across the multiple cavity gaps confirms that the E-field is concentrated between the nose cones as required for the desired mode of interaction between the RF field and electron beam. The electric field value is plotted along a line at one of the drift tube axis as shown in Fig. 4.3 which also indicates that the field is maximum at the cavity gap which is located at 10 mm to 15 mm. The computed R/Q value of the cavity along this line is about 124.8 as indicated in Fig. 4.4 and the simulated Q value for the cavity is about 7600.

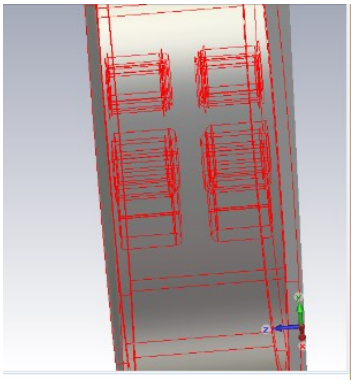

Fig. 4.1: The five beam cavity geometry

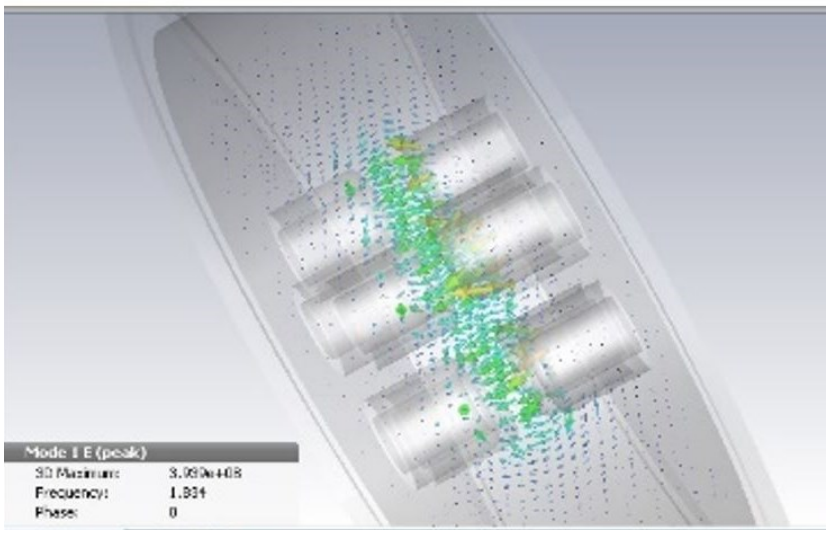

Fig. 4.2: Electric field across the cavity gaps

(The eigen mode frequency is 1834 MHz)

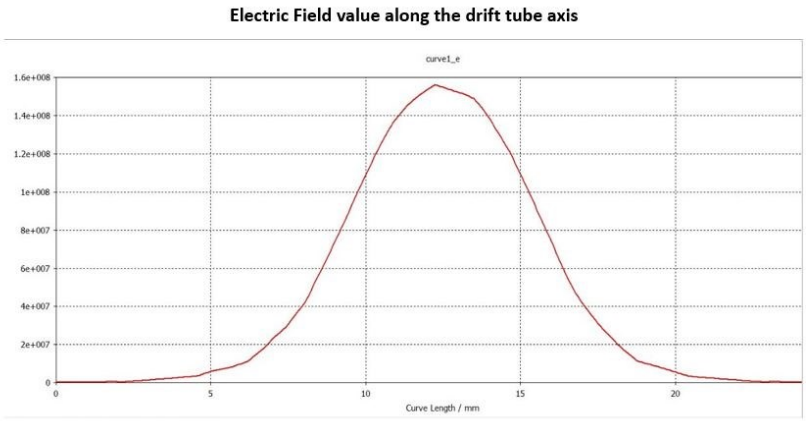

Fig. 4.3: The plot of Electric field along one drift tube axis

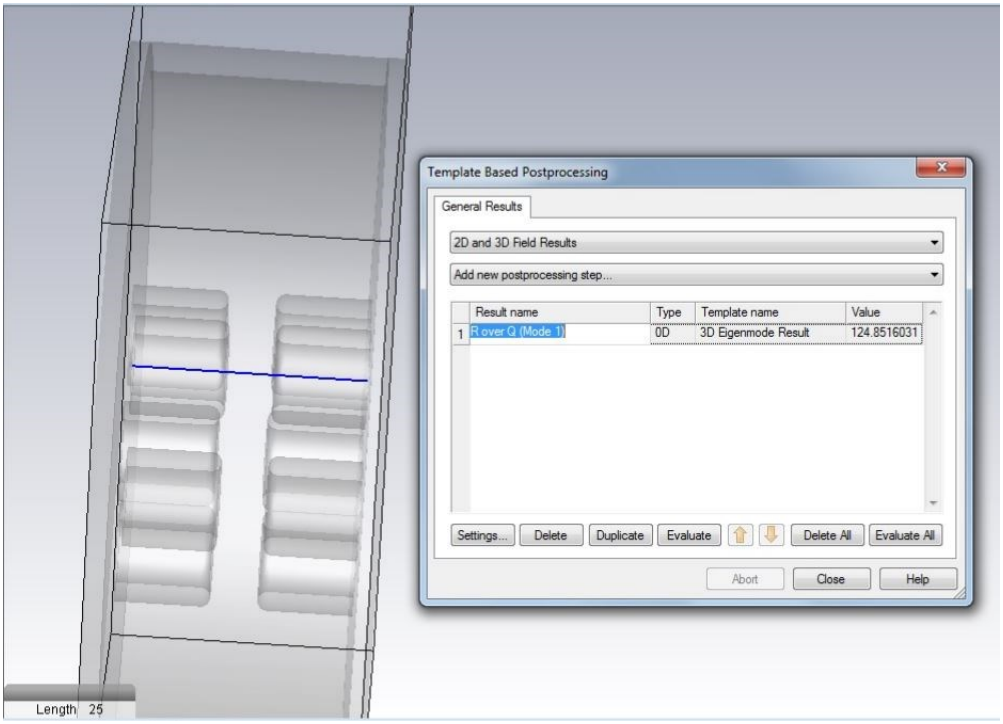

Fig. 4.4: The computed R/Q along one drift tube axis

The optimized dimensions found in the CST Microwave Studio have been modelled again in MAGIC to get the resonant frequency. The eigen mode simulation result after MAGIC simulation is shown in Fig. 4.5.

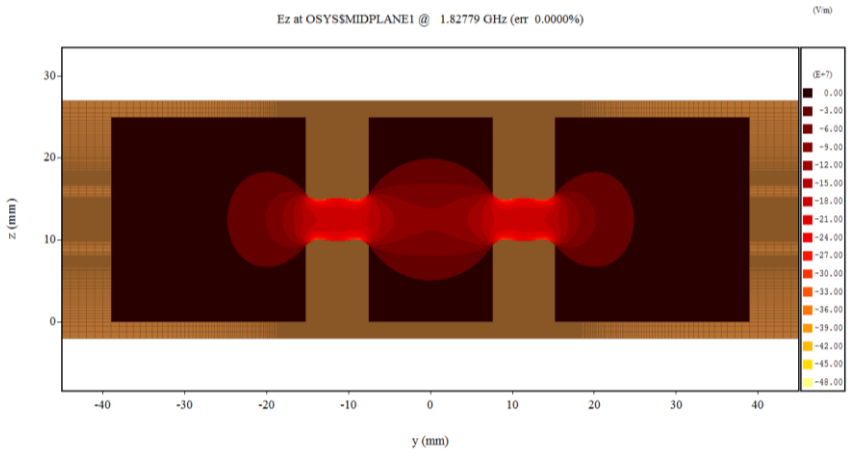

Fig. 4.5: Eigen mode simulation of RF cavity in MAGIC
(the eigen mode frequency 1828 MHz)

4.2 Fabrication and Cold Testing of the Multibeam Cavity

Based on the dimensional design after simulations and verifying it through two different codes i.e. CST Microwave Studio and MAGIC-3D, the five beam cavity has been fabricated by assembly of the piece parts as shown in the Fig. 4.6 where five drift tubes are individually shown.

Fig. 4.6: The piece parts of a five beam cavity

Then the assembled and brazed cavity has been characterized with network analyzer for its resonant frequency and is found to be 1.815 GHz. The simulated frequency for this design of the cavity is 1.8 GHz as shown earlier, therefore giving an error of about 0.83% over the simulated results. The measurement set-up along with screen shot of the measured frequency is shown in Fig. 4.7, the cavity is excited by inserting one probe in one of the drift tube and the reflection coefficient is being observed.

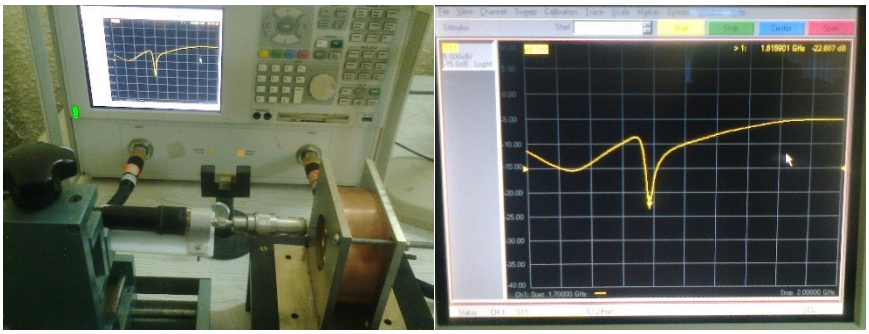

Fig. 4.7: Characterization of the five beam cavity

(the measured resonant frequency is 1815 MHz)

The Table 4.1 summarizes the results after cavity design through simulation and its measured frequency through network analyzer.

Table 4.1: Summary of RF cavity design parameters

Cavity dimensions after optimization through simulation (mm)	Eigen mode frequency found through CST	Eigen mode frequency found through MAGIC-3d	Measured Resonant Frequency of the fabricated cavity
Cavity radius = 39.0 Cavity gap = 5.0 Drift tube inner radius = 3.3 Drift tube outer radius = 5.3 Cavity height = 25.0	1.834 GHz	1.8277 GHz	1.815 GHz

This Chapter has presented the design of a suitable RF cavity for the proposed five beam klystron. The design has been optimized and cross-validated through simulation with two different computer codes. The RF cavity has been fabricated with the simulated design and characterized for its resonant frequency. The measured resonant frequency of the RF cavity in in close agreement with the simulated design.

After completion of the design for electron gun and RF cavity for the five beam L/S band klystron, the beam wave interaction study (considering the five beam tunnels) has been done as a next step towards the design implementation for a multi beam klystron. Chapter 5 covers the beam wave interaction simulation studies done during course of this research work.

Publication Outcome (2):

Deepender Kant, L M Joshi and V Janyani, "Design and Characterization of RF Cavity for a L-Band Multi Beam Klystron", Presented in the international conference IEEE MTT-S International Microwave and RF Conference (IMaRC) 2016 at New Delhi during December 5-9, 2016.

Published in *IEEE Xplore digital library*, '2016, IEEE MTT-S International Microwave and RF Conference (IMaRC) Proceedings' Published on June 08, 2017; DOI: 10.1109/IMaRC.2016.7939619

CHAPTER 5
BEAM WAVE INTERACTION SIMULATIONS IN MULTI BEAM KLYSTRON

The mechanism of amplification in a klystron involves proper velocity modulation followed by density modulation of initially accelerated and collimated electron beam passing through the interaction structure. The design of electron gun and RF cavity is covered in detail in previous chapters. This chapter shall deal with the study of interaction of the RF signal to be amplified with the electron beam so as to produce an amplified signal that will be coupled out from output section to the load. 'Beam wave interaction' is the process occurring in the RF structure of the klystron during which the accelerated electron beam generated by the electron gun transfers its kinetic energy to the external RF field to be amplified. All performance parameters of the device such as its output power, gain, bandwidth, efficiency etc. are decided through this process which in turn depend on various operating parameters such as beam voltage, beam current, beam focusing, RF drive power as well as characteristics of the interaction circuits such as resonant frequencies, quality factors, shunt impedances of various cavities and their placement [126-140]. The challenge to the designer is to optimize all these process parameters to achieve the targeted performance of the device. The interaction process in the present case is involving eight beams which requires other special considerations for multiple beam klystron designs [141-145]. With availability of fast and accurate design codes, the device characteristics is mostly optimized through beam wave interaction simulation.

5.1 Modeling of RF Interaction Structure

Simulation of the RF interaction structure for a klystron starts with simulation of RF cavity for the desired frequency of operation along with its other parameters such as Q, R/Q and design of coupling mechanism for input and output cavities. The design of RF cavity resonating at 1800 MHz has been dealt in detail in Chapter 4. However a larger diameter cavity is normally taken for incorporating a tuning mechanism in the cavity to get the desired frequency range of operation. Generally a combination of capacitive and inductive tuners or purely a capacitive tuner is chosen to tune the cavity. In case of a capacitive tuner, the resonant frequency of the cavity is changed by changing capacitance between suitably designed tuning plunger and the nose cones of drift section. As tuner moves inside the cavity, the capacitance between nose cones and plunger increases resulting in decrease in resonant frequency, being inversely

proportional to effective gap capacitance. On the other hand the cavity resonant frequency increases when the tuning plunger is pulled out. The present study of beam wave interaction simulation has been done at 1800 MHz frequency of operation and for a tunable range of device operation.

The modelling of RF interaction structure involves integration of input cavity, intermediate cavities, penultimate cavity and output cavity. The RF signal is applied at the input cavity through a port and the amplified RF is observed at output cavity port. The parameters of all cavities like their operating frequencies, shunt impedance, quality factors and their mutual spacing can be taken as variables for the simulation which may be varied so as to get the required device performance.

As discussed in detail in Chapter1, velocity modulation of electrons in the cavities by the RF field causes them to get density modulated and the RF current is maximum only at certain locations along the drift tube. Mihran [146] experimentally demonstrated that under the effect of space charge forces, the optimum distances between the cavities of a multi cavity klystron should be in the order 90˚: 90˚: 65˚: 45˚: 30˚and this is irrespective of the maximum RF drive level at the input.

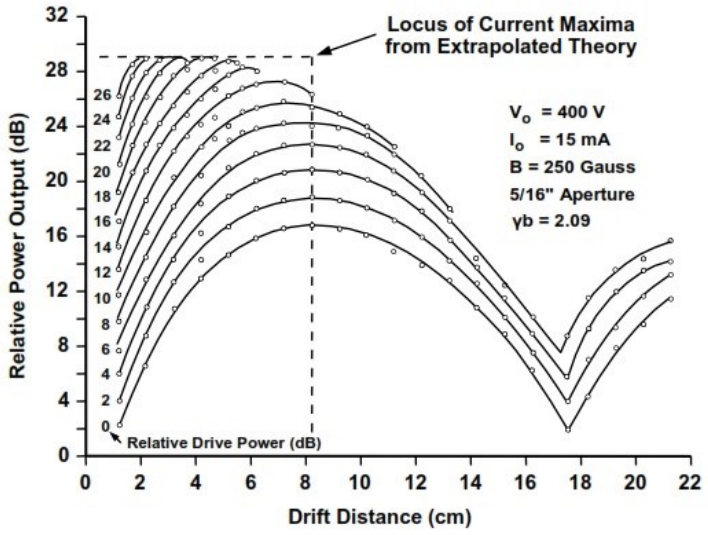

Fig. 5.1: Optimum distance between buncher cavity and output cavity from Mihran's experiment (*Source: T.G. Mihran,, IRE transactions on electron devices, January 1959*)

Explanation to this phenomenon was provided by Webber [147] assuming disk electron model as shown in Figure 5.2.

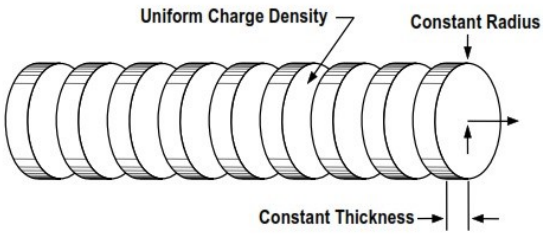

Fig. 5.2: Disk electron model of Webber *(Source: A.S Gilmour, Klystons, TWTs, Crossed-Field Amplifier and Gyrotrons, pp. 231)*

This disk electron model of Webber is adopted in the A-J disk code [122]. This is a very fast 1-D code that can be used effectively for initial estimation of the locations, frequency, Q-factor, R/Q, gap distance of the cavities and electric field profile in between nose cones for optimum operation of the klystron.

5.2 Simulations through AJDISK Code

The process has been simulated initially using 1-D code AJDISK code to get some initial values of parameters for RF interaction structure like cavity frequencies, spacing between the cavities, and the cavity parameters such as Q factors, shunt impedances etc. These parameters are then put for modelling of the RF interaction structure with 3-D code and further optimization of these parameters will lead to their final values.

AJDISK code can be used for single beam simulations only, so initially we have tried to simulate each beam conditions of a five beam structure with assumption that total power will be five times of the power obtained through each beam. However considering the multi beam RF cavity structure, the input parameter 'k' has been optimized separately by computation of electric field profile at each drift gaps using a MATLAB program as given in Appendix 1.

The maximum output power with each beam, as per AJDISK simulation, is shown to be about 204 W with five cavities. However the desired power per beam should be 400 W so as to get total 2 kW RF power (with five beams). So further optimization has been done in CST particle studio (3-D code) which is capable to simulate more realistic computation of multi beam structure. Some results after AJDISK simulations are shown in the following figures, the description of input parameters and output results is according to the demonstration (of AJDISK code) given in Appendix 3, the growth of output power is shown as function of the input parameters. Fig. 5.3 shows an initial AJDISK simulation result with output RF power of 68 W thereafter input parameters are adjusted by iterative simulations so as to get the result as shown in Fig. 5.4 with an output power of 204 W.

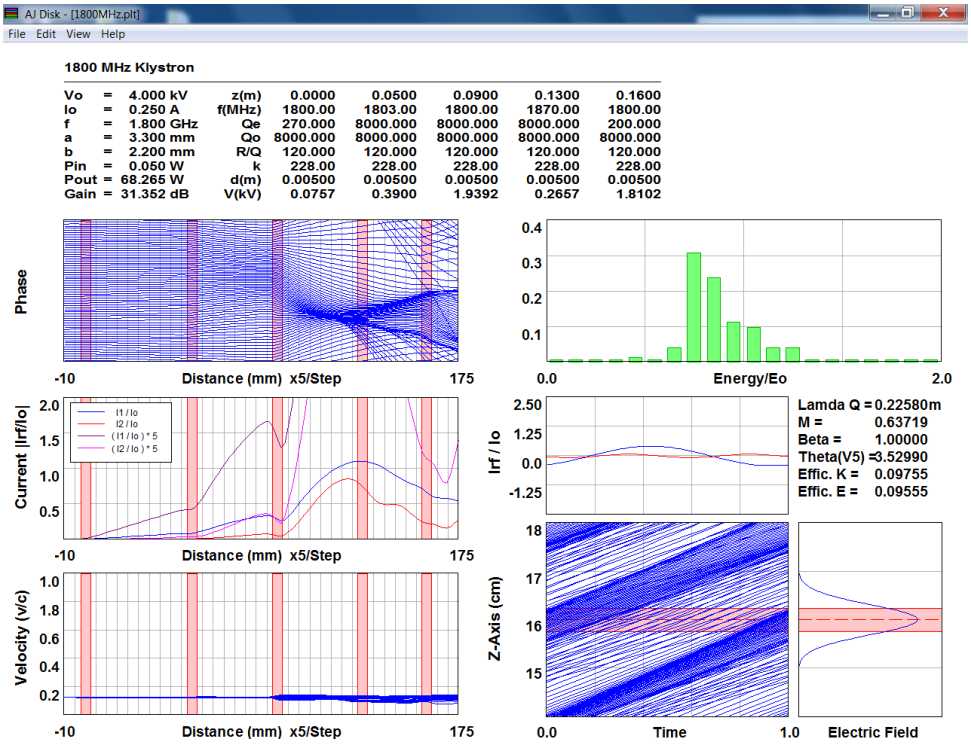

Fig. 5.3: Simulation in AJDISK (output power 68 W)

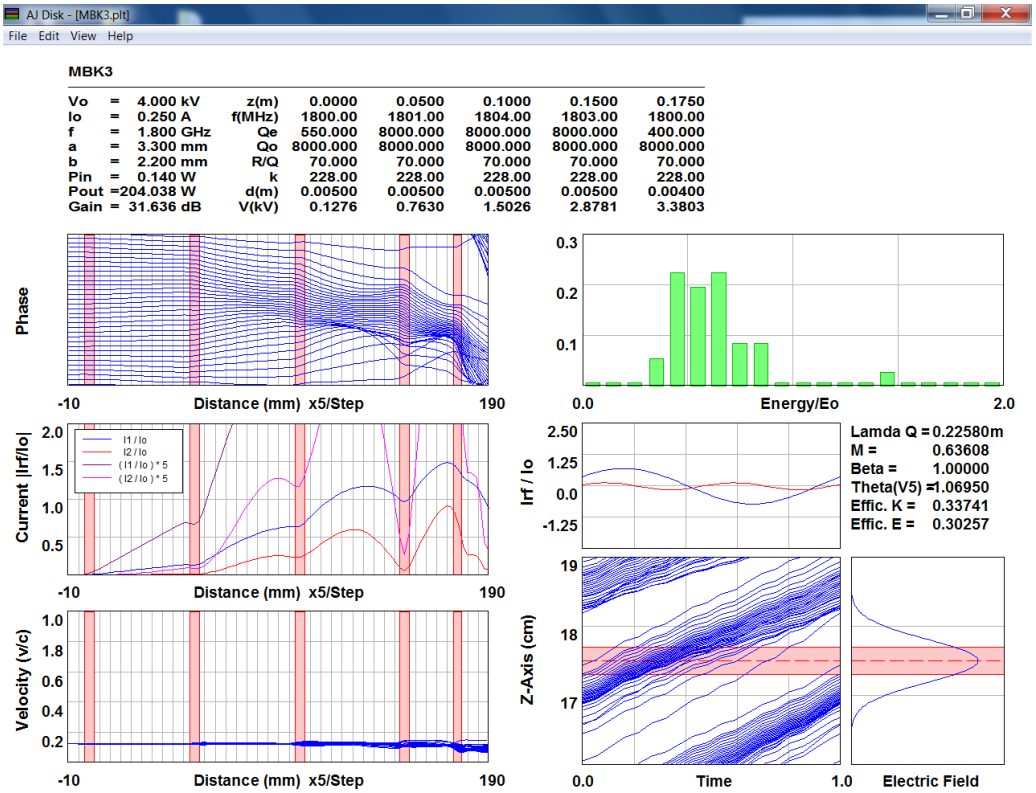

Fig. 5.4: Simulation in AJDISK (output power 204 W)

5.3 Simulation of Beam Wave Interaction in CST

The cavity frequencies and their mutual spacing optimized through AJDISK simulation are used as initial inputs in CST code for 3-D simulation of beam wave interaction process. The final optimization of the beam wave interaction parameters is done in CST, so as to get the required output RF power. The modelling of the RF interaction structure in CST particle studio is done as shown in Fig.5.5 where the AJDISK model of RF interaction structure is chosen for further optimization.

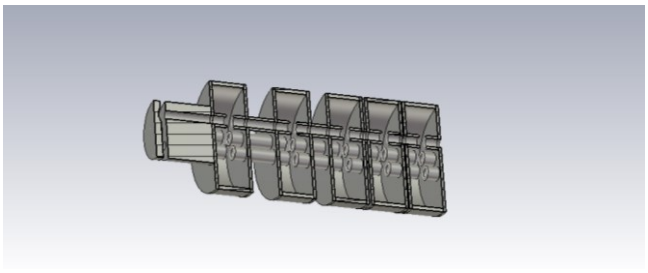

Fig. 5.5: Modelling of RF interaction structure

RF drive power is coupled via a port at the input cavity through a slot cut in its wall as shown in Fig. 5.6. The slot dimensions are to be optimized by iterative simulations in CST Microwave Studio.

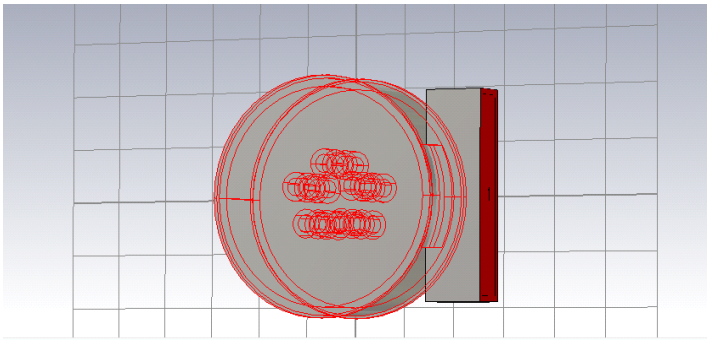

Fig. 5.6: Cavity with Port

A rectangular slot is made on the wall of cavity cylinder, in which a waveguide portion is inserted and a port is defined at the waveguide boundary. The excitation signal is given to the port and reflection coefficient S_{11} is measured at the port. The rectangular dimensions of the slot and external waveguide length are adjusted through simulation to get the desired coupling characteristics. We have found that a slot design of 32mmx 10mm is most optimum for both input and output cavities for RF power coupling while doing simulation for beam wave interaction in CST Particle studio.

A view of RF interaction region along with both the ports is shown in Fig.5.7. The electron gun portion is also shown integrated with RF section, while wireframe view of the structure is shown in Fig. 5.8 indicating the internal five drift sections.

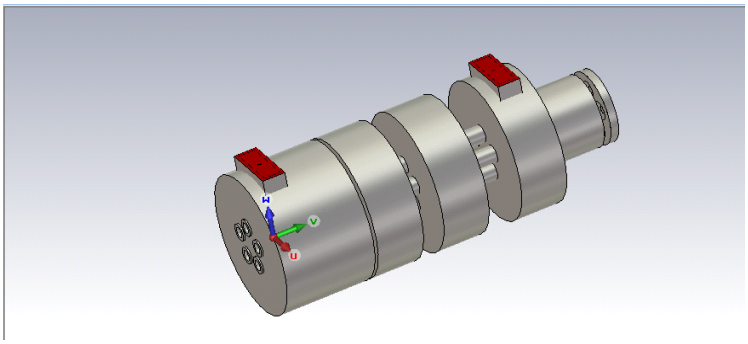

Fig. 5.7: RF interaction structure with ports

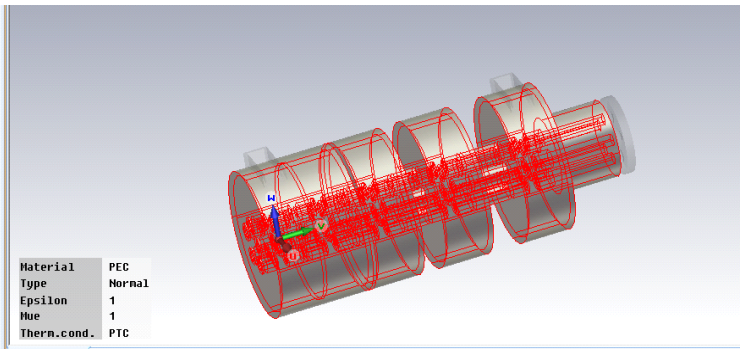

Fig. 5.8: Drift sections within the interaction structure

There were few issues while running the beam wave interaction simulation: after running a few cycles, the computer was not responding due to meshing errors. It was found through the mesh view shown in Fig. 5.9, that there was a common node between anode-cathode region which was responsible for the error. Later efforts were made to carry out the simulation with graded meshing i.e. different mesh size in different portions of the geometry. This improved the program execution and the simulation ran continuous for 3-4 days many times. However every time it stopped abruptly, probably due to lack of hardware resources. The intermediate results of beam transmission are shown in Fig. 5.10 where a velocity modulated electron beam is displayed. However the output port signal has been terminated abruptly after few time of running the simulation, as shown in Fig. 5.11.

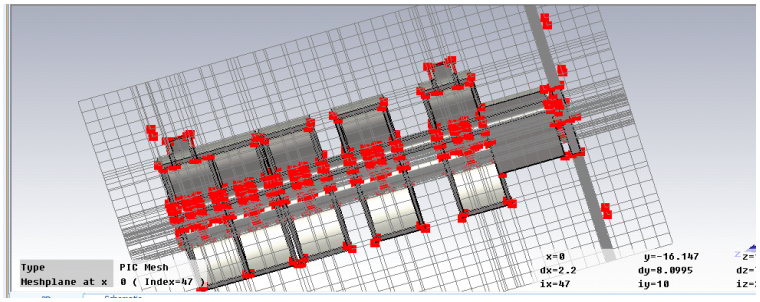

Fig. 5.9: RF interaction region along with mesh view

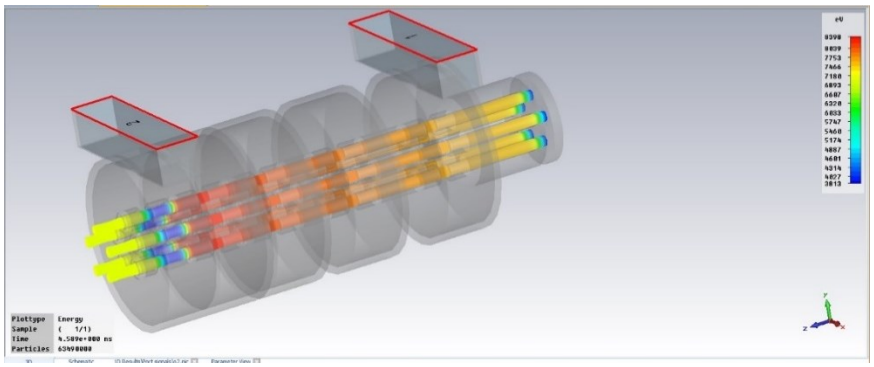

Fig. 5.10: Beam propagation during interaction simulation

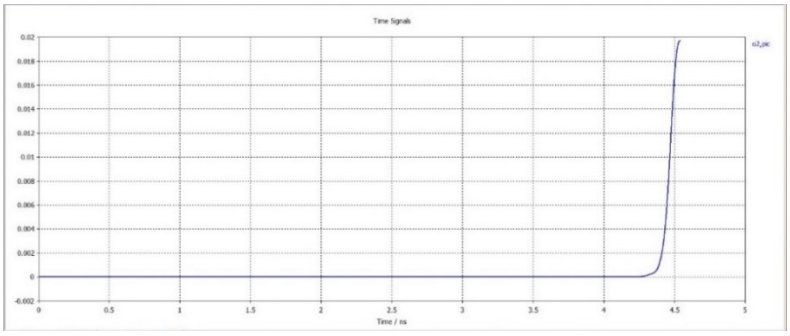

Fig. 5.11: Growth of output port signal during interaction simulation

Later the simulation was run on an upgraded workstation with improved storage memory and also the reasons for termination of solver were identified. It was found that the error was due to a very small discontinuity at the wave guide-cavity wall interface, where a rectangular structure was meeting the cylindrical surface. One patch was used for filling the gap between waveguide and cavity wall, the simulation was terminated abruptly due to improper meshing of this thin patch. However the problem was resolved by selecting 'Automatic' mesh option instead of 'PBA' meshing. Thereafter the simulation did not terminate abruptly.

One of the results, when simulation of beam-wave interaction process started to produce output results, is shown in Figure 5.12 which indicates clearly that electron beam is density modulated and the energy from the beam is being transferred at the output cavity gap for RF amplification

as is also evident from Figure 5.13 showing the growth of output port signal. Both of these results indicated that the beam wave interaction process was being successfully simulated in the 3-D code CST Particle Studio however parametric optimization was required. After doing iterative simulations by variation of parameters like cavity frequencies along with their mutual spacing and RF input conditions, Figure 5.14 shows one of the optimized result of output port signal after a complete run of beam wave interaction. The final amplitude of the output port signal is found as 56.816 as shown by the measure lines which corresponds to an equivalent output RF power 1.61 kW i.e. squared amplitude divided by two.

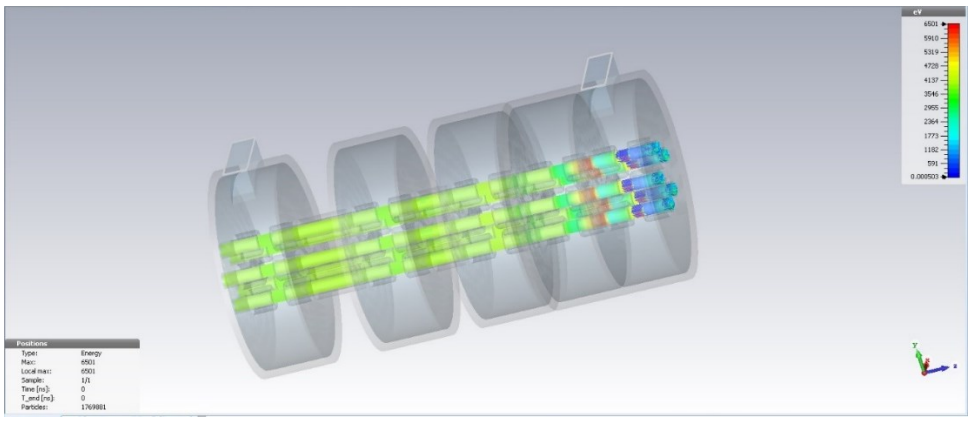

Fig. 5.12: Simulations for beam wave interaction in CST

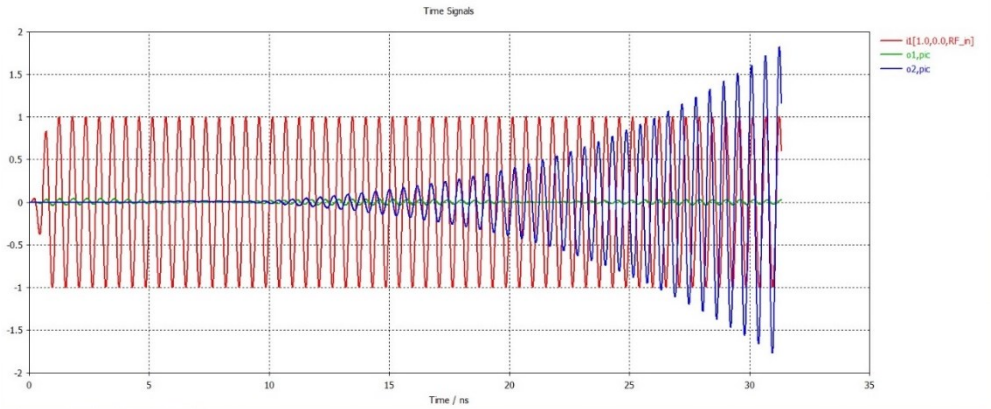

Fig. 5.13: Growth of output port signal in CST

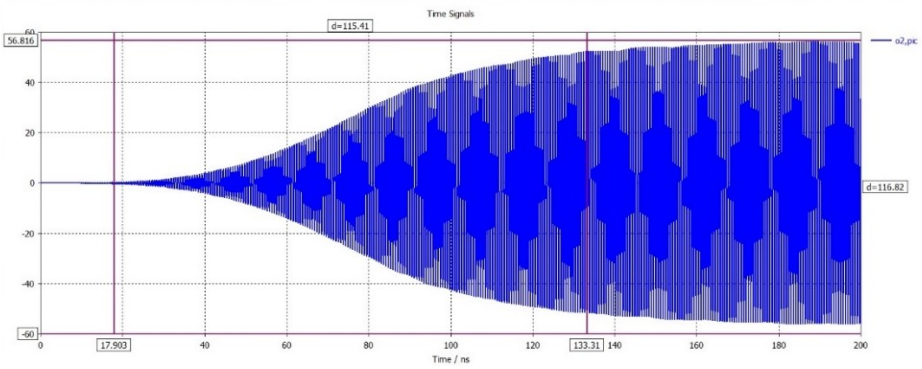

Fig. 5.14: Output port signal showing 1.61 kW RF power

However the above result is not showing the required output RF power, for which the penultimate cavity frequency is tuned further and input RF conditions are adjusted slightly so as to get the simulation result of Fig. 5.15 which shows the required output power i.e. 2 kW.

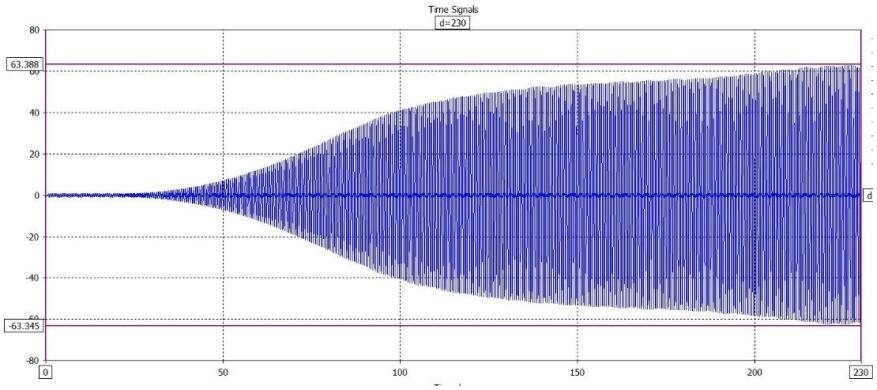

Fig. 5.15: Output port signal showing 2 kW RF power

The beam wave interaction simulations presented in this Chapter have established that with chosen multi beam design parameters, the required RF power can be produced with given efficiency. The design studies on multi beam klystron is concluded here with above mentioned results. The next part of our design study on klystron variants includes some design aspects of a sheet beam klystron. The following Chapter presents the design of a sheet beam RF cavity and its frequency characterization. The chosen frequency for design is 2.1 GHz which lies within the band of above L/S band klystron specifications mentioned in Chapter 1.

Publication Outcome (3):

Deepender Kant, A K Bandyopadhyay, L M Joshi, M V Kartikeyan and V Janyani, "Design Studies for a 2 kW (CW) Power L/S Band Multi Beam Klystron", Published in *IEEE Xplore digital library*, 'IEEE International Vacuum Electronics Conference Proceedings (IVEC 2018)' Published on June 21, 2018; DOI: 10.1109/IVEC.2018.8391591

CHAPTER 6
DESIGN STUDIES FOR A SHEET BEAM KLYSTRON CAVITY

A detailed study of single beam and multi-beam klystrons with cylindrical configuration of electron beams and cavities has been presented in previous chapters. For meeting still higher output power demand with such devices, either beam voltage or beam current should be increased. It is considered impractical to increase the beam voltage beyond 500 kV due to voltage breakdown and arcing issues. Higher perveance beam (i.e. high beam current) is also not a good choice due to increased current density and hence higher space charge forces leading towards lesser efficiency of the device. Also this would require higher confining magnetic fields. The multi beam klystrons provided some solution to this problem but due to multiplicity of parts they are complex and not consistent with low manufacturing costs.

This chapter deals with our design studies on another variant of klystron known as a Sheet Beam Klystron (SBK). The sheet beam klystrons with their lower manufacturing cost and simpler geometry provide a good alternative for high power devices at higher frequencies. In conventional cylindrical beam klystrons the output power of the device scales down as the square of the frequency whereas in sheet beam devices, output power scales down linearly with frequency. As mentioned in Chapter 1, the working of sheet beam klystron is similar to that of conventional klystron but the only difference is that here rectangular beam is used instead of cylindrical beam, resulting an increase in surface area as well as cross sectional area of beam. The key design issue is to form a beam that is as thin and as wide and can carry as much current as consistent with the optics of beam generation as well as with beam confinement [122]. This chapter present the design approach for making a sheet beam RF cavity, the frequency for design is chosen at 2.1 GHz which is having the reference of a SLAC's SBK under design and development for its intended use in their FEL source. However the designed frequency also lies in the range of our L/S band klystron specifications.

A sheet beam is capable to carry higher amount of current with lower charge density which resolves many issues as mentioned above. Besides that, SBK has the following structural advantages.

(i) High aspect ratio sheet beam allows cavities of larger area to dissipate heat produced due to I^2R losses.

(ii) Simplified fabrication of klystron cavity when compared to multi beam klystron. SBK cavity can be made as two plates separately and then combined together.

These characteristics make SBK a promising device for high frequency and high power amplifier applications. There are several challenges in designing a RF cavity [148-150] suitable for efficient interaction with a sheet beam. These include:

1. Achievement of flat field across the overall width of the beam
2. Mode propagation in the drift tube since the drift tube is no longer in cut off for TE modes, leading to oscillations and hence instability
3. Mode competition in increased gap length
4. Need for high performance 3D codes for the design
5. Reduced R/Q of the cavity due to the increased lateral dimension

6.1 Design Aspects of a Sheet beam Klystron Cavity

The single cell SBK cavity is essentially a TE_{10} rectangular waveguide positioned transverse to the direction of beam transport [122]. The electron beam traverses the narrow dimension of the waveguide and the broad dimension is chosen such that the waveguide is cut-off at the operating frequency of SBK. Since the waveguide section is cut-off, the electric field seen by the beam is constant across the width of the cavity. The cut-off waveguide is terminated at both ends by quarter wave matching sections to produce a resonant structure.

Flat field profile is very much essential for the efficient beam wave interaction in SBK. It maintains the uniform shunt impedance across the beam. The shunt impedance refers to the available field to the beam for the given RF power. An ordinary rectangular cavity cannot provide such flat field. So some modification is necessary to get flat field profile. Some of the techniques used are:

- Barbell cavity
- H-block cavity
- Dielectric loaded cavity

The ‘H-block cavity’ is nothing but a variant of barbell structure and used at much higher frequencies such as beyond W-band frequencies where semiconductor fabrication techniques (LIGA etc.) are used. Our proposed design of sheet beam cavity lies in S-band and the conventional barbell structure is easily machinable so it is the optimum choice. The dielectric loading technique is having many other issues like selection of optimal dielectric material with suitable dielectric constant and thickness, also the braze-ability of dielectric material with metallic cavity walls is another problem. The barbell cavity is all metal structure, hence more suitable for the proposed design.

Concept of the barbell cavity:

RF interaction structure in SBK is mostly a barbell type of cavity. Study on single cell barbell cavity is the first step to design complex interaction structure for SBK. The RF cavity used for sheet beam interaction must be specially designed so as to provide a uniform electric field across the overall beam-width which is usually higher due to high aspect ratio of the beam. As mentioned above, in this design, there is a waveguide operated near cut off in the middle and on either side there are quarter wave sections for transforming the short at the waveguide wall to open at the wave guide port. The height of the quarter wave section is slightly larger than that of the central waveguide height. Larger the height difference between the two larger the length of the quarter wave section to get the flat field profile. The dimensions are very sensitive. Any minor change in the dimensions distorts the flat field profile considerably. Hence very precise machining is required.

Consider a simple rectangular waveguide operated near cut off as shown in Fig. 6.1

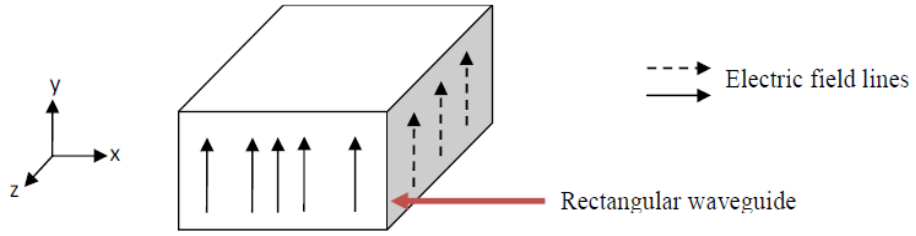

Fig. 6.1: Electric field distribution inside a waveguide operating near cut off

At cut off the slope of the ω-ß diagram is zero. Thus the group velocity is zero. If the waveguide is operated near cut off, the group velocity is very less. So the electric field profile operating at or close to cut off will appear as shown in Figure 6.2. The important directions of concern are the directions perpendicular to the electric field i.e. x and z direction.

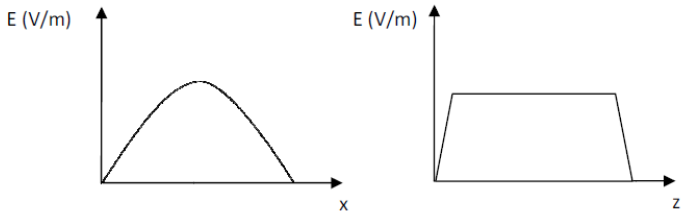

Fig. 6.2: Electric field profile along the x and z direction

Thus the needed flat field profile is available along z direction. Such a component can be used in the SBK provided the direction of the electron beam is parallel to Y-axis.

Another important thing to be considered is that the above mentioned structure is essentially a waveguide and not a cavity. So we need to close this waveguide from either side. For this

purpose a shorted quarter wave section is used. The short on the one side will get transformed to open by the quarter wave section. The three sections forming the barbell cavity are separated for viewing conveniently and are shown in the figure 6.3.

The height of the quarter wave section is greater than that of the middle waveguide section but has the same length as the waveguide section. The width of the quarter wave section is not exactly λ/4. The greater the height difference the greater is the width required to get the flat field profile.

Thus the SBK cavity is not a re-entrant cavity as in conventional cylindrical beam cavity. The structure of the cavity is entirely different and specially designed for interaction with the high aspect ratio sheet beam.

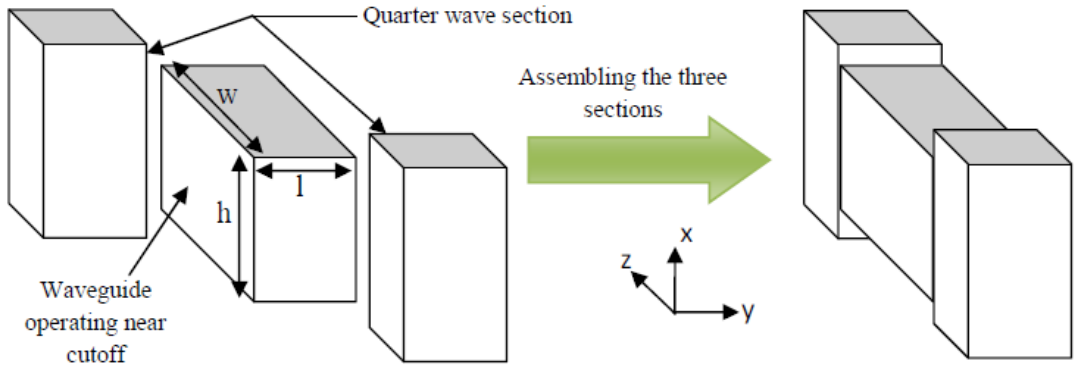

Fig. 6.3: Barbell cavity showing the middle waveguide section and the two quarter wave section

6.2 Simulation of a Sheet Beam RF Cavity

The operating frequency for the proposed sheet beam cavity is 2.1 GHz (i.e. within the S-band, as under present study) and also this refers to a recently published paper of SLAC [113].

As we know for a barbell cavity design, the middle section has to be near cut off.

$$\text{so} \quad \lambda = c / f$$

$$\lambda = \ 3\text{x}10^{8} / \ 2.1 \ \text{x}10^{9} \ \ \text{meter} \ = 142.85 \text{ mm}$$

For a wave to propagate in a waveguide the broader dimension a should be,

$$a >/ \lambda/2 = 71.\ 42 \text{ mm}$$

For the waveguide operation close to the cut off conditions the broader dimension ‘a’ is chosen as 72 mm. So h = 72 mm. Thus now we got one of the middle section dimensions ‘h’. The width of the waveguide depends on the beam width along with the required clearance. The length of the middle section can be considered an equivalent to the parameter ‘cavity gap’ in

the conventional re-entrant cavity. So it depends on the signal wavelength of the microwave to be amplified and we need less length for the cavity to get better coupling coefficient. Since the wavelength is 142.85 mm the cavity length 'l' is chosen as 50 mm initially. The reference paper [113] shows that a beam of dimensions 50.4 mm×4.2 mm has been used at this frequency. So the width of the cavity is chosen as 100 mm, to give margin between the beam and the metal walls. Thus a comfortable margin of 24.8 mm on either side of the beam is given.

To design the two quarter wave sections, we need the help of the 3D CAD tools like CST Microwave Studio (MWS), MAGIC-3D etc. Since the accurate PIC (Particle In Cell) based tool MAGIC-3D is extremely time consuming, for the actual design the CST MWS is used and the MAGIC-3D is used for cross-validation of results.

Figure 6.4 shows the 3D view of the cavity along with its drift tube modelled in CST MWS. The cavity is modelled as vacuum structure while surrounding is taken as PEC. The simulation was started with cavity dimensions (referring to Fig. 6.3) as mentioned in Table 6.1 and varying the width of quarter wave section in the range 30 mm to 50 mm. The dimensions of drift region on both side of the cavity are taken as 95 mm x 8 mm for the simulation.

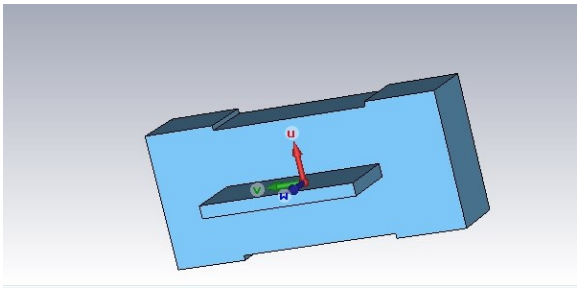

Fig. 6.4: Modelling of a SBK cavity in CST Microwave Studio

Table 6.1: The SBK cavity's initial design parameters

Design Parameter	Value (in mm)
Cavity height	72
Cavity width	95
Cavity length	50
Quarter wave section height	75
Quarter wave section length	50

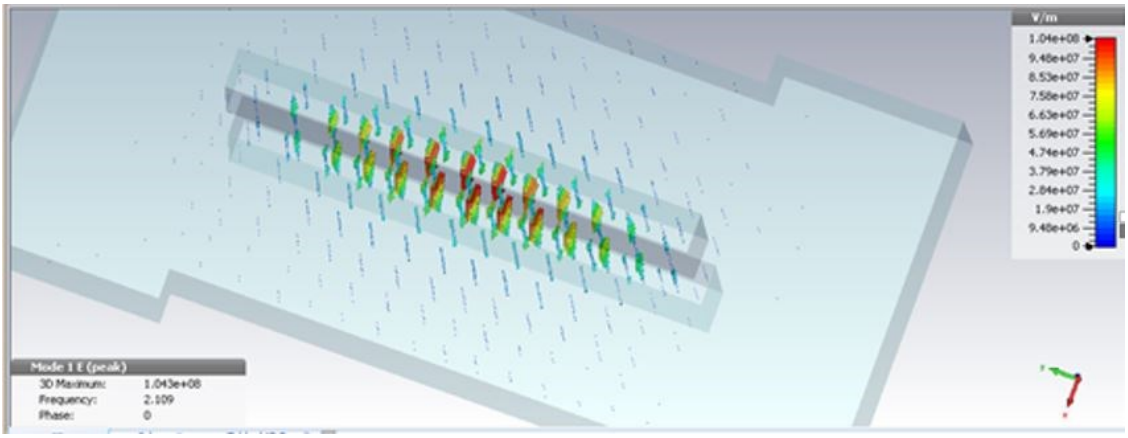

Fig. 6.5: Eigen mode simulation in CST Microwave Studio

The required eigen mode frequency is found 2.109 GHz as shown in Fig. 6.5 after few iterations by varying slightly, the above mentioned parameters along with variation in the width of quarter wave section. The optimized dimensional parameters are given in Table 6.2 for getting the required eigen mode frequency.

Table 6.2: The optimized design parameters of SBK cavity

Design Parameter	Value (in mm)
Cavity height	78
Cavity width	95
Cavity length	50
Quarter wave section height	86
Quarter wave section length	50
Quarter wave section width	36

Although the required frequency has been found yet the desired flat field profile along the beam width direction has not been achieved as is evident from Fig. 6.6 which indicates the electric field profile along beam width direction.

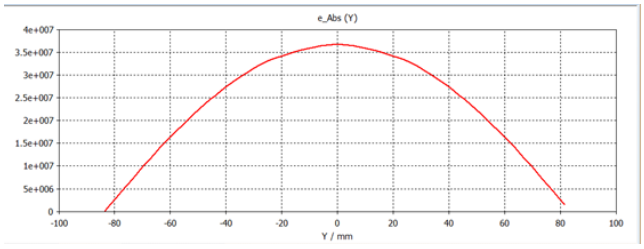

Fig. 6.6: The field profile along beam width direction

Our aim is to get the resonant frequency of SBK cavity along with a flat field profile so further optimization of the design parameters is required. Increasing height of quarter-wave section improved the flatness, but resonant frequency decreases. Hence, width has to be increased above quarter wavelength to get back to resonant frequency. This in turn affects the flatness of field. Cavity height is one parameter which does not affect flatness of field but has an influence on resonant frequency so it can be increased above its minimum value.

Initially we have chosen the quarter wave section height as a variable parameter (in the range 74mm to 100 mm with 26 samples) to get the flat field profile while cavity eigen mode frequency is at 2.1 GHz. The field profile against each sample is shown in Fig. 6.8. The best result among these is highlighted as in Fig.6.9 for side height of 84 mm.

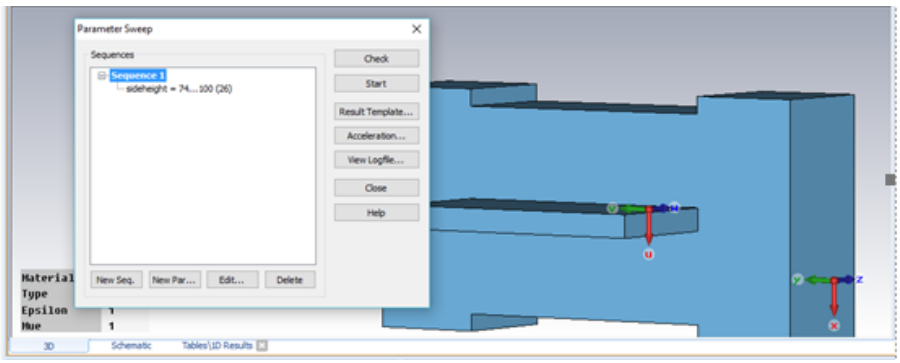

Fig. 6.7: Parameter optimization for quarter wave section height

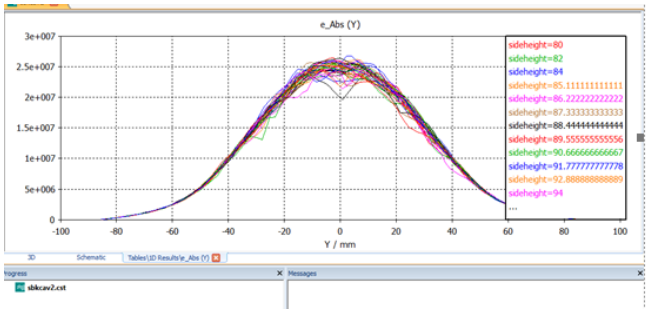

Fig. 6.8: The field profile with side height varying

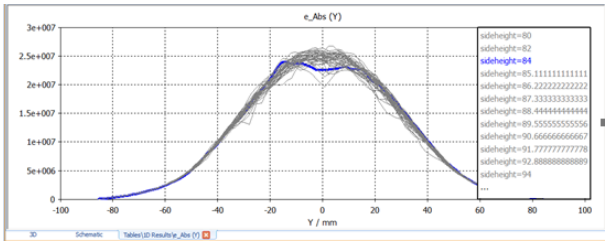

Fig. 6.9: The field profile with side height = 84 mm

However the result of Fig. 6.9 is yet not optimum as desired. So a two parameter optimization trial has been done for which quarter wave section height and width, both are variable parameter a shown in Fig. 6.10, one output result is shown in Fig.6.11. The best result among output results is shown in Fig. 6.12 for side height of 84 mm and side width of 44 mm.

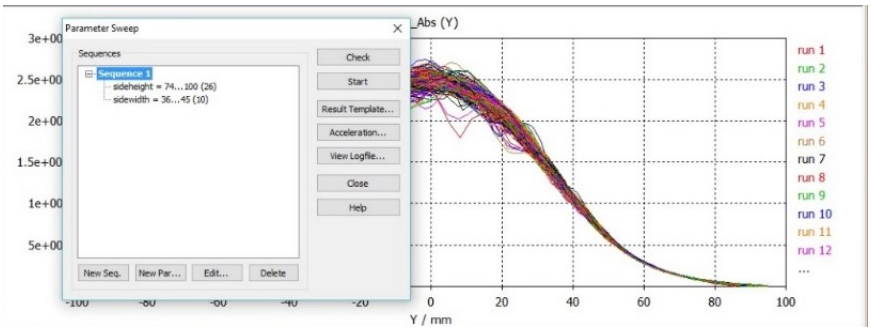

Fig. 6.10: Parameter optimization with two variables

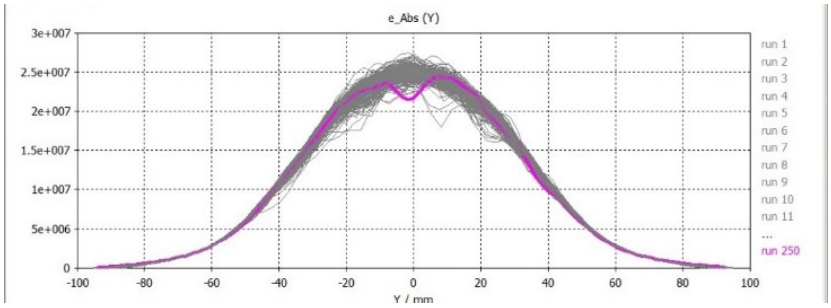

Fig. 6.11: Output result after optimization with two variables

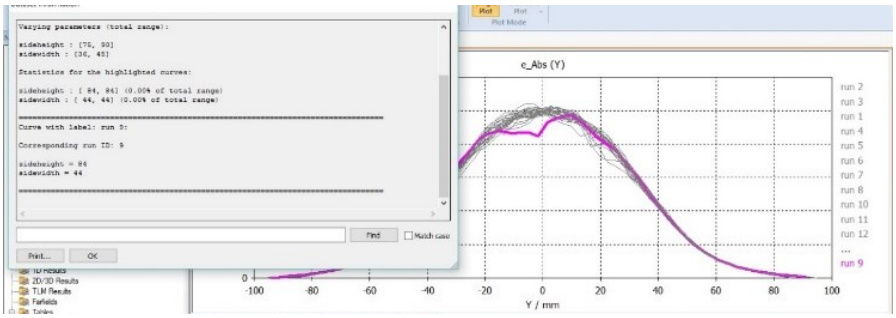

Fig. 6.12: The field profile with side height = 84 mm, side width = 44mm

The field profile as found in fig.6.12 is still not suitable for sheet beam operation. We have taken the cavity cell length as 50 mm in all simulations. Now we will consider this third parameter also as one variable and try to optimize all parameters so as to get the flat field profile along with desired frequency.

After iterative simulation process we have found one electric field profile along the beam width direction (in Y direction for our case) as shown in Fig.6.13 which is quite flat and the resonant frequency of the sheet beam cavity for this case is also at 2.101 GHz as shown in Fig.6.14.

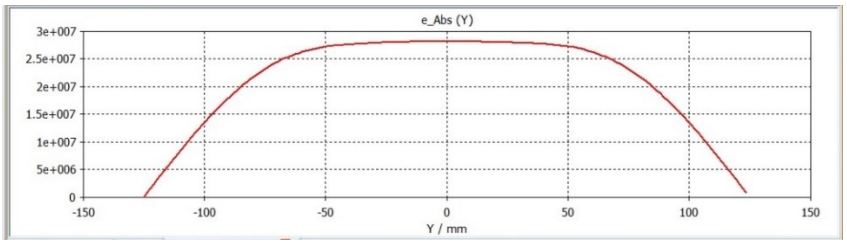

Fig. 6.13: The flat field profile after optimization

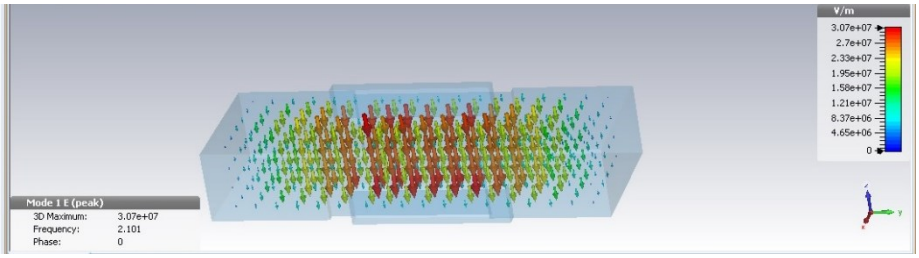

Fig. 6.14: The eigen mode frequency after optimization

Now the desired sheet beam cavity has been designed, it can be seen that an electron beam of 50.4 mm width [113] will see a total flat field while propagating in the designed SBK cavity as shown in Fig. 6.15. The simulated R/Q value for the designed SBK cavity is about 107 ohms as shown in Fig. 6.16. The final design parameters obtained through simulation are given in Table 6.3.

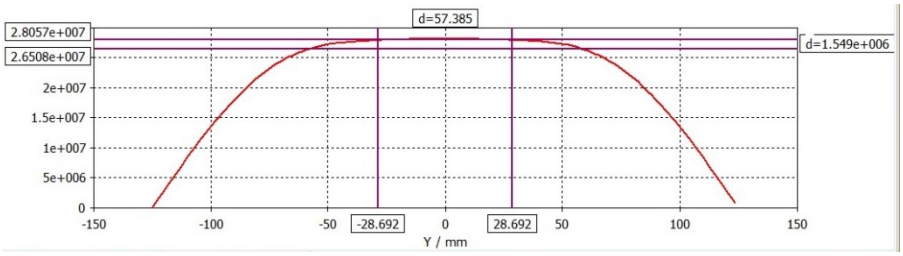

Fig. 6.15: The flat field profile along beam width of 50.4 mm

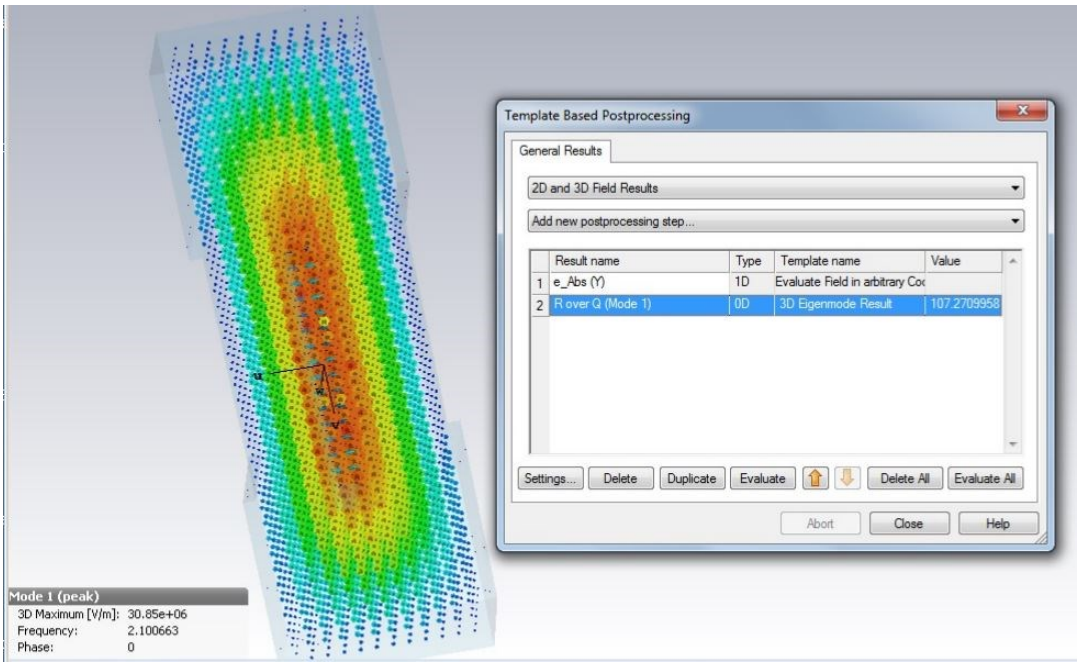

Fig. 6.16: The Simulation of R/Q for the SBK cavity

Table 6.3: The final design parameters of SBK cavity

Design Parameter	Value (in mm)
Cavity height	72
Cavity width	100
Cavity length	45
Quarter wave section height	82
Quarter wave section length	45
Quarter wave section width	75
Drift region dimensions	100 x 8

Simulation of Sheet Beam Cavity in MAGIC-3D:

The sheet beam cavity simulated and optimized through CST Microwave studio has been modelled in MAGIC-3D for verification of results. The geometry of the cavity is shown in Fig. 6.17 and the eigen mode simulation result is shown in Fig. 6.18 where the resonant frequency is found 2.103 GHz as desired. The plot of electric field intensity in the beam widths direction (along Y-axis) and its profile is shown in Fig.6.19. It can be seen that field is quite uniform along beam width direction.

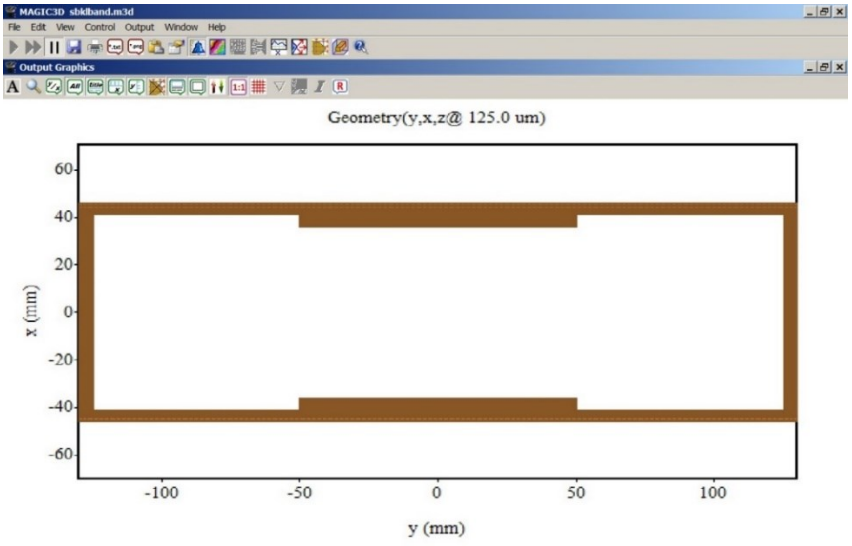

Fig. 6.17: Sheet beam cavity geometry in MAGIC-3D

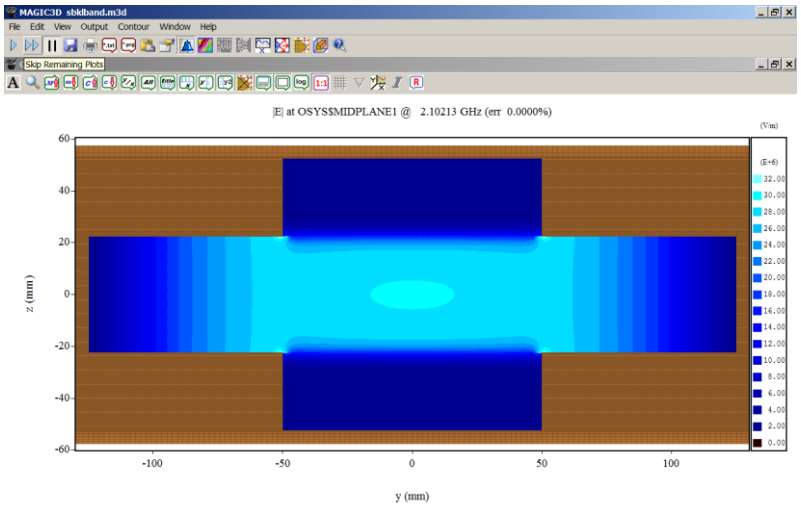

Fig. 6.18: Eigen mode simulation result in MAGIC 3-D

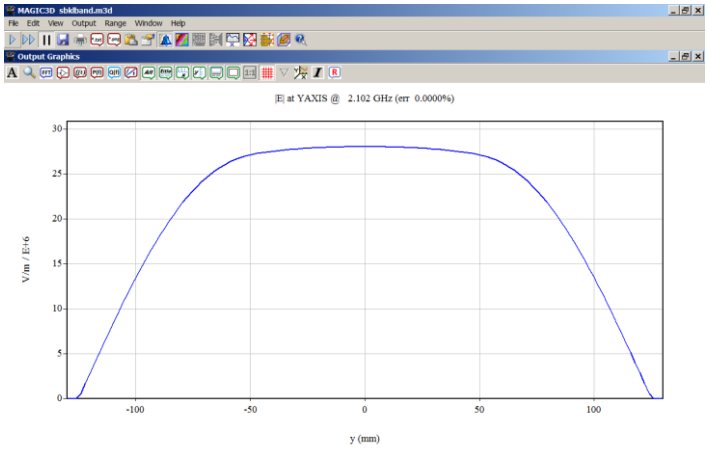

Fig. 6.19: The flat field profile along beam width

6.3 Development and Characterization of a Sheet beam RF Cavity

After optimization of SBK cavity's dimensional parameters through simulation using CST Microwave studio and cross-validation of the simulation results with MAGIC simulations, the engineering design of the sheet beam cavity has been worked out as shown in Fig. 6.20.

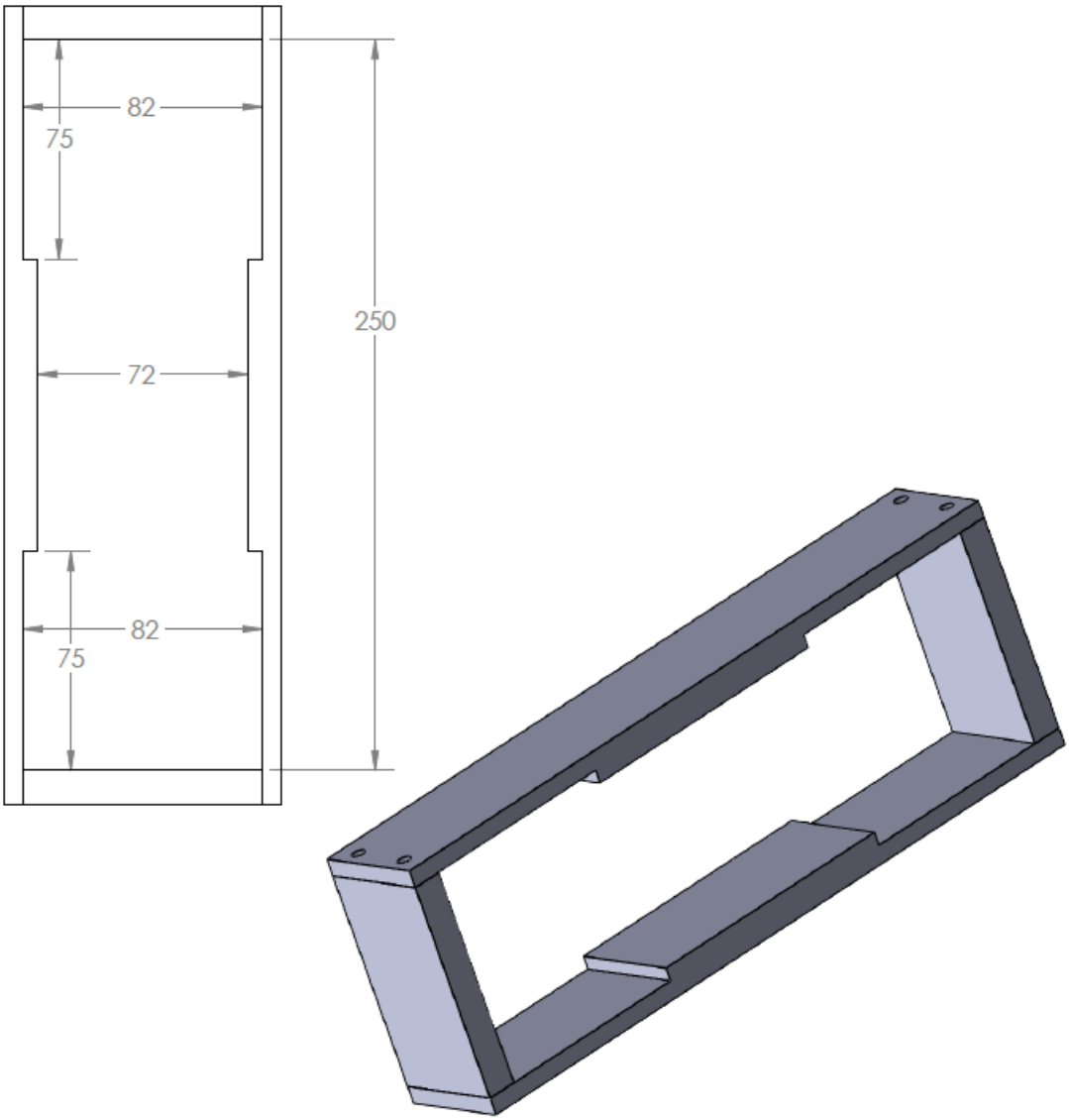

Fig. 6.20: Engineering design of the sheet beam cavity

An Aluminium cavity has been fabricated along with its two cover plates to close the barbell structure, as shown in Fig.6.21. This is used to characterize the cavity through cold measurements. However a practical SBK cavity will be made of OFHC copper.
There is a hole at the centre of the one aluminium plate and six equally spaced holes on its full length. These holes are used for the excitation and perturbation of the cavity. The cavity is placed in between the aluminium plates and screwed tightly.

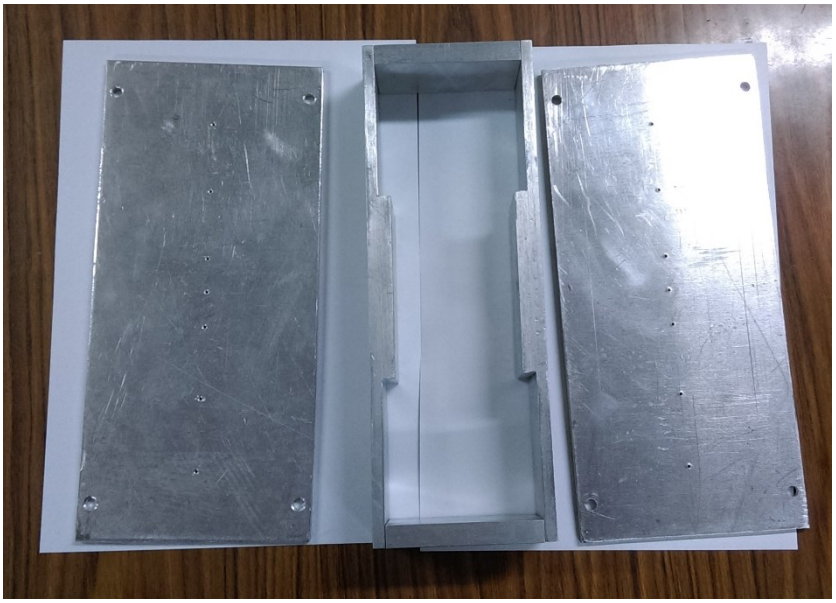

Fig. 6.21: Fabricated sheet beam cavity

The cold testing is done using the Vector Network Analyser with following procedure;

1. Initially calibrate the equipment by E-Cal Kit for desired frequency range (1GHz to 3 GHz).
2. Then the port A is connected to an SMA connector and thereafter SMA to N-type adaptor
3. A thin insulated copper wire is attached to the central conductor of the N-Type connector forming an antenna (Fig.6.22).
4. The open end of the copper is slightly inserted into the cavity via the hole provided in the aluminium plate. The wire is inserted in such a way that it should not touch the walls of the hole, this has been done precisely through 'XYZ moving platform' as shown in test set up of Fig.6.23. Then the depth of insertion of the copper wire (Probe coupling) is varied to get S_{11} in the given frequency range.

The entire set up should be clamped properly to avoid any unwanted fluctuations in the result.

Fig. 6.22: Probe antenna with assembled sheet beam cavity

Fig. 6.23: Cold test set-up for measuring the frequency of SBK cavity

The depth of probe penetration affects the resonant frequencies of the cavity mode. The smaller the penetration better is the accuracy of the observed results. The larger the penetration the other modes will appear more prominently and the frequency of the existing modes will be shifted slightly. This happens because the exciting probe acts also as a perturbing antenna which affects the field pattern considerably depending upon the probe penetration. However the probe coupling is not a realistic situation, since it is not implemented in a cavity installed in an actual device, it is being used here only to characterise the cavity frequency.

A measured result of cavity frequency on VNA screen is shown in Fig. 6.24 where plot of S_{11} parameter gives the resonant frequency 2.1723 GHz which is close to the simulated frequency i.e. 2.1 GHz. Here the excitation probe is inserted slightly deeper at the central hole, so that we are getting a single dip at 2.1723 GHz.

Fig. 6.24: Measured resonant frequency of SBK cavity

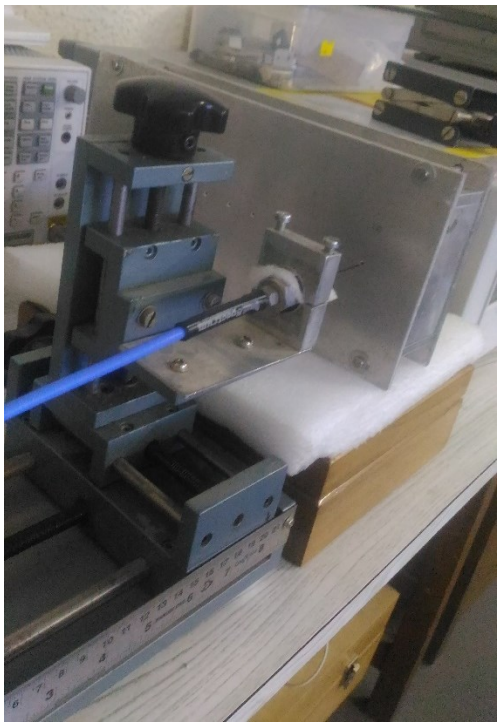

Fig. 6.25: SBK cavity excited through end

In another case the cavity is excited at the end as shown in Fig.6.25. Here the dominant mode is weak but the higher order modes are stronger and hence we get a very small dip for the dominant mode and another dip at 2. 296 GHz as shown on VNA screen in Fig.6.26.

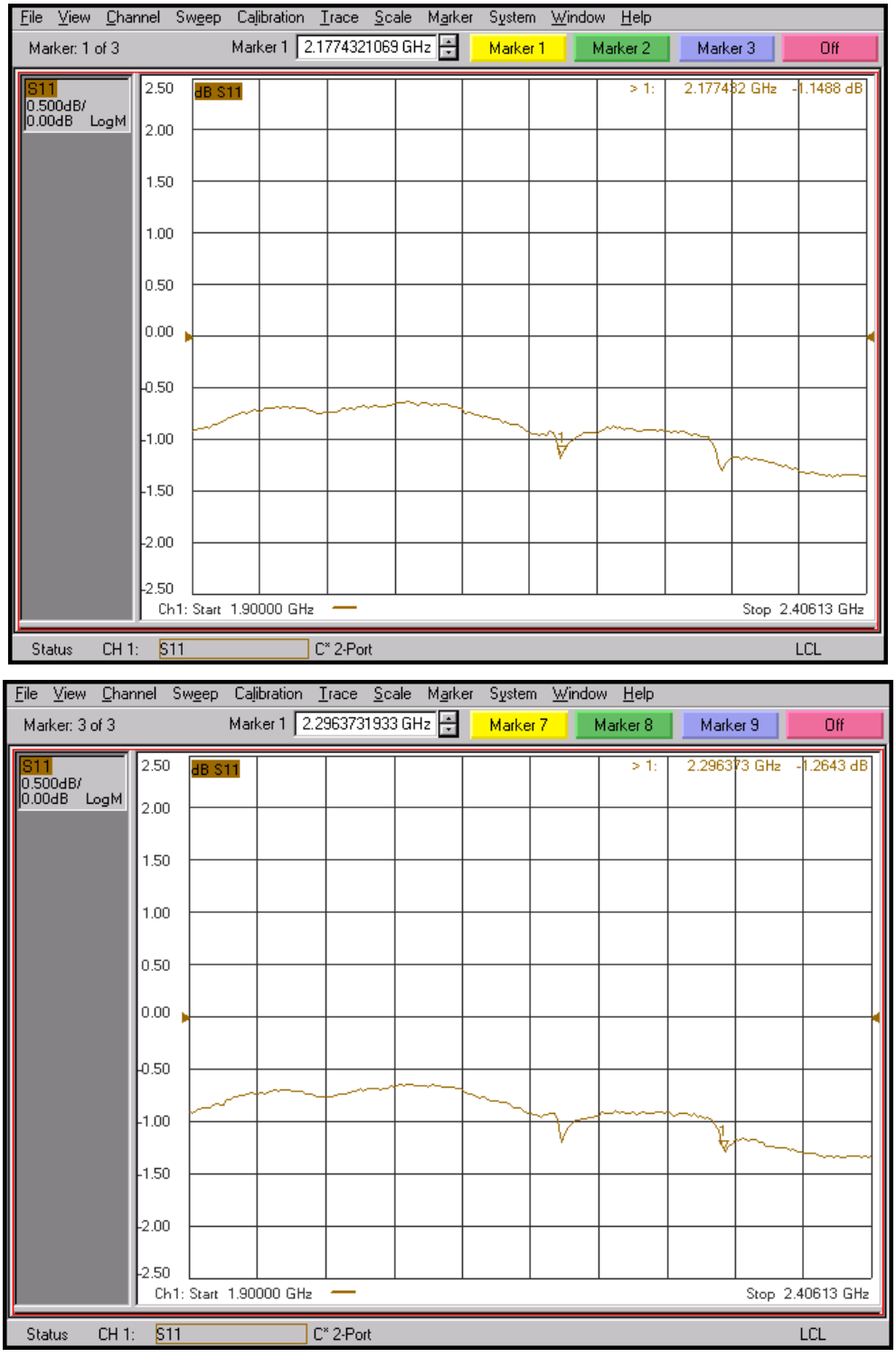

Fig. 6.26: Measured resonant frequencies for first two modes of the cavity

After measuring the second mode frequency of the fabricated SBK cavity, the simulation of the cavity in CST Microwave studio has been run again to check the second mode frequency which is found as 2.263 GHz as shown in Fig.6.27 which confirms that the fabricated cavity is as per simulated design.

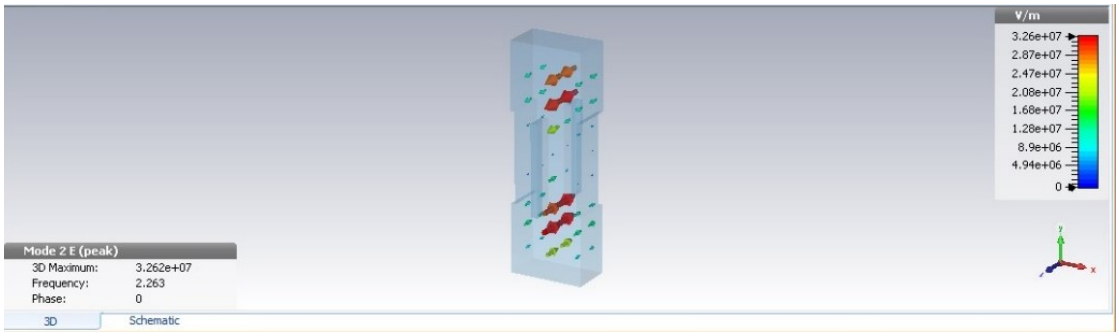

Fig. 6.27: Simulation of SBK cavity for its second mode frequency

In summary, we have designed a sheet beam cavity at 2.1 GHz and cross validated its design through two computational codes. The cold test model of the sheet beam cavity has been fabricated and it resonant frequency for the first two modes has been measured and the measured results are close to the simulated results.

The future work towards the SBK cavity design may be to characterize the cavity for other parameters such as R/Q for which a special measuring arrangements is needed. The cavity fabricated with OFHC copper may be used to measure its 'Q' parameter. The simulated value of 'Q' with Aluminium cavity is 11604 and with Copper it is found 14938 using CST code. We have presented a single cell cavity structure which has a lesser R/Q value than required for good interaction. Normally there are multi-cell cavities used in practical devices for their higher R/Q values [105], the design of multi cell cavities along with tuning and coupling mechanism can be carried out as a next part of this study. Also in continuation of design study on sheet beam klystrons, other design aspects of the device are the design of electron gun for sheet beam generation along with its confinement and beam-wave interaction simulations involving multi-cell cavities.

Up to now we have covered some of the design aspects for newer variants of a conventional klystron amplifier. The next chapter focuses on the design of a complete conventional klystron along with experimental verification of the electron gun design after its development. In later part the experimentally validated electron gun design has been converted into a multi beam electron gun with the same methodology as presented in previous chapters.

CHAPTER 7
DESIGN STUDY OF A 352.2 MHZ, 100 kW CW POWER KLYSTRON

In previous chapters we have gone through some design aspects of newer variants of a klystron amplifier by taking an example of a L/S band klystron. This chapter presents a conventional klystron's complete design through simulations by considering a 352.2 MHz, 100 kW CW power klystron under development at CSIR-CEERI, Pilani for its applications in various accelerator based systems [92], the other specifications of the device are given in the Table 7.1. This will be a large size vacuum electron tube device due to lower operating frequency and hence needs special infrastructure for its development. A beam stick tube has been developed and tested successfully. After experimental verification of the conventional electron gun, the design has been converted to a multi beam electron gun by the methodology presented in Chapter 3.

Table 7.1: Specifications of 352.2 MHz klystron

Parameters	Specifications
Frequency (MHz)	352.2
Output Power (kW)	100.0
Gain (dB)	45
Efficiency (%)	45-50
Beam voltage (kV)	30
Beam current (A)	7
Beam Radius (mm)	20
Fill Factor	.625

7.1 Design and Development of Electron Gun

The design of electron gun [98] has been carried out with given specifications through similar analytical calculations as described earlier in Chapter 3. The computed value of drift tube radius is 32.0 mm by taking beam voltage of 30 kV and frequency of operation i.e. 352.2 MHz and the beam radius is taken as 20.0 mm by considering 0.625 fill factor. Then simulation of

electron gun has been carried out with a planar cathode of 45.0 mm diameter using Trak and MAGIC codes. Some of the simulation results for electron gun are shown as following.

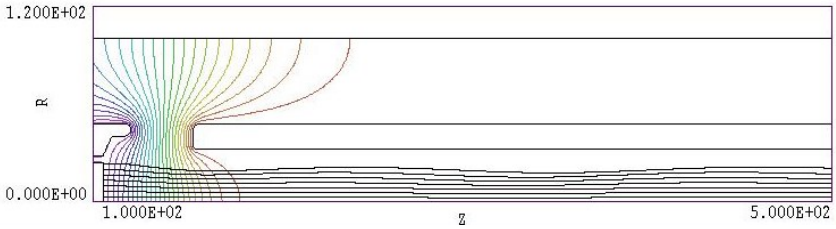

Fig. 7.1: Simulation of Electron-gun with TRAK

The Fig 7.1 shows the laminar flow of electron trajectories under the applied magnetic field of about 200 Gauss which is computed by using Brillouin formula [40]. The simulated value of beam current is 6.98 A in Trak. The design of electrodes optimized through TRAK has been re-simulated in MAGIC for cross-validation, as shown in Fig. 7.2.

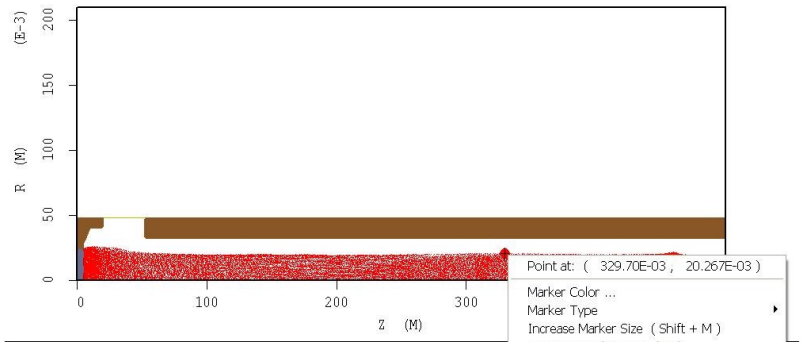

Fig. 7.2: Simulation of Electron Gun in MAGIC

The MAGIC simulation shown in the above figure is indicating the value of beam radius 20 mm as required and simulated current value is 7.02A. After cross-validation of electron gun design with two computer codes, the fabrication of electron gun has been carried out. The complete electron gun assembly has been leak tested and found leak tight. Fig. 7.3 shows the leak testing of electron gun on a helium leak detector.

Fig. 7.3: Leak testing of Electron Gun

7.2 Simulation of RF interaction Structure:

The design of RF interaction region for the klystron has been done using MAGIC-2D code after taking the initial design data optimized using AJDISK (1-D) code as shown in Fig. 7.4 where 101.3 kW RF output power is indicated.

The RF cavities are simulated individually to get their dimensional parameters so as to match their corresponding performance parameters like frequency, Q and R/Q. The Fig 7.5 shows the results of input cavity simulations. A typical RF cavity dimensions obtained after simulation are as follows in Table 7.2 to get the resonant frequency of 352 MHz.

Table 7.2: The dimensional parameters of cavity

Parameter	Dimension (in mm)
Cavity radius	177.5
Cavity height	200.0
Cavity gap	28.0
Drift tube radius	32.0

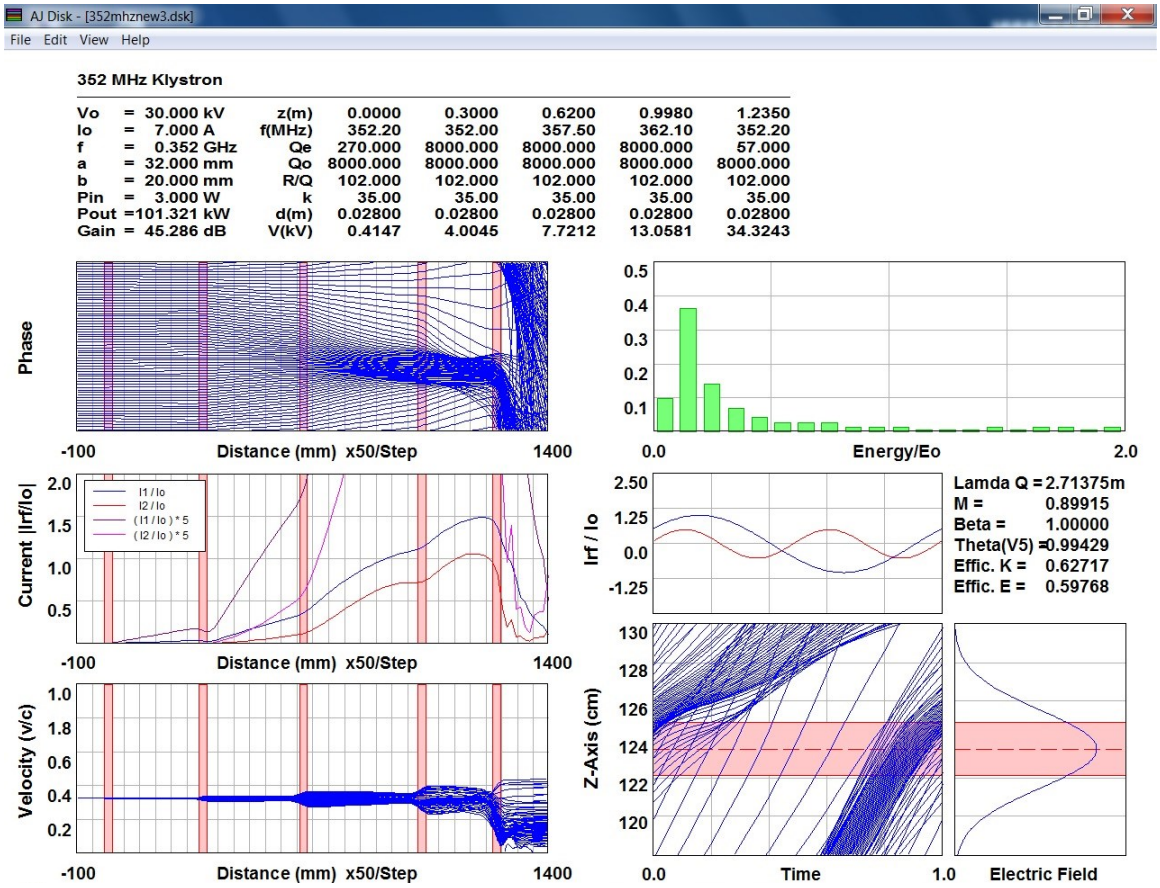

Fig. 7.4: Simulation of output power in AJDISK code (simulated power 101 kW)

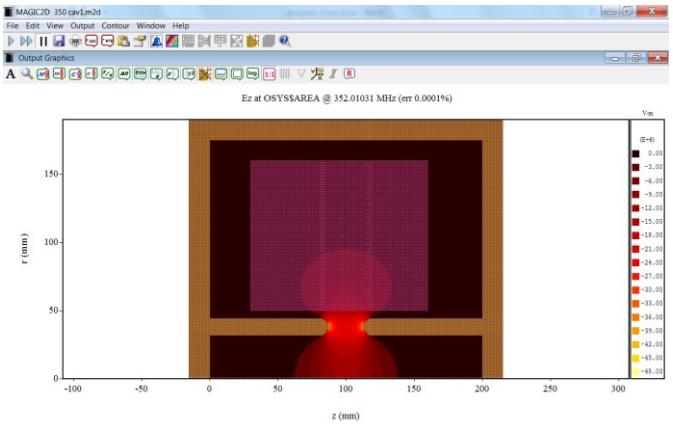

Fig 7.5: Simulation of the input cavity frequency using MAGIC

The intermediate and penultimate cavities have been also simulated using MAGIC as shown by Fig 7.6 and 7.7 which indicate the simulated eigen mode frequencies at 357 MHz and 362 MHz respectively for intermediate and penultimate cavities.

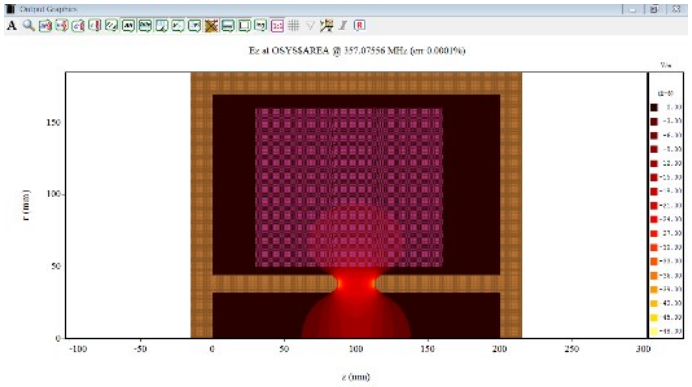

Fig. 7.6: Simulation of intermediate cavities in MAGIC

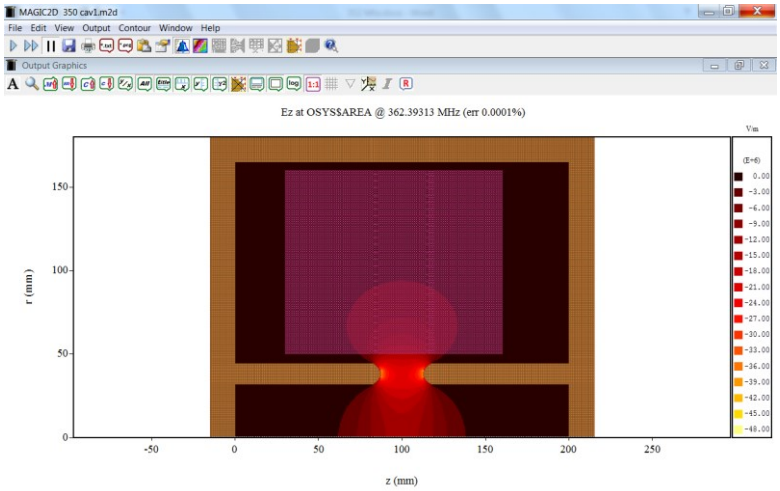

Fig. 7.7: Simulation of the penultimate cavity

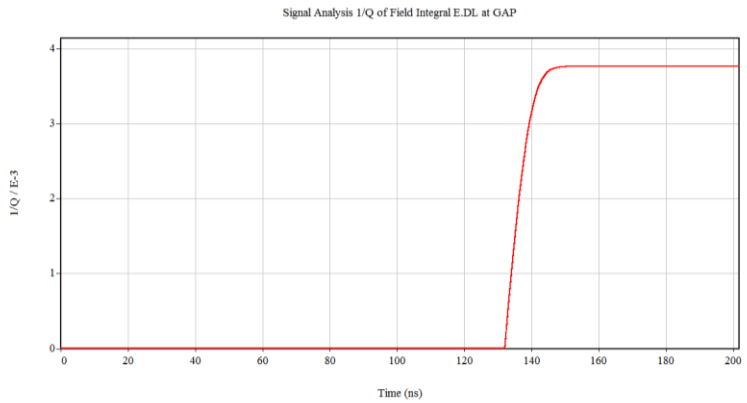

Fig. 7.8: Simulation result for Q of the input cavity

(1/Q = .0037 so that simulated Q value is 270)

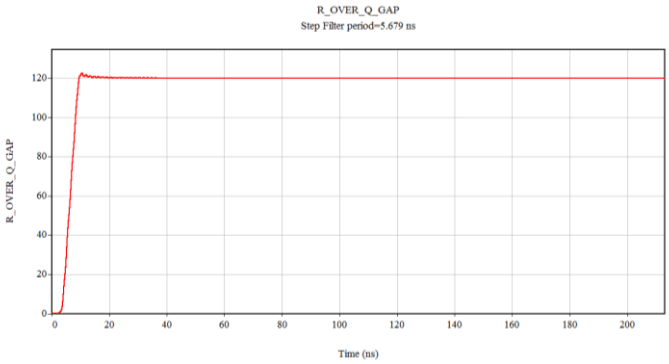

Fig. 7.9: Simulation result for R/Q of the input cavity

Simulation results of some important cold test parameters like Q and R/Q of the input cavity are shown in Fig. 7.8 and 7.9 respectively. The required Q value for the input cavity is 270 as indicated in Fig. 7.4. The MAGIC simulation of the input cavity has been done by varying the value of conductive load so as to obtain the required Q value as shown by Fig. 7.8. Later this load value has been used in beam wave interaction simulations as shown in Fig. 7.12. In practice the input cavity is loaded by the loop coupling of input coupler. The practical input coupler via loop along with a cavity tuner has been simulated in CST Microwave Studio as shown in Fig. 7.10. The resulting S_{11} parameter plot of Fig. 7.11 shows the computed value of loaded Q for input cavity 272.4 along with cavity resonant frequency at 352.2.

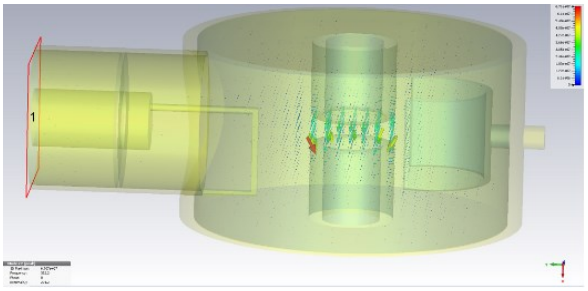

Fig. 7.10: Simulation of the input coupler

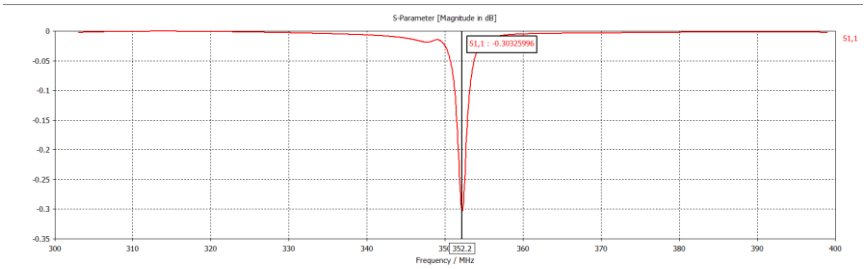

Fig 7.11: Plot of S_{11} parameter vs Frequency for the input cavity

After cold characterization of all cavities, the beam wave interaction process has been simulated and optimized in MAGIC-2D to get the desired RF power at the output cavity port as shown through Fig. 7.12 and 7.13. It may be noted from Fig. 7.13 that the simulated value of output power is 105 kW. The output RF power is measured across a conductive load defined across the output cavity with its loaded Q value of about 39. The value of RF drive power used in the beam wave interaction simulation is about 2.5W as shown in Fig. 7.14. Hence the simulated gain of the device through MAGIC is found as 46.23 dB and its electronic efficiency is 50% for 210 kW input DC power.

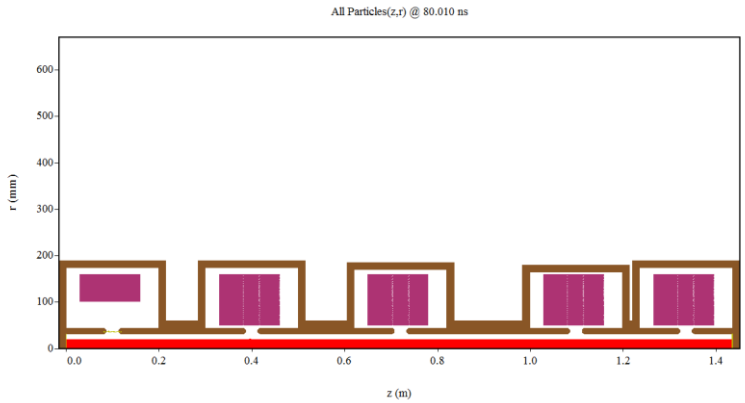

Fig. 7.12: Beam wave interaction simulation in MAGIC 2D

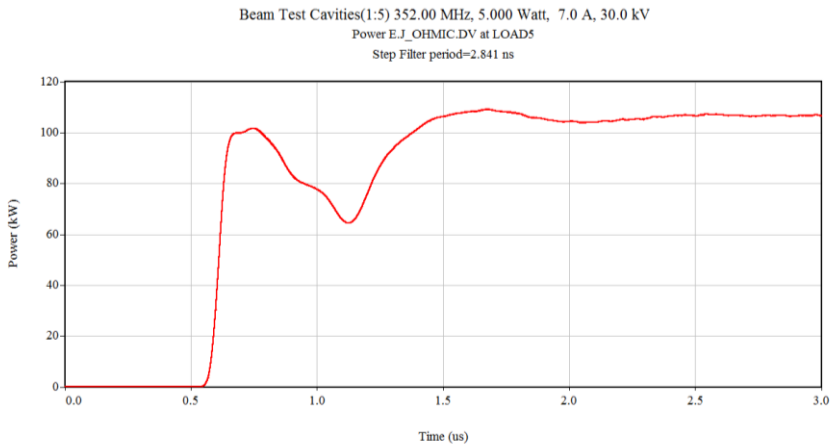

Fig. 7.13: Simulation of RF output power

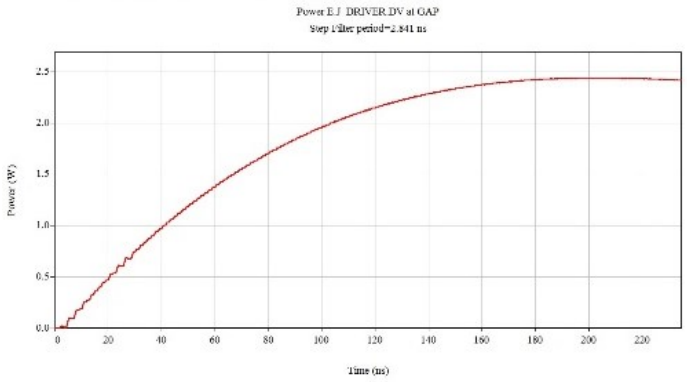

Fig. 7.14: Simulated RF input power

Design of output cavity:

The output cavity is designed to extract the maximum RF power from the interaction region therefore a suitable coupler is required to efficiently couple the RF power to external load. The design of the output cavity along with a door-knob type coupler is simulated in CST Microwave Studio as shown in Fig. 7.15. The resulting S-parameter plot shown in Fig. 7.16 gives its loaded Q value of 39.2 as required for the output cavity. The RF window for this device has been designed and reported separately [151].

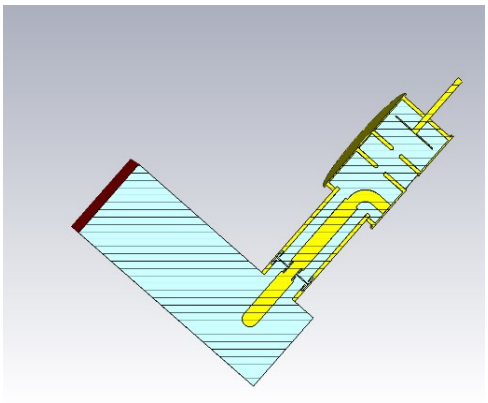

Fig. 7.15: Simulation of the output cavity

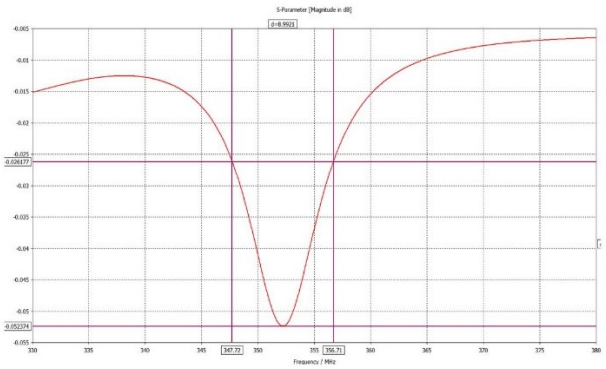

Fig. 7.16: S-parameter plot of output cavity

7.3 Development of RF Cavities:

After optimization of dimensional parameters for the RF cavity through simulations, the cavities have been fabricated with typical design parameters as shown in Table 7.2. The input cavity, second cavity and output cavity are having the same inner radius as mentioned in the Table 7.2. The penultimate and third cavities have been fabricated with 175 mm inner radius due to their higher frequencies i.e. 362 MHz and 357.5 MHz respectively as indicated by Fig. 7.4. However a tuning mechanism through a bellow will be provided in each cavity to tune the cavity frequency within certain range during hot testing of the device, as indicated in simulation of Fig. 7.10.

All the intermediate cavities have been developed and characterized for their frequencies as per requirement whereas the input and output cavities with their RF coupling arrangements are under development. Fig. 7.17 shows some of the fabricated cavity parts including cavity cylinders and the end plates brazed with drift regions. The input cavity cylinder along with one end plate assembly is shown in Fig. 7.18 where a hole in the cavity wall is visible for the required loop coupling.

(a)

(b)

Fig. 7.17: Fabricated cavity parts (a) cavity cylinders (b) end plate assemblies

Fig. 7.18: The input cavity under development

There are several parts required for implementing the tuning of RF cavities as shown in Fig. 7.19 which are used to make the tuner assembly. The movement of tuning paddle inside the vacuum is controlled by a screw from outside so an efficient mechanical design of the tuning mechanism is necessary. Fig. 7.20 shows a complete cavity assembly along with a tuning mechanism.

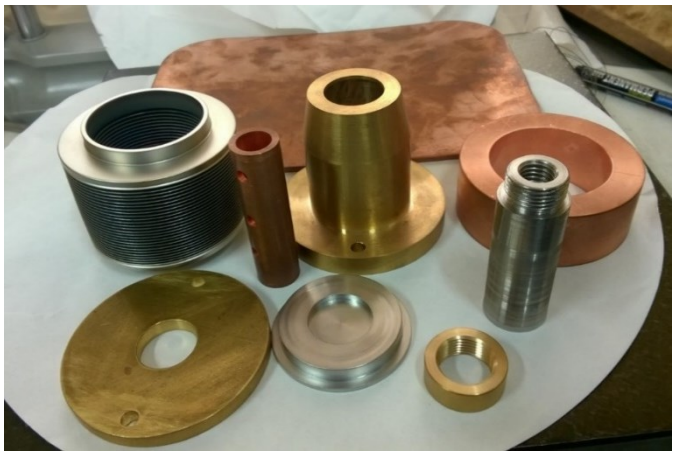

Fig. 7.19: The fabricated tuner parts

Fig. 7.20: Final cavity assembly with tuning mechanism

The measurement for resonant frequencies of the fabricated cavity structures has been done by exciting through a probe near the drift region and observing the S_{11} parameter on a network analyzer as shown in Fig. 7.21. The measured frequencies of the three intermediate cavities without tuner assembly are about 353 MHz, 358 MHz and 363 MHz which are close to our required frequencies. The cavity assembly with tuning mechanism as shown in Fig. 7.20 has been measured to get a tuning range of about 9 MHz by using the capacitive tuning through a paddle movement of about 45 mm inside the cavity cylinder.

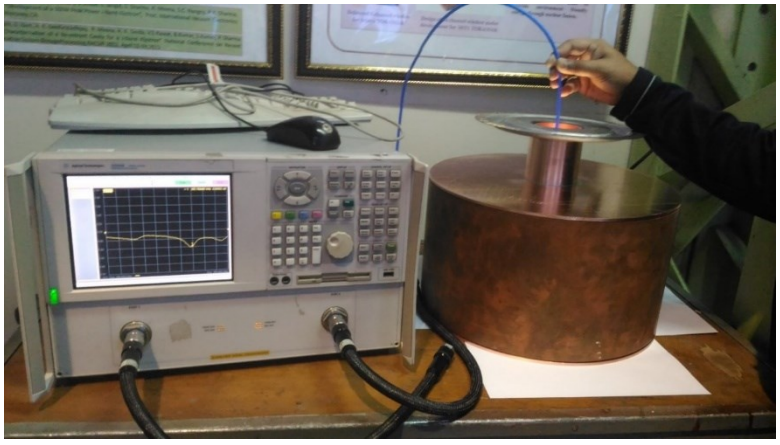

Fig. 7.21: Measurement of resonant frequency for the cavity assembly

7.4 Design and Development of Collector

The collector needs to have optimum design to ensure efficient removal of heat generated and also to stop any back streaming of electrons into the RF interaction region. Thermal analysis of collector for a klystron designer becomes very critical for high CW power tubes, as the energy in the spent electron beam may lead to damage of collector in case of inappropriate thermal management. The thermal design of the collector plays a vital role in deciding the overall efficiency and performance of klystron. This includes some analytical calculations for finding the design parameters of the collector followed by thermal simulations through computer codes, ANSYS (multi-physics) has been used here. The full beam power converted into an equivalent heat load is applied onto the inner surface of collector geometry modelled in ANSYS and cooling conditions are defined on the exterior surface. Design of collector with forced water cooling has been done and cooling channel's dimensions are optimized so as to get the surface temperature of collector below 100^0C to avoid boiling of water. Initially it was designed with smooth outer surface with simulation results as shown in Fig.7.22 indicating the maximum surface temperature of about 171^0C. Later the surface has been grooved for more efficient water cooling due to enhanced surface area [123] and simulation results for a cross section of grooved collector are shown in Fig. 7.23 which indicates the decrease in surface temperature i.e. below 85^0C.

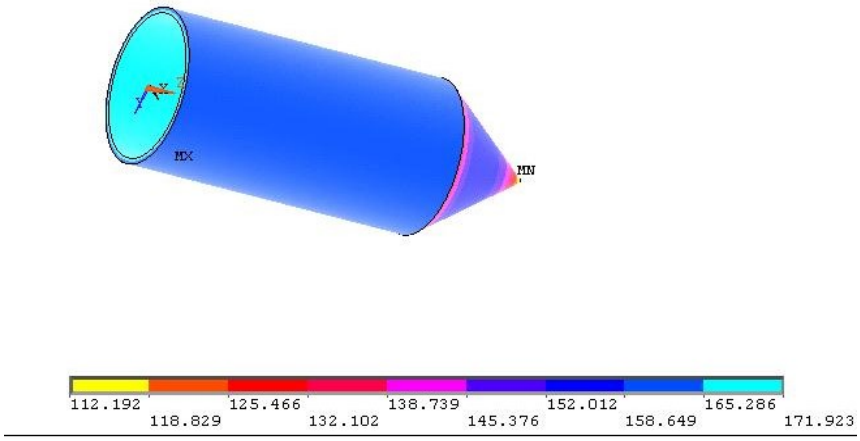

Fig.7.22: Simulation of collector using ANSYS

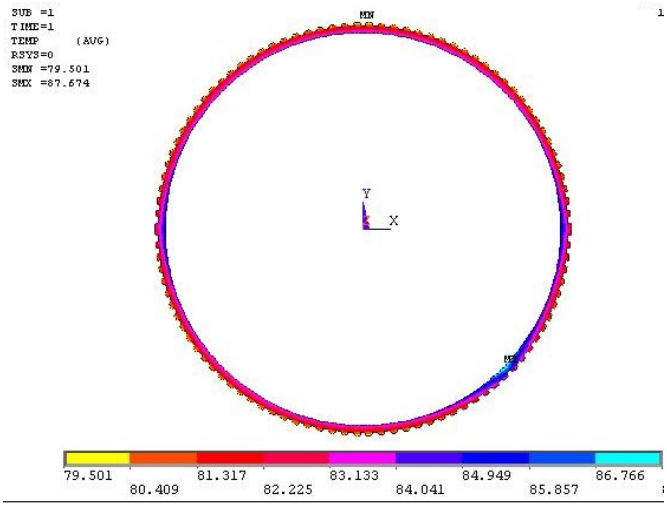

Fig.7.23 Simulation of collector with grooved surface

The optimized cooling parameters including the dimensions of the collector are as follows in Table 7.3, based on the ANSYS results. The collector has been fabricated as per optimized dimensions after simulations as shown in Fig. 7.24.

Table 7.3: The Collector design parameters

S. No.	Design Parameter	Value
1.	Water flow rate (with inlet temp. 20^0 C)	50 gallon per minute
2.	Collector inner diameter	150 mm
3.	Collector outer diameter	165 mm
4.	Conical length	125 mm
5.	Annular space between water jacket and collector	4.0 mm
6.	Number of cooling ducts on the exterior surface	130 ducts of 2.0 mm x 2.0 mm

Fig.7.24: Fabrication of Collector

7.5 Development and Testing of a Beam Stick Tube

After finalization of electron gun and collector design and their fabrication, a beam stick tube has been developed which consists of a drift region surrounded by an electromagnet sandwiched between electron gun and collector, to check the beam transmission and also to characterize the electron gun and collector design. A simulation result of beam stick tube using Trak is shown in Fig. 7.25 which displays the beam trajectories dispersing into the collector as there is no magnetic field applied after the end of drift region. The design schematic of beam stick tube is shown in Fig. 7.26 and the actual device is shown in Fig. 7.27 along with its hot testing set up.

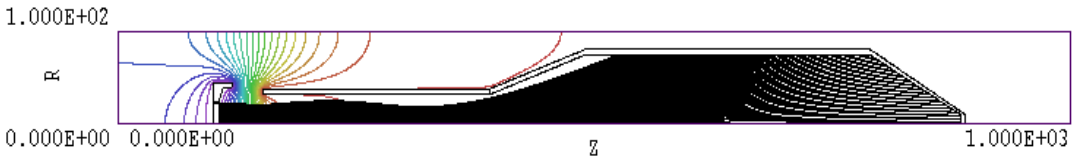

Fig. 7.25: Simulation of the beam stick tube using Trak

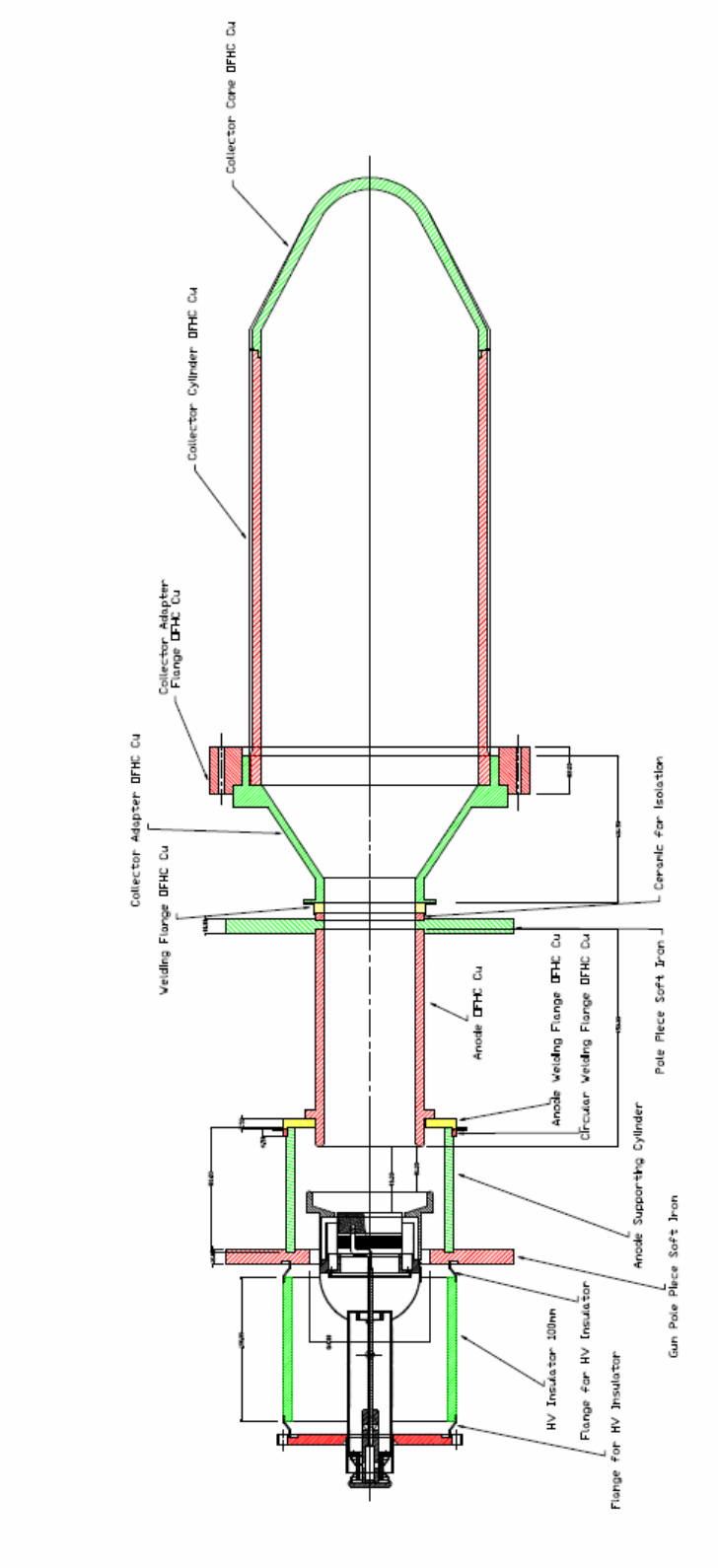

Fig. 7.26: Schematic of the beam stick tube

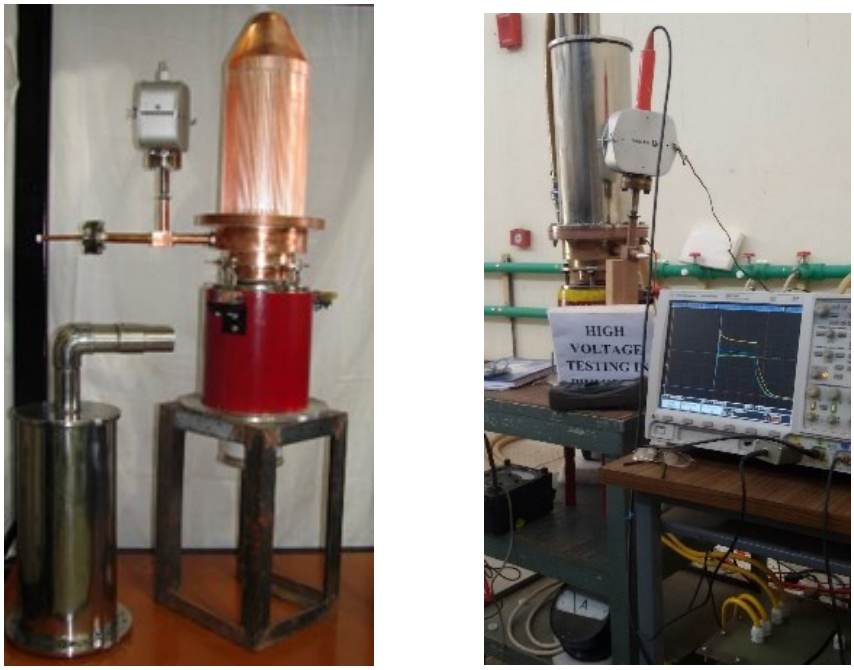

(a) (b)

Figure 7.27. (a) Developed beam stick tube along with electromagnet (b) Hot testing of beam stick tube

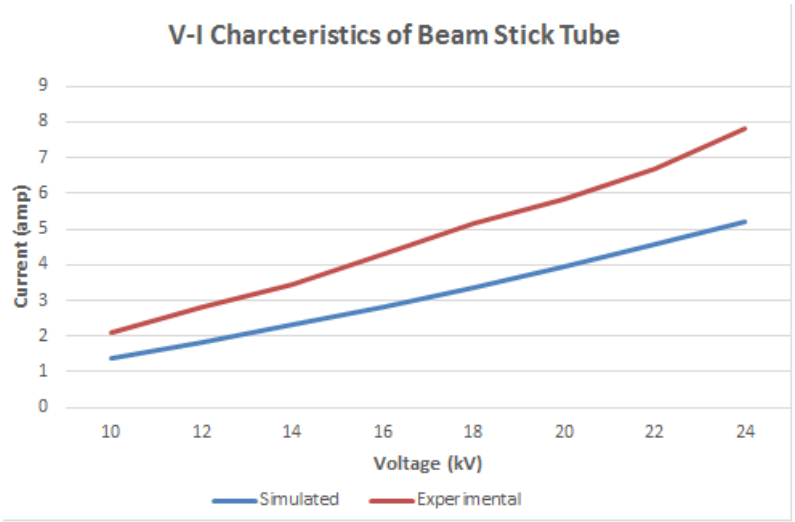

Fig.7.28 Measured Characteristics of beam stick tube

The beam stick tube has been tested successfully and the measured V-I characteristics are shown in Fig.7.28. There is some deviation found in the measured current w.r.t. the simulated value. It has been found that this is due to 90-95% beam transmission achieved so far which can be improved further by increasing the axial magnetic field.

7.6 Conversion of Single Beam Gun Design into Multi Beam Gun Design

In this section some simulation work has been reported for converting the existing single beam electron gun design of 352.2 MHz klystron into an equivalent five beam design using the methodology as discussed in Chapter 3. It will reduce the operating voltage and hence the size of associated power supplies. It is found that the five beam electron gun can be operated at about 50% less beam voltage. The beam voltage and beam current parameters for this five beam klystron can be derived using scaling laws as reported in Chapter 2. The equation 2.14 is used to compute the beam voltage V_{MBK} and it is found 15.8 kV by putting the existing value of 30 kV with single beam design and taking N as 5 which is the number of beams. The beam current for each beam-let in the five beam design can be calculated by multiplying the beam perveance with 3/2 power of V_{MBK} i.e.

Beam current in each beam = Beam perveance * $(15800)^{3/2}$ *(Eq. 7.1)*

It is to be mentioned here that the beam perveance in each beam is taken same as of the single beam design which is 1.35 μP. [as per assumption (i) of scaling laws mentioned in Chapter 2]. Therefore the computed value of beam current per beam let in MBK is 2.7 A. We can compute the beam current density per beam let of MBK using Eq. 2.16 which is found as 1.06 A/cm^2. The beam current density along with beam current value are used to get the beam radius which for the present case is calculated to be 9.0 mm. The drift tube radius of each tunnel is found to be 14.4 mm for the fill factor of 0.625 as taken in the single beam case.

Now a five beam RF cavity has been simulated in CST Microwave studio to get the target frequency of 352.2 MHz. By iterative simulation process it has been found that by placing five drift tunnels at 80 mm diameter PCD (also considering the tool margin for fabrication) in a cavity cylinder of 162 mm ID, the eigen mode solver gives the resonant frequency of 352.5 MHz, as shown in Fig. 7.29 where electric field lines are shown near gaps and eigen mode frequency is displayed. The cavity diameter is slightly lesser than the single beam case which was taken 177.5 mm, however the gap spacing is same as in both cases i.e. 28 mm.

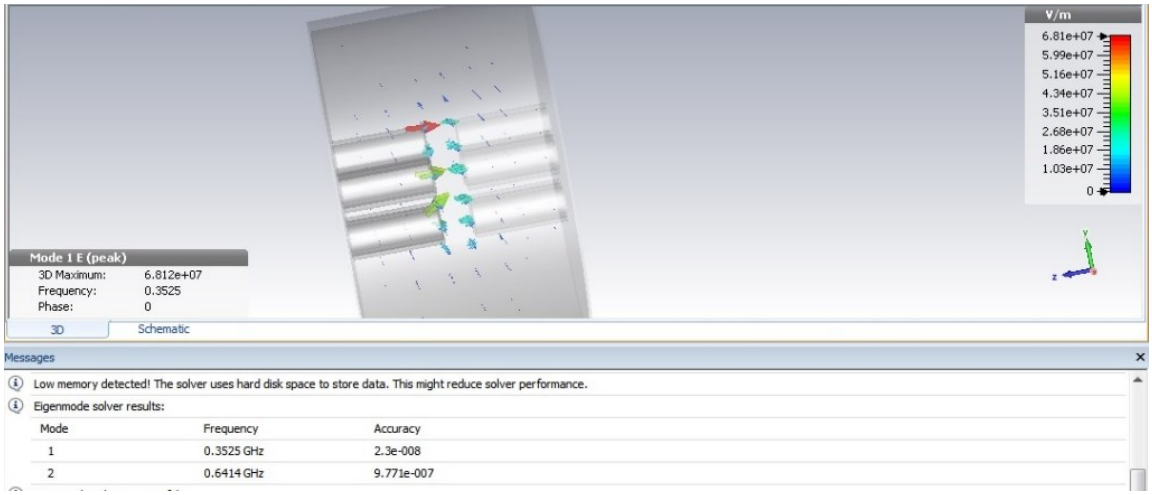

Fig.7.29: Simulation of five beam cavity for 352 MHz

Simulation of Electron Gun

Once the target frequency has been simulated through the proposed configuration of drift tubes in a cavity structure then the electron gun design may be simulated with a matching orientation of emission surfaces. The electron gun for the desired five beam klystron has been simulated in two steps, first the single beam gun has been optimized using TRAK code to find the proper electrode shapes and spacing so as to achieve the required value of current. A planar cathode surface has been chosen and confined flow focusing [40] has been used for focusing of the electron beam. The simulation of a single beam electron gun under the effect of focusing field is shown in Fig.7.30. The computed beam current is 2.7 A with a beam voltage of 15.8 kV.

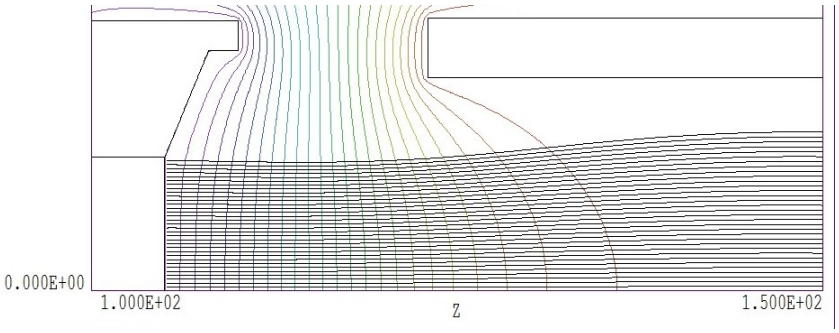

Fig. 7.30: The simulated electron gun in TRAK

The value of required magnetic field for focusing of electron beam with the mentioned beam parameters has been found using the well-known relation by Brillouin [40].

$$(B_b)^2 = \frac{69\, I_b}{(V_b^{0.5})R_b^2} \qquad \textit{(Eq. 7.2)}$$

Where B_b is the Brillouin field value in Gauss, V_b is the beam voltage and R_b is the beam radius. Thus the calculated value of B_b is 135 gauss and for confined flow focusing the value of the required magnetic field is taken 2-3 times [40] of Brillouin field value so the chosen value for the focusing magnetic field is taken about 350 Gauss. It is noted in Fig. 7.20 that the electron beam is laminar with no interception but with minor scalloping, under this value of magnetic field. The plot of required axial magnetic field after TRAK simulation is shown in the Fig. 7.31.

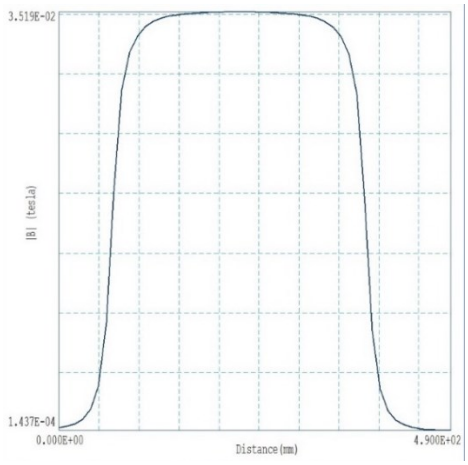

Fig. 7.31: The simulated magnetic field in Trak

Once the single beam gun design is optimized in Trak code then a five-beam structure has been modelled in CST particle studio with similar structural parameters of each beam let as per Trak design. The structure is shown in Fig. 7.32 where five planar cathodes on a single surface and the anode cylinder with five drift tunnels are placed at the optimized distance simulated through Trak.

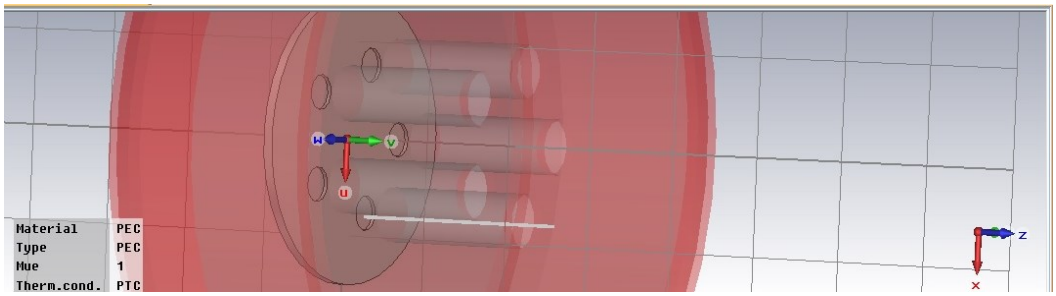

Fig. 7.32: Geometry of the five beam electron gun

An electromagnet has been designed to provide the required magnetic field along each drift tunnel axis and it is placed around the anode cylinder. The simulation of electromagnet has been carried out along with electron gun structure so as to get the desired value of magnetic field (350 gauss) at the drift tunnel axis, as shown in Fig. 7.33. The value of NI for simulated

electromagnet design is 3000 with 50A current and 60 turns in the coil. The electron trajectories in presence of applied magnetic field are shown in Fig. 7.34 which are well focused along the simulated drift section length. The collision information reveals that there is no beam interception at any of the drift axis and the dissipation is only at the termination.

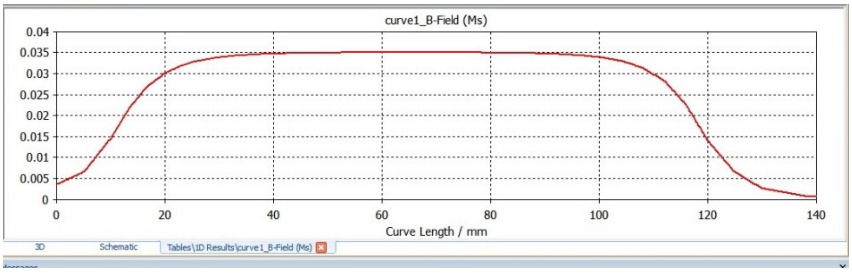

Fig.7.33: Simulated value of Magnetic Field on Drift tube axis

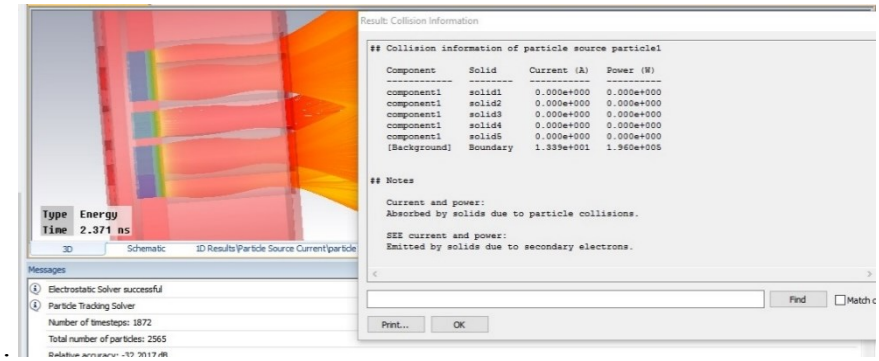

Fig. 7.34: Beam trajectories with focusing magnetic field

The simulated value of total beam current is about 13.5 A as shown in Fig. 7.35 and it is clear that total current of the five beam structure is almost five time of its single beam value as obtained through Trak.

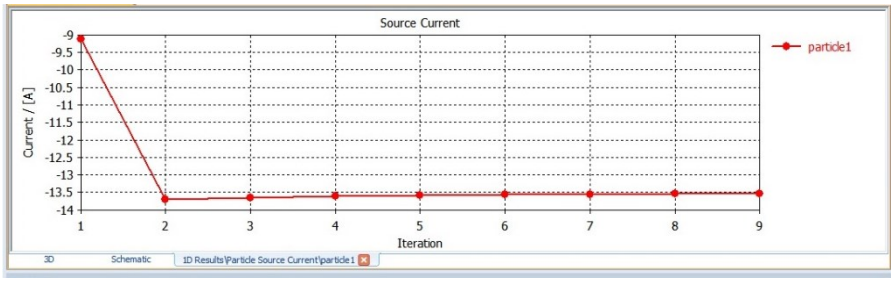

Fig. 7.35: Simulated value of the beam current

Once the Multibeam gun design is completed through CST then the same optimized dimensions are modeled in Opera-3d code to validate the results (Fig.7.36). The simulated value of focusing field is shown in Fig. 7.37 (same as in CST).

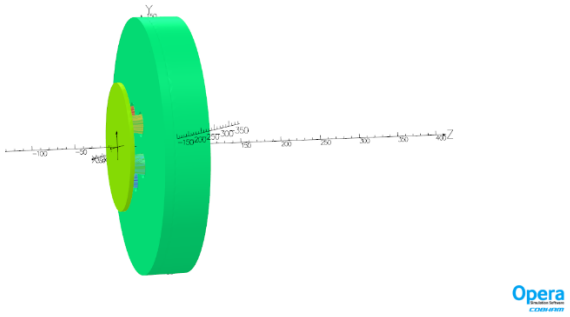

Fig. 7.36: Modelling of Electron gun in Opera

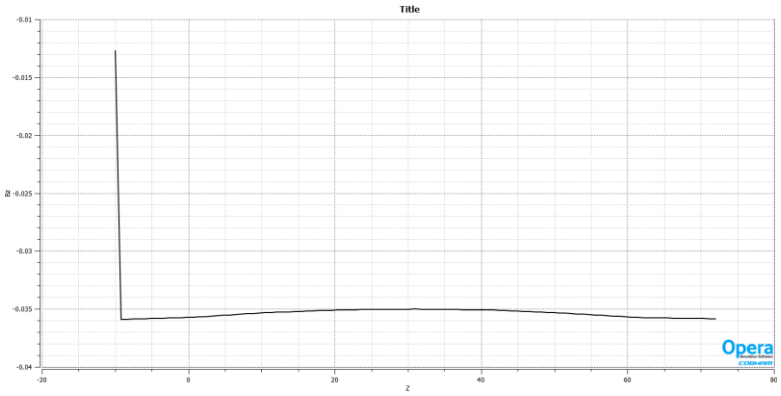

Fig. 7.37: Simulated value of magnetic field in Opera

The electron trajectories under the effect of simulated magnetic field are shown in Fig.7.38 which seem to be laminar.

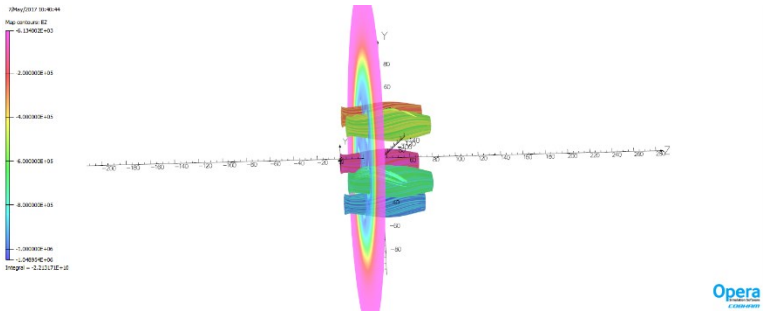

Fig. 7.38: Simulated Trajectories in Opera

The collision information can be drawn by measuring the current at two patches defined before and after the anode as shown in Fig. 7.39 and 7.40, it is found that no beam current is dissipated during propagation through anode as simulated by opera code.

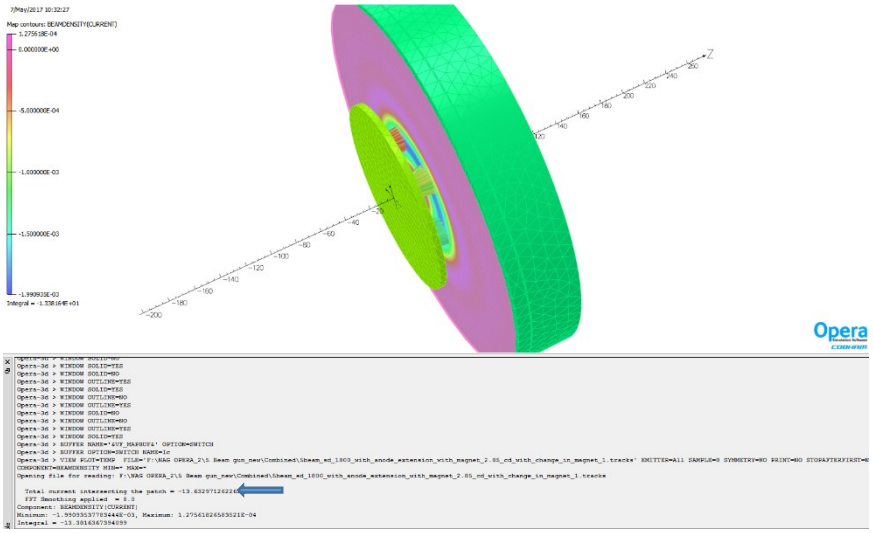

Fig. 7.39: Measured current before anode

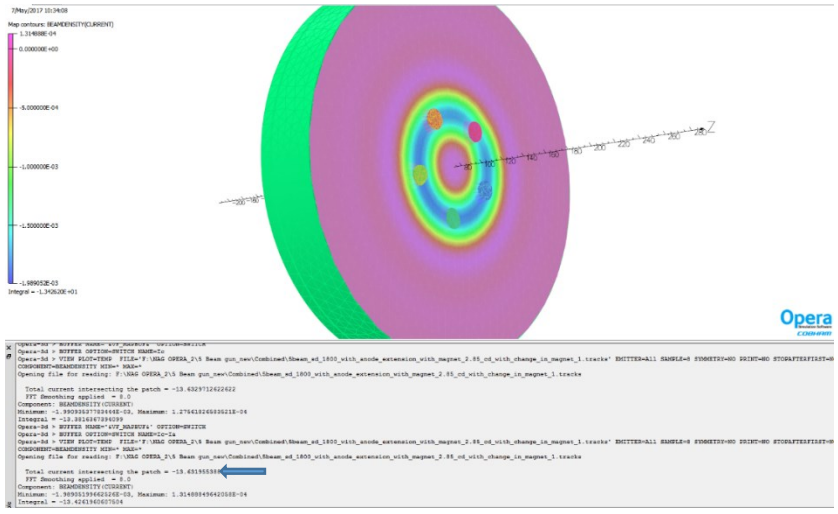

Fig. 7.40: Measured current after anode

Therefore a design of electron gun for a five beam 352.2MHz Klystron (with 100 kW RF output power) has been proposed after simulation through computer aided design codes. The five beam gun design will operate at about half of the operating voltage of single beam gun design. The results of multi beam electron gun have been cross-validated by two different codes i.e. CST particle studio and Opera-3D.

The work presented in this chapter has following publication outcomes;

Publication Outcome (4)

Deepender Kant, LM Joshi, V Janyani, "Thermal Analysis of Collector for a 100 kW (CW) Power Klystron" , 8th National Conference on Thermophysical Properties (NCTP-2015) at MNIT, Jaipur December 14-16, 2015

Later published *in 'Advanced Science Letters' Volume 22, Number 11, November 2016 pp 3781-3783* **doi: 10.1166/asi.2016.8053**

Publication Outcome (5)

Deepender Kant, L M Joshi and V Janyani, "Design of RF Interaction Structure for a 352.2 MHz, 100 kW (CW) Power Klystron", Presented in the Asia Pacific Microwave Conference (APMC) 2016 at New Delhi during December 5-9, 2016. *Published In IEEE Xplore digital library ' 2016, IEEE* Asia Pacific Microwave Conference *(APMC) Proceedings'*

Published on May 18, 2017; DOI: 10.1109/APMC.2016.7931307

Publication Outcome (6)

Deepender Kant, LM Joshi, Vijay Janyani, "Design of a Multi beam Electron Gun for 352.2 MHz, 100 kW (CW) Power Klystron"

Journal of Electromagnetic Waves and Application (published by Taylor and Francis) , Published online: 28 Sep 2017. DOI: 10.1080/09205071.2017.1381648

CHAPTER 8
Summary and Conclusion

The Microwaves and millimeter waves are popularly used in communication systems, electronic warfare, remote sensing and navigation, spectroscopy, industrial heating, material processing, waste remediation, imaging in atmospheric and space applications, thermonuclear fusion, particle accelerators for many societal as well as strategic applications. This demands various types of sources for microwave generation and amplification. The microwave tubes based on the vacuum technology and solid state semiconductor devices provide different options of the devices. In general, microwave tubes are preferred to solid state devices for their advantages in terms of higher power, gain, bandwidth, reliability, life, etc. The selection of a particular device depends upon the selected application and hence the operating frequency and power level.

The designing of microwave tubes with higher power level poses several challenges such as DC power dissipation, RF losses, maximum attainable electron density, heat transfer, material breakdown and the technological limitations of fabrication as the operating frequency increases to the mm wave range. In the category of slow wave devices i.e. where a slow waveguide mode, with phase velocity less than the speed of light, is destabilized, the traveling wave tube (TWT) is the most popular microwave tube and has the largest market among all tubes. The klystron belongs to the O type, longitudinal space-charge interaction, slow-wave, kinetic energy conversion type device. Klystrons are high gain, high output power but narrowband amplifiers that find wide use in various communication and radar systems, material processing and particle accelerators for medical, industrial and scientific applications including nuclear waste transmutation and energy production by sub-critical reactors.

The conventional klystron technology has been quite matured and there is a great demand of high power microwave sources with improved performance features like efficiency, gain, bandwidth, compact size and low weight. New variants of klystron amplifier like Multi Beam Klystron (MBK), Sheet Beam Klystron (SBK) and Extended Interaction Klystron (EIK) are capable to provide the solution to the desired performance features. The objective of the research work presented in this thesis was to investigate different design aspects of some of the new variants of conventional klystron. In this regard some defined goals were set to carry out this study such as design of a multi beam electron gun, design of focusing system for confinement of multiple beams, beam wave interaction simulations in a multi beam klystron

and to understand the design aspects of a sheet beam cavity. The complete design approach of a conventional klystron was also taken-up as a part of the study.

Following a research paper by SLAC, it was noted that some scaling laws with certain assumptions can be used to convert an existing single beam klystron design into an equivalent multi beam design. These laws were initially applied to convert the design parameters of existing RF cavities of single beam S-band and C-band klystrons under development at CSIR-CEERI into their equivalent multi beam design parameters. The study was carried out through simulation in CST Microwave Studio. The designs of two types of multi beam cavity structures were simulated i.e. one at 5 GHz frequency, another at 2856 MHz frequency. It was found that a significant reduction in the operating voltage of the device can be found by choosing an appropriate number of beams which results in the reduction of device size as well as the associated power supplies. This is covered in detail in Chapter 2.

After setting a design approach for the multi beam cavities by applying the scaling laws, a target for study of various other design aspects of a 2 kW L/S band multi beam klystron was set up. The proposed device specifications were set as per an immediate requirement for some communication application by defense forces which was also the major source of motivation for taking upon this study. The work was started by the design of beam formation and its confinement i.e. the design of a multi beam electron gun. The number of beams were chosen as five and the design parameters of the five beam electron gun were found initially by applying scaling laws along with some reference design parameters of an existing 1 kW single beam klystron which was developed earlier at CSIR-CEERI for similar kind of applications. The proposed five beam klystron will be actually an improved and multi beam version of the existing device. The newer version with higher output power and efficiency will be suitable to fulfill the required device performance. The design of a five beam electron gun for the proposed device has been done by using planar cathode structures. Initially the design was simulated by using an applied magnetic field analytically and the spacing of gun electrodes along with their mutual placement were optimized. Later an electromagnet was designed for the required focusing field by implementing the following two conditions;

(i) Electron gun side pole piece is put behind the cathode, instead of between cathode and anode

(ii) The pole pieces on both sides have similar holes matched with the drift section for a better coupling of the magnetic field inside the drift tunnels.

The design of electron gun along with electromagnet was simulated in CST Particle Studio and the required value of beam current was found without any beam interception while traversing

the beam through the five drift regions. A sensitivity study of the electron gun design was also done to see the effect for misalignment of axis of electromagnet with respect to the device's main axis. The above mentioned work is covered in detail in Chapter 3.

After optimization of the beam optics, the design of a compatible RF cavity for the proposed five beam klystron was done. The design was optimized and cross-validated through simulation with two different computer codes i.e. CST Microwave Studio and MAGIC-3D. The RF cavity has been fabricated with the simulated design parameters and characterized for its resonant frequency. The measured resonant frequency of the RF cavity was found in close agreement with the simulated design as discussed in Chapter 4.

Once the design of electron gun and RF cavity is finalized, the next step towards the realization of device is to optimize the interaction parameters of RF interaction region. The performance parameters of the device such as its output power, gain, bandwidth, efficiency etc. are decided through beam wave interaction process which in turn depend on various operating parameters such as beam voltage, beam current, beam focusing, RF drive power as well as characteristics of the interaction circuits such as resonant frequencies, quality factors, shunt impedances of various cavities and their placement. The process was simulated with the proposed device parameters through Particle-In-Cell (PIC) code of CST Particle Studio. The interaction parameters were optimized and it was established that with chosen multi beam design parameters, the required RF power can be produced with given efficiency.

Chapter 6 dealt with the next part of design study on klystron variants where some of the design aspects of a sheet beam klystron RF Cavity were investigated. The design of a sheet beam RF cavity and its frequency characterization were presented. The frequency for design was chosen as 2.1 GHz which lied within the band of above L/S band klystron. This cavity was designed and simulated to establish a flat field profile along the beam direction as required for a sheet beam operation of the device. The design was cross-validated through CST Microwave Studio and MAGIC-3D codes. The cold test model of the sheet beam cavity was fabricated and its resonant frequencies for the first two modes were measured and the measured results were found in close agreement with the simulated results. The details of sheet beam cavity development are covered in Chapter 6.

In addition to investigating multi beam and sheet beam variants of klystron, as discussed in Chapters 2 to 6, design of a high CW power conventional klystron was also investigated during the course of this research work. The targeted specifications were for some important applications in Department of Atomic Energy. The Chapter 7 of the thesis presented a complete design approach of a conventional klystron. The electron gun and corresponding focusing field

for this high power device were designed using MAGIC and Trak codes. The electrical, mechanical and thermal designs of collector were explored for optimum performance using electron optics and ANSYS codes. A beam stick tube consisting of the electron gun, the collector and a dummy drift section with provision of an electromagnet for transporting the beam from gun to collector was then designed and developed. The beam stick tube was hot tested and V-I characteristics of the electron gun and beam transport through drift section were measured, validating the simulated design. While development of this high power tube was continued to meet immediate requirements, a multi beam version of the same tube is under consideration for improved performance. The design of the multi beam electron gun for this device has been done with the same methodology as presented in Chapter 3.

8.1 Conclusion

In conclusion, the thesis presents methodologies for design of various components of a multi beam klystron. The focusing in a multi beam klystron is a challenging task which has been studied through some simulations and a methodology has been developed for the same. This approach has been adopted to design some electron guns with different specifications. The results after beam wave interaction studies with the designed parameters have established the suitability of the proposed design approach for designing of multi beam klystrons. A study on the design of a sheet beam klystron cavity has also been done as another newer variant of klystron amplifier. Limitations of resources in terms of finance, manpower and infrastructure did not allow practical realization of devices designed during course of this research. However a strong design base has been created to take-up specific klystron variants to meet upcoming demands with minimum lead time.

8.2 Future Work

The high power, high gain and wide band klystrons are required in substantial numbers in various high power microwave based systems and the demand shall further grow in foreseeable future. In this context the design base created through the work presented in this thesis shall provide a valuable contribution to take-up development of specific devices. There are still some gaps to be filled before a particular device may be taken-up for development which are indicated by the following points;

(1) The experimental validation of the five beam electron gun.

(2) Optimization of the beam wave interaction process for improving the device performance.

(3) The design of coupling and tuning mechanism in the multi beam cavity keeping in view of its asymmetric structure.

(4) Development of sheet beam cavity made out of OFHC copper and its characterization for other parameters like Q and R/Q.

(5) The designing of coupling and tuning mechanism in sheet beam cavities.

(6) The design study on multi-cell sheet beam cavity structures.

(7) The design study for a sheet beam electron gun including the generation and confinement of sheet beam.

(8) The confinement of sheet beam through magnetic field puts another major challenge in the form of 'diocotron instability' as discussed in Chapter 1 and hence needs more research work to be undertaken when designing a complete sheet beam device.

(9) The beam wave interaction simulations in SBK may be carried out.

It is expected that once the necessary resources are available, specific device development would be taken-up using the knowledge base generated in the present research work.

References:

[1] **The birth of the term "Microwaves"** *G. Pelosi* Proceedings of the IEEE. Vol. 84, Feb. 1996, p-326.

[2] **Microwave Devices and Circuits**, *S. Y. Liao* Englewood Cliffs, Prentice Hall, New Jersey 1985.

[3] **Microwave Tubes** *A. S. Gilmour*, Artech House, Norwood 1986.

[4] **Microwave Electron Tube Devices**, *S. Y. Liao,* Printice Hall, New Jersey 1988.

[5] **High Power Microwave Sources** *V. L. Granatstein and F. Alexeff*, Artech House, Norwood 1987.

[6] **Foundation of Microwave Engineering,** *R. E. Collin,* McGraw Hill, New York 1966.

[7] **Microwave Tube Transmitters** *L. Sivan*, Champman & Hall, London 1994.

[8] **Microwave Electronics** *I. Lebedev*, Mir, Moscow 1964.

[9] **Foundation of Microwave Electronics** *M. Chodorow and C. Susskind*, McGraw Hill, New York 1964.

[10] **Microwave Engineering and Applications** *P. Gandhi*, Pergamon, New York 1981.

[11] **Travelling Wave Tubes** *J. R. Pierce,* Princeton, D. Von Nostrand, New Jersey 1950.

[12] **Microwave Tubes and Semiconductor Devices** *G. D. Sims and I. M. Stephenson,* Blackie & Sons, London 1963.

[13] **Power Travelling Wave Tubes** *J. F. Gittins*, English University Press, London 1964.

[14] **Principles of Electron Tubes** *J. W. Gewartowski and H. A. Watson*, D. Van Nostrand, New Jersey 1965.

[15] **Microwave filters, impedance matching networks and coupling structures** *Mathaei et al.*, McGraw Hill, New York 1964.

[16] **Time Harmonic Electromagnetic Fields** *R. F. Harrington*, McGRaw Hill, New York 1961.

[17] **Fundamentals of Electromagnetics** *M. A. Wazed Miah*, Tata McGraw-Hill, New Delhi 1982.

[18] **Microwave Circuits** *J. L. Altmann*, D. Van Nostrand, New Jersey 1964.

[19] **Microwave Tubes 1920-1990: A review of ideas and progress** *H. Steyskal*, IETE Review, Vol. 9, 1992, pp. 81-85.

[20] **Unconventional microwave tubes: First report** *J. Zhang and R. G. Carter*, Report No. MRG/94/2, Lancaster University, February, 1994.

[21] **Microwave, Millimeter wave and submillimeter wave vacuum electron devices** *R. Chatterjee,* Affiliated East-West Press, New Delhi 1999.

[22] **Beam and wave electronics in microwave tubes** *R. G. E. Hutter*, D. Van Nostrand, New Jersey 1960.

[23] **High electron mobility transistor based on a $GaNAl_xGa_{1-x}N$ heterojunction** *M. A. Khan, A. Bhattarai, J. N. Kuznia, and D. T. Olson*, Appl. Phys. Letters 63, 1214,1993.

[24] **AlGaN/GaN high electron mobility transistors with InGaN back-barrier***T. Palacios, A. Chakraborty, S. Heikman, S. Keller, S. P. DenBaars, and U. K.Mishra* IEEE Electron Device Letters, vol. 27, no. 1, pp. 13–15, Jan. 2006.

[25] **BGaNHFET for W-band power applications** *M. Micovic, A. Kurdoghlian, P. Hashimoto, M. Hu, M. Antcliffe, P. J. Willadsen, W.S. Wong, R. Bowen, I. Milosavljevic,*

A. Schmitz, M. Wetzel, and D. H. Chow, IEEE International Electron Devices Meeting, 2006.

[26] **AlN/GaN insulated-gate HFETs using cat-CVD SiN** *M. Higashiwaki, T. Matsui, and T. Mimura,* IEEE Electron Device Letters 27, 16, 2006.

[27] **AlGaN/GaN Ka-band 5-W MMIC amplifier** *A. M. Darwish, K. Boutros, B. Luo, B. D. Huebschman, E. Viveiros and H. A.Hung,* IEEE Transactions on Microwave Theory and Techniques, pg 4456– 4463, 2006.

[28] **5 W GaN MMIC for millimeter-wave applications** *K.S. Boutros, W.B. Luo, Y. Ma, G. Nagy and J. Hacker* IEEE Compound Semiconductor Integrated Circuit Symposium, 2006, pages 93–95, 2006.

[29] **Ka-band AlGaN/GaN HEMT high power and driver amplifier MMICs** *M. van Heijningen, F.E. van Vliet, R. Quay, F. van Raay, R. Kiefer, S. Muller, D. Krausse, M. Seelmann-Eggebert, M. Mikulla and M. Schlechtweg* European Gallium Arsenide and Other Semiconductor Application Symposium (EGAAS) 2005, pages 237–240, 2005.

[30] **Field plated GaN HEMTs and amplifiers** *Y. F.Wu, A. Saxler,M. Moore, T.Wisleder, U.K. Mishra and P. Parikh* IEEE Compound Semiconductor Integrated Circuit Symposium (IEEE Cat. No.05CH37701), page 4, 2005.

[31] **A K-band AlGaN/GaN HFET MMIC amplifier on sapphire using novel super lattice cap layer** *M. Nishijima et al.* Microwave Symposium Digest, 2005 IEEE MTT-S International, 2005.

[32] **Ka-band MMIC power amplifier in GaN HFET technology** *M. Micovic, et al*. Microwave Symposium Digest, 2004 IEEE MTT-S International, pages 1653–1656,2004.

[33] **Applications of SiC MESFETS and GaN HEMTs in power amplifier design** *W. L. pribble et al.* Microwave Symposium Digest, IEEE MTT-S International, 2002.

[34] **Vacuum Electronics** *R.K. Parker, R.H. Abrams, Jr., B.G. Danly, and B. Levush* IEEE Trans. MTT, vol. 50, pp. 835-845, Mar. 2002.

[35] **Vacuum Electronics: Status and Trends** *B. Levush, et al.* IEEE Radar Conference, April 17–20, 2007, Boston, MA.

[36] **State-of-the-art of high power gyro-devices and free-electron masers** *M. Thumm* FZKA Report 5728, Institute fur Technische Physik, Karlsruhe, 1996.

[37] **Gain and bandwidth of the gyro-TWT and CARM amplifier** *K. R. Chu and A. T. Lin* IEEE Trans. Plasma Sci., vol. 16, 1988, pp. 90-104.

[38] **Comparative study of axial and azimuthal bunching mechanisms in electromagnetic cyclotron instabilities** *K. R. Chu and J. L. Hirshfield* Phys. Fluids, vol. 21, 1978, 461-466.

[39] **Cyclotron resonance devices** *R. S. Symons and H. R. Jory* Adv. Electron Phys., vol. 51, 1986, pp. 1-75.

[40] **Principles of klystrons, Travelling Wave Tubes, Magnetrons, Crossed Field Amplifiers and Gyrotrons** *A. S. Gilmour.*

[41] **Traveling-wave valve-New amplifier for centimetric wavelengths** *R. Kompfner* Wireless World Nov.1946,Vol52, pp 369-372.

[42] **From History to Future of Satellite TWT Amplifiers** *Dr. Günter Kornfeld* Thales Electron Devices GmbH, Germany.

[43] **Achievements and new Development Trends of Satellite Communication TWT´s** *E. Bosch, P. Heumüller, F. Bossert, H. Bradatsch, G. Kornfeld, R. Lotthammer and H. Strauß* Proceedings of Second European Conference on Satellite Communications, Liège, Belgium, Oct. 1991,ESA SP-332.

[44] **Satellite TWT-Amplifiers using the Microwave Power Module Concept and Radiation Cooled Collectors** *G.K. Kornfeld* Proc. IEDM Conference, San Francisco, Dec. 1994.

[45] **High Power C- and Ku-Band Amplifiers in Hybrid Solid State / Vacuum Technology** *R.A.Nunn, E.Bosch, P.Heumüller, G.Kornfeld (AEG); J.B. Klatskin, J. Martinetti,G. Pallace,P. Palena (Martin Marietta Astro Space); R. Schellhase, P.V. de Santis, J.L. Stevenson(Intelsat)* Proceedings of the ESTEC Workshop on Satellite *TWTA´s,* May 1994.

[46] **A 12 GHz 110 to 170 W High Efficiency TWTA for Broadcasting Satellites** *Y. Morishita, H. Hoshino, H. Nakagawa, S. Hamada, K. Kubo, K. Katakami, Y. Yoshida, A.Shiraiwa, Y. Iwanami, T. Takesue* Proceedings of the ESTEC Workshop on Satellite *TWTA´s,* May 1994.

[47] **Improved High Power Ku-Band TWTA´s for DBS Applications** *E. Sosa, R. Tamashiro and G. Lewis* Proceedings of the AIAA-94-0923, San Diego Conference, June 1994.

[48] **K-band TWT using using new diamond rod technology** *S. L. Aldana and R. N. Tamashiro* Proceedings of the ESTEC workshop on Satellite TWTA's, May 1991.

[49] **Twystrode experiments with tapered and untapered helices** *M.A. Kodis, N.R. Vanderplaats,E.G. Zaidman, B. Goplen, D.N.Smith and H.P. Freund* Proceedings of IEDM Conference, San Francisco, Dec. 1994.

[50] **TWT Amplifier for Satellite Communications with 200 W of RF-Power in Ka-Band and 300 W in Ku-Band** *F. André, E. Bosch, R. Nunn, H. Seidel* Proceedings of 2nd International Vacuum Electronic Conference, May 2001 in Noordwijk, Netherlands.

[51] **Advances in Space TWT Efficiencies** *D.S. Komm, R.T.Benton, H.C. Limburg, W.L. Menninger, X. Zhai* Ab Proceedings of IEEE International Vacuum Electronic Conference, May 2000 in Monterey, USA.

[52] **Review Paper on Space TWTs** *G. Fleury* Proceedings of IEEE International Vacuum Electronic Conference, May 2001 in Noordwiik.

[53] **Wavelength limit of rising sun system and comparison with the unstrapped magnetrons for mm wave range** *W. Praxmarer* Nachrichtentechnik (Berlin) 1954.

[54] **Possibility of generating mm waves with pulsed multi slot magnetrons of rising sun type** *W. Praxmarer* Nachrichtentechnik (Berlin) 1954.

[55] **High power mm wave radar transmitters** *G. W. Ewell, G. S. Ladd and J. C. Butterworth* Microwave Journal, Vol. 23, No.8, August, 1980.

[56] **Current status of crossed-field devices** *Mac Master*, IEEE IEDM, 1988, p. 358.

[57] **Cathode driven crossed-field amplifier, Product feature** *Raytheon Microwave and Power Tube Division, USA,* Microwave Journal, 1988, p. 208.

[58] **Vacuum Electronic High Power Terahertz Sources** *J.H. Booske, R.J. Dobbs, C.D. Joye, C.L. Kory, et al.* IEEE Trans. Terahertz Science and Technology, vol.1, no.1, 2011.

[59] **GYROTRONS High Power Microwave and Millimeter Wave Technology** *M.V. Kartikeyan, E. Borie, M.K.A. Thumm,* Springer, 2003.

[60] **A review of terahertz sources** *R.A. Lewis* J. Appl. Phys. vol. 47, 2014.

[61] **Recent Advances in the Worldwide Fusion Gyrotron Development** *M. Thumm* IEEE Trans. Plasma Sci., vol. 42, no. 3, pp. 590-599, March 2014.

[62] **Plasma physics and related challenges of millimeter-wave-to-terahertz and high power microwave generation** *J.H. Booske,* Physics of Plasmas, vol. 15, no. 5, pp. 055502 (16 pp.), Feb. 2008.

[63] **The potential of the gyrotrons for development of the sub-terahertz and the terahertz frequency range: A review of novel and prospective applications** *T. Idehara, T. Saito, I. Ogawa, S. Mitsudo, Y. Tatematsu, S. Sabchevski* Thin Solid Films, vol. 517, pp.1503-1506, 2008.

[64] **Development of THz Gyrotrons at IAP RAS and FIR UF and Their Applications in Physical Research and High-Power THz Technologies** *M.Y. Glyavin, T. IdeharaS.P. Sabchevski*, IEEE Trans. on Terahertz Science and Technology, vol. 5, pp. 788-797, 2015.

[65] **High Power THz Technologies Opened by High–Frequency Gyrotrons: Special Issue** *T. Idehara (Editor),* Journal of Infrared Millimeter and Terahertz Waves Vol. 33, 2012.

[66] **Gyrotron Development for High Power THz Technologies at IAP RAS** *V.L. Bratman, A.A. Bogdashov, G.G. Denisov, M.Yu. Glyavin, et al.,* Journal of Infrared Millimeter and Terahertz Waves Vol. 33, pp 715-723, 2012.

[67] **Terahertz Gyrotrons: State of the Art and Prospects** *M.Yu. Glyavin, G.G. Denisov, V.E. Zapevalov, A.N. Kuftin, et al.,* Journal of Communications Technology and Electronics, vol. 59, pp. 792–797, 2014.

[68] **Gyrotrons for High-Power Terahertz Science and Technology at FIR UF** Toshitaka Idehara and Svilen Petrov Sabchevski; Review Article.

[69] **A Quarter Century of Gyrotron Research and Development** *Victor L. Granatstein, Baruch Levush,B. G. Danly and R. K. Parker,* IEEE Transactions on Plasma Science Vol. 25 No. 6, December 1997.

[70] **High power linear beam tubes** *A. Staprans, E. W. Mccune, and J. A. Reutz* Proc. IEEE, Vol. 61, 1973, pp. 299-330.

[71] **Performance of SLAC linear collider klystrons** *M. A. Allen et al.,* IEEE Proc. , Particle Accelerator Conference, Washington DC, 1987.

[72] **Development of 2 GHz, 1 MW klystron for plasma heating** *S. Miyake et al.* IEEE IEDM, p.784, 1986.

[73] **Compact Multibeam Klystron** *M. Bres et al.,* IEEE IEDM, 1986.

[74] **Klystron performance using multistage depressed collector** *McCune et al.* IEEE p. 157, IEDM 1987.

[75] **Power Klystron Today** *M. J. Smith and G. Phillips*, 1995.

[76] **Radio frequency power generation** *R G Carter* DOI: 10.5170/CERN-2013-001.45.

[77] **R.F. Power Generation** *R.G. Carter* Proc. of the CERN Accelerator School 'RF for Accelerators' Denmark, 8–17 June 2010.

[78] **Thales Electron Devices** www.thalesgroup.com France.

[79] **1.2 MW Klystron for Asymmetric Storage Ring B factory** *W. R. Frowkes et al.* Proceedings of Particle Accelerator Conference 1995 , Texas.

[80] **A 3.0 MeV KOMAC/KTF RFQ Linac** *J. M. Han et al.*

[81] **RF system developments for CW and/or long pulse linacs** *Michael Lynch;* Los Alamos National Laboratory, USA.

[82] **Litton Electron Devices,** USA.

[83] **A 375 MW Modulator for a 150MW Klystron at the S-Band Linear Collider Test Facility at DESY** *S. Choroba, M. Bieler, J. Hameister, Y. Chi,* Proceedings of Linac 96.

[84] **Toshiba Electron Tubes and Devices,** Japan.

[85] **High Power CW Klystron for Fusion Experiments** *Ph.Thouvenin, A.Beunas, F.Peauger , B.Beaumont , L.Delpech , F.Kazarian* IEEE Conference Proceedings 2004.

[86] **High Power Klystrons: Theory and Practice at the Stanford Linear Accelerator Center** *George Caryotakis,* SLAC Publications.

[87] **Baron Gen3 Radar** http://www.baronweather.com

[88] **Comparison of Transmitters of Weather Radars** *Oguzhan Sireci* Turkish State Meteorological Service, Turkey.

[89] **High-power, high-efficiency klystrons for industrial heating** *Shintaro Arai et al.*

[90] **Electron Beam RF Linac for Cargo Inspection** *R. C. Sethi et al.* BARC Internal Report No: APPD/RFAS/2/2003.

[91] **Industrial and Agricultural Applications of Accelerators at RRCAT** *Jishnu Dwivedi* Workshop on Asian Forum for Accelerator and Detectors (AFAD) 2012.

[92] **Accelerator-driven sub-critical reactor system (ADS) for nuclear energy generation** *S. S. Kapoor* PRAMANA-Journal of physics pp. 941–950 December 2002.

[93] http://www.rrcat.gov.in/technology/accel/mal/arpf.html.

[94] **Linac for Medical Applications** *Subrata Das, R. Krishnan, A. P. Bhagwat, S. N. Pethe* ieeexplore.ieee.org Conference Proceedings 2009.

[95] **Eine neue Methode zur Erzeugung kurzer, ungedämpfter, elektromagnetischer Wellen grober Intensität***, Heil, A. A., O. Heil Zietschrift Für Physik,* Verlag Von Julius Springer, Berlin.

[96] **On Resonators Suitable for Klystron Oscillators** *Hansen, W. W., R. D. Richtmyer*, Journal. Of Appl. Physics,10, Pg. 189-199.

[97] **U. S. Patent No. 2.242.275 ,** *R. H. Varian,* Applied on October 11, 1937.

[98] **Synthesis of the Pierce gun** J R M Vaughan, IEEE Trans. Electronics Devices, ED-28 Vol 1, PP. 37-41, 1981.

[99] **Extended interaction klystron technology at millimeter and sub-millimeter wavelengths** *Brian Steer etal.* CPI.

[100] **Toshiba/KEK MBK for TESLA** *Yong Ho Chin.*

[101] **Development of 10MW L-Band MBK for European X-FEL Project** *Yong Ho Chin* ieeexplore.ieee.org Conference Proceedings 2007.

[102] **Design of a C-Band High Efficiency Multi-Beam Klystron** *Zening Liu, Jiaru Shi,Maomao Peng, Huaibi Chen* Proceedings of IPAC, Copenhagen, Denmark.

[103] **Research and development of Multi-Beam Klystrons in China** *Yaogen Ding et al.* IEEE International Vacuum Electronics Conference (IVEC), 2009.

[104] **Research Progress on X-Band Multi-Beam Klystron** *Yaogen Ding Bin Shen, Jing Cao, Yongqing Zhang, Cunjun Ruan, Hong-hong Gu, Ding Zhang, Caiyin Wang, Ming Cao*, IEEE International Vacuum Electronics Conference (IVEC), 2008.

[105] **A Sheet Beam Klystron Paper Design** *G. Caryotakis,* 5th MDK *workshop,* Geneva, 2001.

[106] **Design of a 11.4 GHz, 150-MW, Sheet Beam,PPM-Focused Klystron** *G.Caryotakis et al.* 6th workshop on high energy density and high power RF.

[107] **Design and Cold test of High Frequency Interaction Structure for X-Band Sheet Beam Klystron** *Ding Zhao, Cunjun Ruan, Yuan Liang, Shuzhong Wang, Changqing Zhang, Xiudong Yang.* IEEE 14th International Vacuum Electronics Conference (IVEC), Paris, 2013.

[108] **Researches on an *X*-Band Sheet Beam Klystron** *Ding Zhao, Xi Lu, Yuan Liang, Xiudong Yang, Cunjun Ruan, and Yaogen Ding,* IEEE Transactions on Electron Devices Vol 61 No.1 Jan. 2014.

[109] **The Development of X-band and W-band Sheet Beam Klystron in IECAS** *Cunjun Ruan, Ding Zhao, Xiudong Yang, Changqing Zhang, Shuzhong Wang* IEEE International Vacuum Electronics Conference (IVEC), Monterey, CA, USA, 2014.

[110] **Test and Development of a 10 MW 1.3 GHz Sheet Beam Klystron for the ILC** *D. Sprehn et al.* Proceedings of IPAC'10, Kyoto, Japan.

[111] **W-Band Sheet Beam Klystron Simulation** *E. R. Cobly, G. Caryotakis, W. R. Fowkes, D. N. Smithe.* Conference on High-Energy Density Microwave 1998, California.

[112] **Design and Construction of a W-band Sheet Beam Klystron** *G. Scheitrum* 7th Workshop on High Energy Density and High Power RF, 13-17 June 2005, Greece.

[113] **S-Band Sheet Beam Klystron Research and Development at SLAC** *Aaron Jensen, Fazio Haase, Jongewaard, Martin, Neilson, Sprehn and Vlieks.* IEEE 14th International Vacuum Electronics Conference (IVEC), Paris, 2013.

[114] **200 kW CW Sheet Beam Klystron Research and Development** *Aaron Jensen, Michael Fazio, Andrew Haase, Erik Jongewaard, and Jeffrey Neilson* IEEE International Vacuum Electronics Conference (IVEC), Monterey, CA, USA, 2014.

[115] **Design Aspects of a 1 KW Tunable D/E Band Klystron,** Journal of the IETE, Vol.39, pp345-350, Nov.-Dec.1993.

[116] **High-power multibeam klystron with reversive magnetic focusing system** *A.V.Malykhin, P.V.Nevsky, V.I.Pasmannik, E.P.Yakushkin* SRPC "TORIY", Moscow.

[117] **A Medium Power Electrostatically Focused Multiple-Beam Klystron** *Bernard Vancil, Robert Mueller, Kenneth W. Hawken, Edwin G. Wintucky and Carol L. Kory* IEEE Transactions on Electron Devices Vol 54 No.10 October 2007.

[118] **Effect of Aperture in a Pole Piece for Focusing of Multi Beam Electron Gun** *Ashok Nehra, L.M. Joshi, S. Kaushik and R.K. Gupta* IEEE International Vacuum Electronics Conference (IVEC) 21-24 Feb. 2011.

[119] **Electron Gun for Multiple Beam Klystron using Magnetic Focusing** Patent No. US 6,768,265 B1 dated July 27,2004.

[120] **Method and Apparatus for Magnetic Focusing of Off-axis Electron Beam,** Patent No. US 7, 005,789 B2 dated Feb 28, 2006.

[121] **Low-voltage Multi-Beam Klystron** Patent No. US 2013/0229109 A1 dated Sep 05, 2013.

[122] **Modern Microwave and Millimeter-wave Power Electronics** *Barker, Booske, Luhmann Jr. & Nusinovich;* John Wiley & Sons, Inc.

[123] **Cooling of Electronic Equipments** *Allan W. Scott,* John Willey and sons.

[124] **A review of the development of Multiple-beam Klystron and TWTs** *Gregory S Nusinovich, B. Levush, and D.K. Abe*, Research report, Naval Research Laboratory, USA, March, 2003.

[125] **Electromagnetic Theory and Applications in Beam Wave Electronics** *B N Basu*, World Scientific Publishing Co. Pte Ltd. Singapore.

[126] **Design consideration for high power multicavity klystron** *Paul J Tallerico,* IEEE Trans. Electron Devices, vol. ED-18, no. 6, June 1971.

[127] **Electron Beam Coupling in Interaction Gaps of Cylindrical Symmetry** *Branch, G. M. Jr.* IRE Transactions on Electron Devices, May, 1961.

[128] **Electron bunching and output gap interaction in Broad band klystrons** *T G Mihran G. M. branch and G. J. Griffin* IEEE Transactions on Electron Devices Vol ED-19 No.9 Sep 1972.

[129] **Design and Demonstration of a klystron with 62 percent efficiency** *T G Mihran* IEEE Transactions on Electron Devices Vol ED-18 No. 2 Feb 1971.

[130] **Computer modeling and investigation of most efficient interaction processes in multicavity klystrons** *A. V. Aksenchik et al.,* Radio Engineering and Electron Physics Vol. 28, No. 2, February 1983.

[131] **Three-dimensional evaluation of energy extraction in output cavities of klystron amplifiers** *H. G. Kosmahl, and L. U. Albers* IEEE Trans. Electron Devices, Vol. ED-20, No. 10, October 1973.

[132] **A high-efficiency klystron with distributed interaction** *M. Chodorow and T. Wessel-Berg* IRE Trans. Electron Devices, Vol. ED-8, No. 1, January 1961, pp. 44–55.

[133] **Criteria for Vacuum Breakdown in RF Cavities** *W. Peter et al.* Particle Accelerator Conference, Santa Fe, NM, 1983.

[134] **The current and velocity distributions in a velocity modulated Brillouin focused electron beam** *A. S. Gilmour, Jr., G. C. Dalman, and L. F. Eastman* Proceedings of 4th International Congress on Microwave Tubes, Eindhoven, the Netherlands,1963.

[135] **Radial and axial current and velocity distributions in large-signal velocity-modulated electron beams** *A. S. Gilmour, Jr.* IEEE Transactions on Electron Device, Vol ED-19 No. 7, July 1972.

[136] **A study of the broadband frequency response of the multicavity klystron amplifier** *K. H. Kreuchen, B. A. Auld, and N. E. Dixon* Journal of Applied Physics, May 1957.

[137] **The linear theory of the clustered-cavity klystron** *R. S. Symons and J. R. M. Vaughan* IEEE Transactions Plasma Science, Vol 22 No.5 October 1994.

[138] **Special features of bunching and energy exchange in a relativistic multiresonator klystron** *A. N. Sandalov and A. V. Terebilov* Radio Engg. and Electron Physics Vol. 28 No.9 September 1983.

[139] **Effect of the velocity distribution in a bunch on the kinetic energy extraction efficiency in a klystron** *Y. I. Vasil'yev, V. I. Kanavets, and A. V. Terebilov* Radio Engg. and Electron Physics Vol. 28 No.4 April 1983.

[140] **Synthesis of an electron bunch and the conditions for realizing it in a klystron** *V. A. Kochetova, A. V. Malykhin, and D. M. Petrov* Radio Engg. and Electron Physics Vol. 26 No.1 Jan 1981.

[141] **Multiple-beam Klystron Amplifiers: Performance Parameters and Development Trends** *A.N. Korolyov, E.A. Gelvich, Y.V. Zhary, A.D. Zakurdayev, and V.I. Poognin*, IEEE Trans. Plasma Sci., vol. 32, no. 3, pp. 1109–1117, Jun. 2004.

[142] **High‐power Four Cavity S‐band Multiple‐beam Klystron Design** *K T Nguyen, D K Abe, D E Pershing, B Levush, E L Wright, and H Bohlen*, IEEE *Trans. Plasma Sci*., vol. 32, no. 3, pp. 1119–1135, June 2004

[143] **On the opportunity of bandwidth increasing in Multibeam klystron with planar layout of the beam** Galdetskiy, A.V. IEEE International Vacuum Electronics Conference (IVEC) 2011.

[144] **S-band multibeam klystron with bandwidth of 10%** *Y. Ding et al.* IEEE Transactions on Electron Devices Vol 52 No. 5, May 2005.

[145] **The design and demonstration of a wideband multiple-beam traveling wave klystron** *W. J. Pohl.* IEEE Transactions on Electron Devices ED-12 No. 6, June 1965.

[146] **The effect of space charge on bunching in a two-cavity klystron** *T G Mihran* IRE Transactions on Electron Devices Vol ED-6 No. 1 Jan 1959 pp54-64.

[147] **Ballistic analysis of a two-cavity finite beam klystron** *S. E. Webber,* IRE Transactions on Electron Devices Vol. 5 No. 2 April 1958 pp. 98-108.

[148] **Sheet-Beam Klystron RF Cavities** *David Yu, et al.* Proceedings of particle Accelerator Conference, pp - 2681 - 2683 vol.4, 1993.

[149] **Cavity Design for an X-band Sheet Beam Klystron** *Wang Ruan et al.* IEEE International Vacuum Electronics Conference (IVEC) 2010, Monterey, CA, USA.

[150] **Study of RF Structure for W band Sheet Beam EIK** *Shuyuan Chen et al.* IET International Radar Conference 2015, Hangzhou, China.

[151] **Computer Simulation and Analysis of 350-MHz High-Power Coaxial RF Window and T-bar Transition** *Sandeep Vyas, Narendra Shekhawat, Shivendra Maurya, and V.V.P. Singh* IEEE Transactions on Plasma Science, vol. 40, no.10, October 2012.

Appendix 1

Calculation of Gaussian 'k':

Gaussian 'k' gives the shape of the electric field distribution across the gap of the klystron cavity. The normalized electric field distribution is given by the equation:

$$f(z) = \frac{k}{\sqrt{\pi}} e^{-k^2 (z - z_{center})^2} \quad \text{..... (i)}$$

where,

z = axial distance along the drift tube of the cavity

z_{center} = mid-point of the gap-length of the cavity

The Gaussian distribution of a quantity x is given as:

$$f(x) = \frac{1}{\sigma\sqrt{2\pi}} e^{-\frac{1}{2\sigma^2}(x-\mu)^2} \quad \text{..... (ii)}$$

where,

σ =standard deviation of the distribution *f(x)*

μ = mean of the distribution *f(x)*

Comparing equation (i) with equation (ii), we get

$$k = \frac{0.707}{\sigma}$$

Since, k is inversely proportional to σ,higher the value of k sharper is the electric field profile at the gap.

The following steps were followed to find out the value of *k*:

1) A straight line is drawn along the drift tube of the cavity.
2) Z-component of the electric field distribution was calculated along the curve.
3) The field distribution is exported as 'Plot data (ASCII)'.

4) A MATLAB program, as given below, has been used to calculate the value of *k*. This program does a Gaussian curve fitting over the procured set of values and generates the value of *k* along with the fitted curve.

```
clc; clear all; close all;
%e_dat=dlmread('efld2ghz00_1.txt');
e_dat=dlmread('efield1.txt');
max1= max(e_dat(:,1));
max2= max(e_dat(:,2));
e_dat(:,2)=e_dat(:,2)/max2;
e_dat(:,1)=e_dat(:,1)/1000;
cfn=fit(e_dat(:,1),e_dat(:,2),'gauss1')
plot(e_dat(:,1),e_dat(:,2),'o');
holdon;
plot(cfn);
kk=1/cfn.c1
```

5) A sample result is shown below.

```
cfn =

     General model Gauss1:
     cfn(x) =  a1*exp(-((x-b1)/c1)^2)
     Coefficients (with 95% confidence bounds):
       a1 =       1.024  (1.02, 1.029)
       b1 =      0.0021  (0.002098, 0.002102)
       c1 =   0.0006669  (0.0006637, 0.00067)

kk =

   1.4996e+03
```

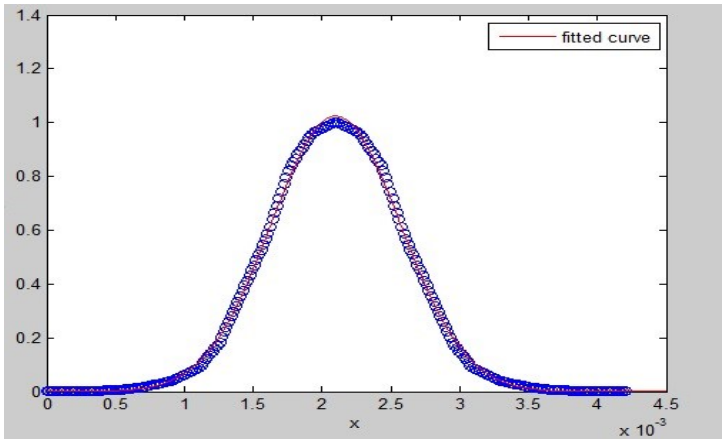

Appendix 2

List of Publications:

1. Deepender Kant, LM Joshi, Vijay Janyani, "Design of a Multi Beam Klystron Cavity from Its Single Beam Parameters", 2nd International Conference on Communication Systems (ICCS-2015) at BKBIET Pilani, October 18-20, 2015.
   (Peer reviewed international conference with publication in the 'Journal of American Institute of Physics')
   AIP Conf. Proc. 1715, 020049 (2016) doi: 10.1063/1.4942731

2. Deepender Kant, LM Joshi, V Janyani, "Thermal Analysis of Collector for a 100 kW (CW) Power Klystron" , 8th National Conference on Thermophysical Properties (NCTP-2015) at MNIT, Jaiur December 14-16, 2015
   Later published *in 'Advanced Science Letters' Volume 22, Number 11, November 2016 pp 3781-3783* **doi: 10.1166/asi.2016.8053**

3. Deepender Kant, L M Joshi and V Janyani, "Design of RF Interaction Structure for a 352.2 MHz, 100 kW (CW) Power Klystron", Presented in the international conference Asia Pacific Microwave Conference (APMC) 2016 at New Delhi during December 5-9, 2016. *Published In IEEE Xplore digital library 'Proceedings of IEEE* Asia Pacific Microwave Conference (APMC)-*2016'* (Published on May 18, 2017; DOI: 10.1109/APMC.2016.7931307)

4. Deepender Kant, L M Joshi and V Janyani, "Design and Characterization of RF Cavity for a L-Band Multi Beam Klystron", Presented in the international conference IEEE MTT-S International Microwave and RF Conference (IMaRC) 2016 at New Delhi during December 5-9, 2016. *Published In IEEE Xplore digital library 'Proceedings of IEEE MTT-S International Microwave and RF Conference (IMaRC) 2016'*
   (Published on June 08, 2017; DOI: 10.1109/IMaRC.2016.7939619)

5. One patent application has been filed with title 'A Novel Approach for Focusing of Electron beam in a Multi-beam Klystron'. The details of application number, date of filing etc. are indicated as following.

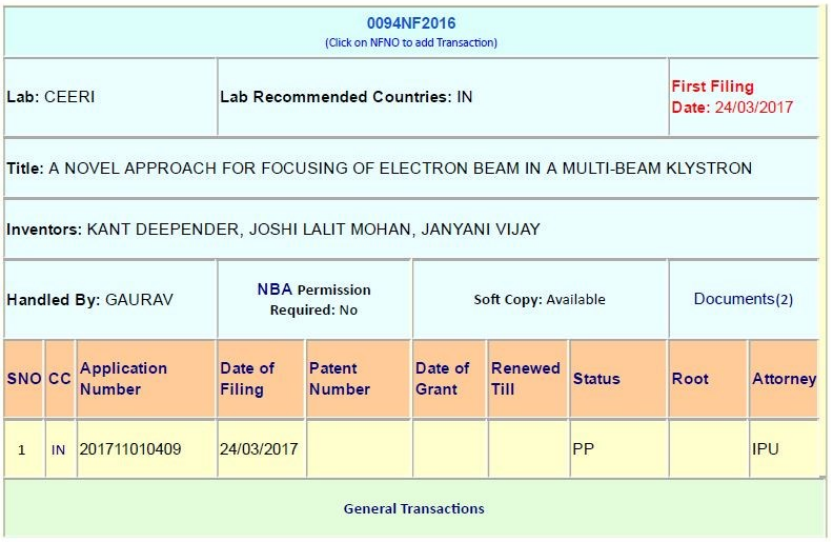

0094NF2016
(Click on NFNO to add Transaction)

Lab: CEERI	**Lab Recommended Countries:** IN	**First Filing Date:** 24/03/2017
Title: A NOVEL APPROACH FOR FOCUSING OF ELECTRON BEAM IN A MULTI-BEAM KLYSTRON		
Inventors: KANT DEEPENDER, JOSHI LALIT MOHAN, JANYANI VIJAY		
Handled By: GAURAV	**NBA Permission Required:** No	**Soft Copy:** Available / Documents(2)

SNO	CC	Application Number	Date of Filing	Patent Number	Date of Grant	Renewed Till	Status	Root	Attorney
1	IN	201711010409	24/03/2017				PP		IPU

General Transactions

6. Deepender Kant, LM Joshi, Vijay Janyani, "Design of a Multi beam Electron Gun for 352.2 MHz, 100 kW (CW) Power Klystron" Journal of Electromagnetic Waves and Application (published by Taylor and Francis) , Published online: 28 Sep 2017. **DOI: 10.1080/09205071.2017.1381648**

Appendix 3

Introduction of computational codes:

CST Studio Suite: *(www.cst.com)*

CST STUDIO SUITE is a software package which can simulate and solve all electromagnetic problems from Low frequency to Microwave and optic as well as thermal and some mechanical problems. It has generally seven studios:

- Microwave Studio: for RF and Microwave problems like antenna design
- EM Studio: for low frequency problems like RFID, electrostatics, magnetostatics, etc.
- Design Studio: a schematic workflow to design lumped circuits and also join the results of the other studios in order to design a system assembly
- Particle Studio: for particles and beam simulation like e-Gun, microwave tubes, etc.
- MPHYSISCS Studio: for some mechanical and thermal simulations
- Cable Studio: for design and simulation of cables in bundle, harness, etc.
- PCB Studio: for simulation of PI and SI in multi layered PCBs.

We have used Microwave studio and Particle Studio for our study;

CST MICROWAVE STUDIO® is a specialist tool for the 3D EM simulation of high frequency components. CST MWS's unparalleled performance is making it first choice in technology leading R&D departments. CST MWS enables the fast and accurate analysis of high frequency (HF) devices such as antennas, filters, couplers, planar and multi-layer structures and SI and EMC effects. Exceptionally user friendly, CST MWS quickly gives you an insight into the EM behaviour of your high frequency designs.

CST PARTICLE STUDIO® is a specialist tool for the fast and accurate analysis of charged particle dynamics in 3D electromagnetic fields. Powerful and versatile, it is suitable for tasks

ranging from designing magnetrons and tuning electron tubes to modelling particle sources and accelerator components. The particle tracking solver can model the behaviour of particles through static fields, and with the gun iteration, space charge limited emission. The particle-in-cell (PIC) solver, which works in the time domain, can perform a fully consistent simulation of particles and electromagnetic fields. The CST desktop looks like as shown in Figure A1

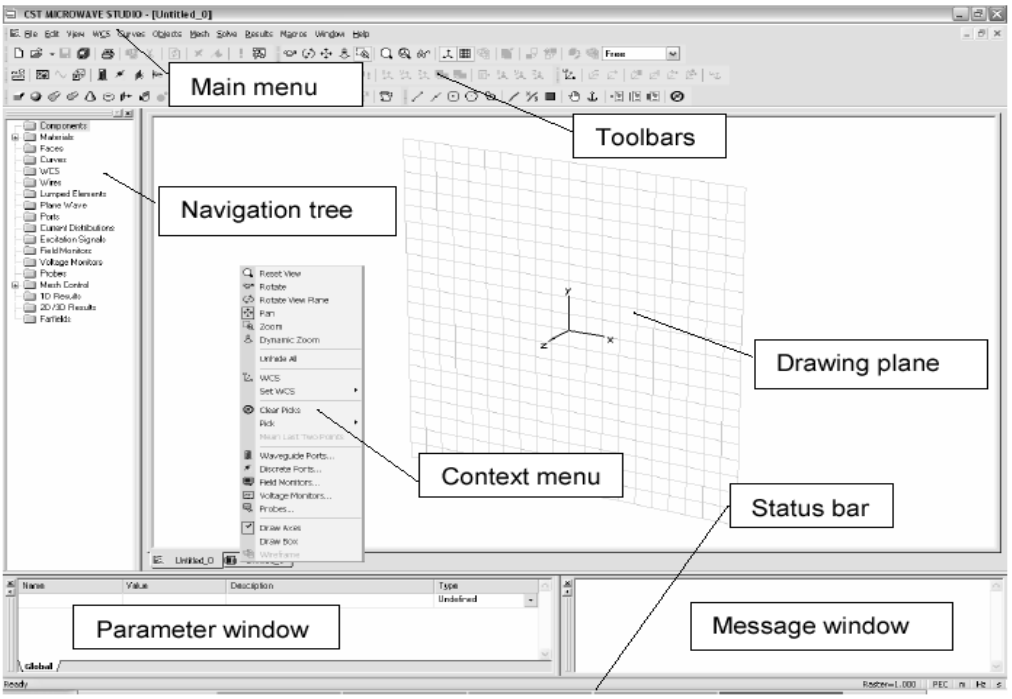

Fig A1: Picture of CST Desktop

AJdisk*:* ***(****www-group.slac.stanford.edu)*

The AJ disk is a considerably improved 1-dimensional klystron code previously known as "Japan disk". It was rewritten in C++ (from FORTRAN) and runs much faster. The code employs the "disk model", in which electrons are represented by disks of charge inside a cylindrical drift tube. Typically, 32 disks (max=64) are employed within a period 1/f. Output power and efficiency are calculated by integrating disk velocity at the exit of the output cavity, and by forming the product of the induced current and voltage at the output cavity

Steps to follow:

To get started, double click on the AJ Disk executable. (ajdisk.exe)

Next, select "file" from AJ Disk's menu, and from within the "file" menu select "open." Now, select the file to be opened and press the "open" button. The input window looks like as in

Fig.A2 where we put the desired input for the getting the desired results. If the "OK" button is clicked then the simulation will begin.

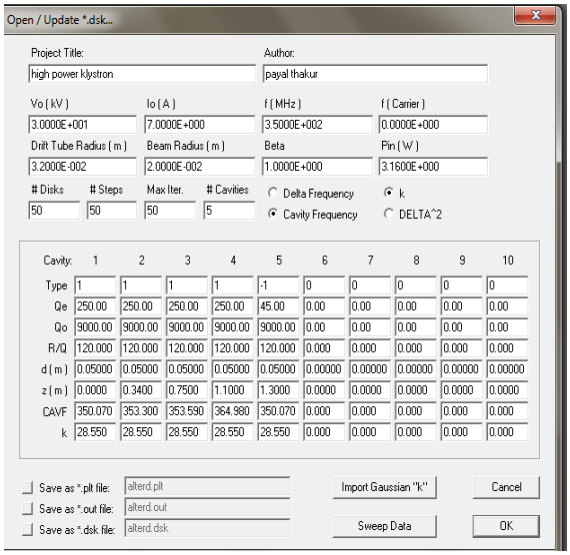

Fig. A2: The input window

The 1st line contains the project's title and the author's name.

The 2nd line contains,

Vo (kV) - the beam voltage in kV

Io (A) - the beam current in Amps

f (MHz) - the drive frequency in MHz

f (Carrier) - this variable is no longer used (set to zero)

The 3rd line contains,

Drift Tube Radius (m.)- The radius of the drift tube in meters Beam Radius (m.)

The radius of the beam in meters. Beta- the radial coupling coefficient (set to one)

Pin (W) - the drive power in watts

The 4th line contains,

Disks - the number of disks

Steps- - the number of integration steps per rf cycle

Max Iteration - the maximum number of iterations. Program stops if not converged by 30 iteration.

Cavities - the number of klystron cavities

The 5th line contains the cavity type which is,

1 for fundamental mode cavities, 2 for 2nd harmonic cavities, -1 for output cavities, 0 for unused cavities

The 6th line contains the Qe's (the external Q's)

The 7th line contains the Qo's (the Ohmic Q's)

The 8th line contains the R/Q's

The 9th line contains the gap widths in meters, d (m)

The 10th line contains the distances of the cavities from the input gap in meters, z (m), and is measured from gap center to gap center.

The 11th line contains the cavity frequencies, if "Cavity Frequency" has been selected or cavity detuning from the drive frequency if "Delta Frequency" has been selected

The 12th line contains the parameter "k"

Which determines the shape of the electric field distribution across the klystron gap.

One example results' window after AJ-disk run is shown in Fig. A3 followed by its description.

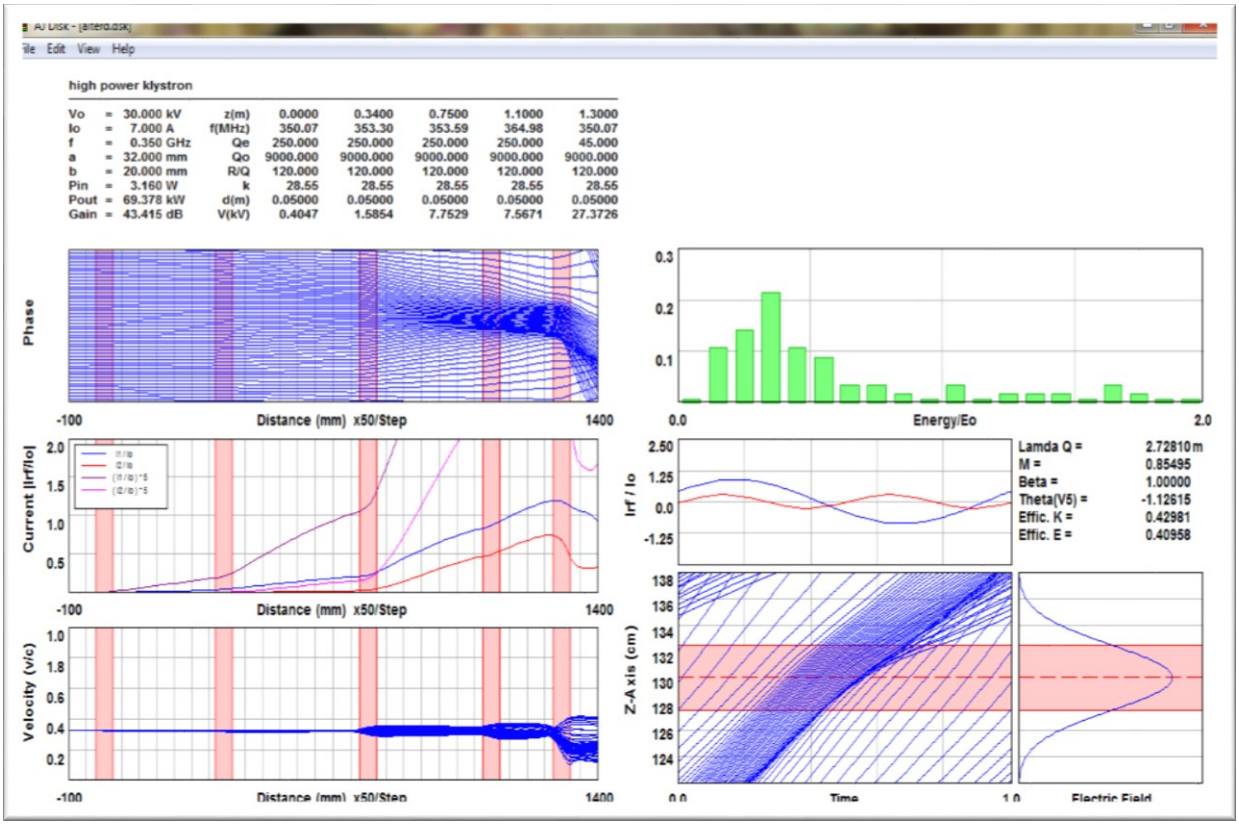

Fig. A3: The output results

Text Block: The text block at the top of the figure shows the user input as well as some of the numeric results of the simulation, such as, gain, cavity voltage, and output power.

Applegate Diagram: Shows the disks in one period and how their phase changes as a function of axial distance. Primary display in analyzing simulation results.

Current Diagram: Shows the fundamental and second harmonic components of the beam current as a function of axial distance.

Velocity Diagram: Shows the velocity spread as a function of axial distance.

Energy Distribution: The energy distribution of the spent beam.

I_{rf}/Io Diagram: The fundamental and second harmonic of the induced current at the output cavity as a function of time.

Electric Field Diagram: The approximated Gaussian distribution of the electric field at the output gap.

The interaction between the electron beam and the RF signaling the rf section of the klystron resulting in amplification of later, was simulated using 1-d code AJDisk. Here the electron beam, is considered to be made up of a number of disks of charges, which are of same diameter as that of bunched beam. In this code it is assumed that focusing is strong enough so that beam diameter does not change due to space charge forces due to unbunched beam.

The model calculates the bunching of the beam in the drift space as the result of interaction of the bunched beam with RF at the gap cavities and the energy extraction at the output gap the cavity parameter such as frequency Qs, R/Q and gap length and separation between successive cavities were given as input. Here the separation between successive gaps was estimated on basis of plasma, plasma wavelength and other parameters.

MAGIC: *(www.orbitalatk.com)*

The MAGIC Tool Suite is an electromagnetic (EM) particle-in-cell (PIC) simulation code employing the finite difference time domain (FDTD) method for simulating plasma physics processes - those that involve interactions between space charge and EM fields. Beginning from a specified initial state, the code simulates physical phenomena as they evolve in time. The full set of Maxwell's time-dependent equations is solved to obtain EM fields. Similarly, the complete Lorentz force equation is solved to obtain relativistic particle trajectories, and the continuity equation is solved to provide current and charge densities for Maxwell's equations. This approach is commonly referred to as EM FDTD-PIC. It provides self-consistent interaction between charged particles and EM fields. In addition, the code has powerful algorithms to represent structural geometries, material properties, incoming and outgoing waves, particle emission processes, and background plasmas. The software is applicable to broad classes of physics problems involving low to high density electrons, ions and neutral gases.

The FDTD-PIC software dynamically solves Maxwell's equations (specifically Ampere's Law and Faraday's Law.) In addition, particle modeling assumes the relativistic Lorentz force. Capabilities of the models include: Cartesian, polar, and cylindrical coordinate systems. Grid mesh is orthogonal, but may be graded in size. Allows complex geometries, although the realization is on an index cubic conformal mesh. Both two dimensional (with three velocities, 2&1/2 D) and full three dimensional (3D) versions of the software. Multiple particle species and creation models: explosive emission, beam emission (prescribed current model), high field emission (Fowler-Nordheim model), thermionic emission (current prescribed by temperature function), and beam injection (import model). External static magnetic field specification by import from other software, as well as functional prescription. Initialization of EM fields. Eigenmode solver for cavity circuits. EM material properties include: perfect conductors, dielectric materials (permittivity), lossy materials (finite electrical conductivity), artificial magnetic loss materials (finite magnetic conductivity, and Convolutional Perfectly Matched Layer materials (CPML). Graphical interface for diagnostics. Diagnostic sampling includes: 2D Contour plots, phase space plots, 1D spatial range plots, 1D time history plots, 2D and 3D geometry views.

ANSYS: *(www. ansys.com)*

ANSYS is finite element analysis software enables engineers to perform the following tasks:

- Models or transfer CAD models of structure, products, components, or systems.
- Apply operating loads or other design conditions.
- Study physical responses, such as stress levels, temperature distributions, or electromagnetic fields.
- Optimize a design early in the development process to reduce production costs.
- Do prototype testing in environment where it otherwise would be undesirable or impossible (for example, biomedical application).

The ANSYS program has a comprehensive graphical user interface (GUI) that gives users easy, interactive access to program functions, commands, and documentation and reference material. ANSYS is used by engineers worldwide in virtually all fields of engineering:

- Structural
- Thermal
- Fluid (CFD, Acoustics, and other fluid analysis)

- Low and High-Frequency Electromagnetics.

Thermal analysis calculates the temperature distribution and related thermal quantities in a system or component. Typical thermal quantities of interest are:

- Temperature distributions
- Amount of heat lost or gained
- Thermal gradients
- Thermal fluxes

Thermal simulations play an important role in the design of many engineering applications, including internal combustion engines, turbines, heat exchangers, piping systems, and electronic components. In many cases, engineers follow a thermal analysis with a stress analysis to calculate thermal stresses (that is, stresses caused by thermal expansions or contractions). ANSYS supports two types of thermal analysis:

Steady state analysis:

It determines the temperature distribution and other thermal quantities under steady state loading conditions. A steady-state loading condition is a situation where heat storage effects varying over a period of time can be ignored. This type of thermal analysis we have worked with.

Transient analysis:

It determines the temperature distribution and other thermal quantities under condition that vary over a period of time.

Opera: *(www.cobham.com)*

Opera provides the complete tool chain for electromagnetic with multiphysics design, simulation and analysis of results, for use on 32- or 64-bit platforms. It consists of a powerful 2D/3D modeller for creating design models (or importing from CAD), plus a choice of specialized finite element simulation tools:

- Static electromagnetic fields (the widely used 'Tosca' tool)
- Low/High frequency time-varying electromagnetic fields
- Thermal and stress analysis (standalone or coupled)
- Linear and rotating machinery design
- Superconducting magnet quenching

- Particle beams including space charge effects
- Permanent magnet magnetization/ demagnetization
- Electric field analysis in conducting /dielectric media

Following simulation, a programmable interactive post-processor allows users to view and analyze the simulation, and perform additional calculations. Subsequent improvement of designs is easy. Model parameters may be changed at will to rapidly perform 'what-if?' investigations. Or, designs can be automatically improved with the aid of Opera's Optimizer. This optional tool is uniquely powerful and fast, and will even optimize competing objectives simultaneously. Opera is available in 2D or 3D variants, for economy and speed of design.

Brief Bio Data

Deepender Kant has completed his Bachelor of Engineering (Honours) in Electronics and Communication from University of Rajasthan in 2002 and M.Tech. in Electronics Engineering from IIT-BHU, Varanasi in 2011. Presently he is serving as a senior scientist at CSIR-CEERI, Pilani and doing research for design and development of various klystrons with different specifications. His areas of interest include High Power Microwaves (Generation and Applications), Computer Aided Design of RF components. Specifically he has worked for design and modelling of Electron Guns, RF interaction structures including RF Cavities, RF couplers/window and high power testing of microwave devices. He has also been involved with thermal design aspects for various microwave tube sub-assemblies like collector, cooling of RF cavities etc. He is a life member of IETE, VEDA and IPA.